PROJECT FINAL REPORT
TO THE
MICHIGAN GREAT LAKES PROTECTION FUND

PROJECT TITLE: **THE DRY DEPOSITION OF SPECIATED MERCURY TO A FOREST ECOSYSTEM (GL00-002)**

and

THE AIR-SURFACE EXCHANGE OF SPECIATED MERCURY TO AGRICULTURAL CROPS AND SOILS (GL01-017)

PRINCIPAL INVESTIGATOR: **Frank J. Marsik, PhD**
Department of Atmospheric, Oceanic and Space Sciences
2455 Hayward, Room 2109
Ann Arbor, MI 48109
(734) 763-5369

CO-PI: **Gerald J. Keeler, PhD**
Department of Atmospheric, Oceanic and Space Sciences
2455 Hayward, Room 1531
Ann Arbor, MI 48109

SUBMITTED TO: **Ms. Emily Finnell**
Assistant Project Manager
Office of the Great Lakes
Hollister Building
P.O. Box 30473
Lansing, MI 48909-7973
(517) 241-7927

SUBMITTED: **August 22, 2003**

INTRODUCTION

Mercury is a known neurotoxin that can result in a number of adverse health effects in wildlife and humans (Myers *et al*., 2000; Rodgers *et al*., 2001; Chan *et al*., 2003). Having both natural (volcanic, geothermal) and anthropogenic sources (mining/smelting of ores, fossil fuel burning, chlor-alkali production and waste incineration), mercury can be found in the atmosphere in three primary forms: elemental gaseous mercury [Hg(0)], reactive gaseous mercury [RGM, as Hg^{+2} or Hg_2^{+2}] and particulate mercury [Hg(p)]. Atmospheric mercury is predominantly (>95%) found as Hg(0) (Steinnes, 1990; USEPA 1997; Schroeder and Munthe, 1998). With an atmospheric residence time of approximately one year due to its highly volatile characteristics, Hg(0) can be transported and deposited far from its original source (Swain *et al*., 1992; Sorensen *et al*., 1995; Fitzgerald *et al*., 1997). In contrast, both the RGM and Hg(p) have relatively short atmospheric residence times and thus are typically deposited closer to their respective emission sources. Once transported into a particular area, mercury in its various forms may experience exchanges with the environment via precipitation (wet-deposition), particle deposition, as well as gaseous air-soil (Carpi and Lindberg, 1998; Zhang *et al*., 2001), air-vegetation (Lindberg *et al*., 1992; Leonard *et al*., 1998) and/or air-water exchange (Lindberg *et al*., 1995; Poissant and Casimir, 1998).

This research project is particularly interested in the exchange of the relevant forms of mercury with vegetation. Numerous studies have shown that mercury can enter vegetation both via the soil and the atmosphere. Grigal (2002) notes that both greenhouse and laboratory studies have shown that mercury uptake from soil is limited, as roots act as significant absorption sites, thus acting as a barrier to mercury transport to

the foliage. The affinity of mercury for root biomass is related to the significant cation-exchange capacity of the roots. Mercury adsorption onto root material (in the form of $HgCl_2$ and CH_3HgCl) has been found to reduce the uptake of essential soil nutrients resulting in damage to the root system of the plant (Godbold, 1991). Bishop *et al*. (1998), however, have proposed a mechanism for the translocation of mercury via xylem sap flow in conifers. In its elemental form [Hg(0)] mercury has been found to be transported through the transpiration stream with subsequent volatilization to the atmosphere (Kozuchowski and Johnson, 1978; Leonard *et al*., 1998; Lindberg *et al*., 2002) for both aquatic and terrestrial plants. While mercury is a natural component of soils (Schroeder and Munthe, 1998), mercury may be added to soils via atmospheric deposition (both wet and dry). In the case of agricultural lands (both orchards and row crops), mercury may be directly applied to the ecosystem through the use of mercury-containing fungicides, fertilizers, municipal sludges and seed preservatives (Steinnes, 1990). It should be noted, however, that agricultural use of mercury-containing products has been reduced considerably in the past two decades.

Significant research has indicated that the soil is not the only source of mercury to plant biomass. In fact, a large number of studies have suggested/shown that the uptake of ambient atmospheric mercury, primarily as Hg(0), is the dominant pathway for mercury to enter plant foliage (Lindberg *et al*., 1998; Fleck *et al*., 1999; Melieres *et al*., 2003; Erickson *et al*., 2003). Hanson *et al*. (1995) found evidence of the existence of a plant species-specific "compensation point" for mercury exchange with vegetation. They suggested that when ambient mercury levels are below the compensation point, emission

of Hg(0) was likely, while foliar uptake of mercury was likely when ambient concentrations were above the compensation point.

While species-specific compensation points are not know for most plant species, there is substantial evidence of the foliar uptake of ambient mercury by many types of plants. Using large gas-exchange chambers to study the uptake of mercury by plants grown in background and mercury enriched soils, Ericksen *et al*. (2003) found that the uptake of mercury was independent of the soil mercury concentration. Their results also showed that for the species studied, *Populus tremuloides* (Quaking Aspen), approximately 80 percent of the mercury in the above ground biomass was found in the foliage. Using small gas chambers, they suggested that nearly all of the mercury found in the foliage had originated from the atmosphere. Similar results have been suggested in studies by Cho and Park (2000) and Melieres *et al*. (2003). For deciduous trees (and seasonal plants), this uptake of ambient mercury through the growing season can result in a significant input of mercury to the soil via litterfall (dropping of leaves) at the end of the growing season (Iverfeldt 1991; *Rea et al*., 1996; Melieres *et al*., 2003).

Our ability to understand the impact of mercury on sensitive ecosystems requires a complete understanding of the processes associated with the cycling of the relevant forms of mercury through these different ecosystem types. Within the State of Michigan, two of the predominant land-use types are hardwood forests and agricultural croplands. For this reason, these two ecosystems were chosen for study. Of particular importance is our need to obtain a better understanding of the processes influencing the dry-deposition of mercury to an ecosystem. An understanding of these processes is essential to the success of current and future modeling efforts aimed at investigating the likely ecosystem

impacts of potential mercury emissions reduction scenarios. As a result, one of the primary objectives of this work has been to obtain in situ measurements of mercury dry-deposition to each of the ecosystems studied. Additionally, a single-layer "bigleaf" dry-deposition model (NOAA Inferential Model) (Hicks, *et al*., 1987) was used in conjunction with the meteorological and ambient-chemical data collected during a series of measurement intensives in an effort to test the model's ability to predict mercury dry-deposition to each of the canopies studied. While this and other inferential models have been used to estimate the dry-deposition of ozone, acidic gaseous and particulate species to various land surface types, this study represents the first effort to apply such models in an ecosystem level study of the dry-deposition of speciated mercury. It is believed that the lessens learned from this study will help us to improve the models used to predict mercury dry-deposition, thus allowing us to narrow the uncertainties associated with the modeling of mercury dry-deposition in transport-deposition models.

1. SITE DESCRIPTIONS

Pellston, Michigan Site

The 2001 Mercury Air-Canopy Exchange (MACE) study was performed on the grounds of the University of Michigan Biological Station near Pellston, Michigan (45.6ºN; 84.4ºW) during the month of June 2001. Meteorological and chemical measurements associated with our mercury dry-deposition study were performed from ~30 meter scaffolding tower located within a mixed-hardwood forest with an average canopy height of 20 meters. The primary species within the forest include *Acer rubrum* (red maple), *Betula papyrifera* (white birch), *Quercus rubra* (red oak), *Fagus grandifolia* (American beech) and *Populus grandidentata* (bigtooth Aspen) (Rea *et al*., 2000). The

forest was relatively dense with a few openings. For the period studied, the overall leaf area index (LAI) was measured to be 3.2.

Clarksville, Michigan Site

The 2002 MACE study was performed at the Michigan State University's Clarksville Horticulture Experiment Station (CHES) in Clarksville, Michigan (42.9ºN; 85.3W). Established in 1974, research on small fruits and tree fruits for Michigan growers is the primary focus of this 440-acre station located in Ionia County. Studies performed at the facility include variety development and evaluation, fruit thinning and growth regulator studies, dwarf rootstocks for fruit trees, weed control, integrated pest management, and new pruning and training practices. In addition, herbicide testing is also conducted on corn and soybeans, which are planted for alternate growing seasons. The first set of mercury air-canopy exchange measurements were performed over a *Malus domestica* (Apple) orchard during the month of August 2002. Averaging between 3.5 and 4.0 m in height, the trees are planted in rows that are approximately 7 m apart. The average LAI for the orchard at the time of our work was 4.3. The surface soils in measurement area have been characterized as a sandy loam of the Riddles Series.

The second set of mercury air-canopy exchange measurements were performed over a *Glycine Max* (Soybean) canopy during the month of September 2002. Averaging between 0.9 and 1.0 m in height, the soybeans were planted in rows approximately one meter apart. At the time of our measurements, the average LAI ranged from 2.7 in areas of senescence and 4.2 in areas of predominantly green foliage. The surface soils in this measurement area have also been characterized as a sandy loam of the Riddles Series.

2. PROJECT GOALS AND METHODOLOGY

Using newly developed mercury measurement and analysis techniques, this project proposed to directly measure speciated, ambient concentrations of mercury, and the dry-deposition of total mercury, over: (a) a mixed-hardwood forest in Northern Lower Michigan (UM Biological Station in Pellston) and (c) agricultural crops and soils in West Michigan (MSU Clarksville Horticulture Experiment Station near Clarksville). Combining this chemical information with simultaneous micrometeorological measurements of the temperature, relative humidity, wind direction/wind speed, global radiation, and the turbulent flux of momentum, model estimates were to be obtained of the dry-deposition of mercury to these ecosystems. These model estimates were then to be compared with our direct measurements to test the ability of the model to predict mercury dry-deposition.

A number of additional meteorological measurements were also performed during the field studies: (1) to assist us in the interpretation of the measured and modeled results and (2) to allow us to estimate the surface layer fluxes of elemental mercury to/from the Apple and Soybean canopies. These measurements included: surface wetness, precipitation, and surface fluxes of heat, water vapor flux and carbon dioxide. The following table summarized the measurements performed during each study. A description of the chemical and meteorological measurements/analyses follows.

Summary of Chemical and Meteorological Measurements Locations

	MEASUREMENT HEIGHT (meters Above Ground Level)		
VARIABLE	**Hardwood Forest**	**Apple Orchard**	**Soybean Field**
Hg (0)	35	6.4 and 3.8	3.2 and1.0
RGM	28	3.1 (between trees)	1.8
Hg (p)	28	3.1 (between trees)	1.8
Dry-Deposition	33	1.8 (between trees)	1.7
Temp/RH	24	1.8	1.5
Wind Dir/Speed	36	3.8	2.8
Global/Net Radiation	24	3.8	2.0
Turbulent Fluxes	35	5.4	3.2
Avg. Canopy Height	~20	~3.6	~0.9

All chemical samples were collected using a daytime/nighttime sampling strategy in order to provide insight into possible differences which may be related to the varying atmospheric stability between the daytime (typically neutral to unstable atmospheric conditions) and nighttime (with relatively stable atmospheric conditions) periods. These periods were determined based upon the whether the net radiation was positive (DAYTIME, net surface absorption of solar radiation typically leading to neutral to unstable, turbulent atmosphere) or negative (NIGHTTIME, net surface emission of radiation typically leading to stabilization of the atmosphere and thus suppression of turbulence). The following period definitions were used for each study, respectively:

Pellston (June 2001)	Daytime:	0700 to 2000 EDT
	Nighttime:	2100 to 0600 EDT
Clarksville (Aug 2002)	Daytime:	0800 to 1900 EDT
	Nighttime:	2000 to 0700 EDT

Clarksville (Sep 2002)	Daytime:	0830 to 1830 EDT
	Nighttime:	1930 to 0730 EDT

Automated Hg Sampling and Analysis

During each measurement intensive, ambient concentrations of Hg(0) over the canopy were measured using a Tekran® Model 2537 Mercury Vapor Analyzer. During both Clarksville measurement intensives, this instrument was connected to a Tekran® Model 1110 Synchronized Two Port Sampling Unit. The Tekran® Model 2537 Mercury Vapor Analyzer allows for the automated measurement of five-minute average concentrations of vapor-phase mercury by using two, alternating gold amalgamation traps and cold-vapor atomic fluorescence spectrometry (CVAFS). During any given five-minute period, one trap is being sampled upon while the other is being analyzed. The instrument itself was placed within a commercially available doghouse to protect it from direct sunlight and precipitation.

During the two measurement intensives performed at the Clarksville site, the Model 1110 Synchronized Two Port Sampling Unit was employed to allow for the measurement measure the Hg(0) concentrations at two levels above the vegetation by automatically switching between these levels at ten-minute intervals. This procedure allowed both gold amalgamation traps to sample at each level before the switch occurred, allowing us to obtain ten-minute average vapor-phase mercury concentrations that were based upon the two five-minute average concentrations measured using both traps. This sampling strategy allowed us to avoid potential errors that could have been introduced by the existence of trap-to-trap biases. Efforts to avoid trap-to-trap biases were made by carefully matching the two traps installed in the instrument. Additionally, prior to (and

after) each measurement intensive, line-bias tests were performed to insure that the sampling lines used in the gradient measurement would provide the same reading with inlets were at the same level. Any existing bias noted between sample lines during these tests were removed from the gradient data during post processing of the data.

Manual RGM Sampling and Analysis

For all three measurement intensive, manually deployed KCl coated quartz annular denuders were used in the measurement of ambient RGM. The collection and thermal desorption of these denuders have been studied extensively (Landis *et al*., 2002). In these laboratory investigations, the capture efficiency of known concentrations of $HgCl_2$ was >97%, and the thermal desorption process was found to be quantitative. In field measurements, precision determined by collocated samples was 15% and breakthrough onto a backup denuder for samples ≤ 5 h was <6%. The mean field blank was 2 pg, resulting in a method detection limit of 3 pg m^{-3} for two hour samples. Manual denuders were also sampled at 10 l min^{-1}. The actual flow was measured using a URG Corp. (Chapel Hill, NC) URG-3000-02C dry gas meter. Manual denuders were analyzed within twelve hours after collection in an on-site laboratory. The manual denuders were thermally desorbed at 500ºC and RGM was quantified as Hg(0) using a Tekran® 2500 CVAFS analyzer. The Tekran® 2500 analyzer was calibrated daily just before analysis using a Tekran® Model 2505 primary calibration unit.

Hg(p) Sampling and Analysis

Total and fine-fraction particulate mercury samples (TPM and PM2.5, respectively) were collected using 47mm quartz fiber filters. A strict clean-handling

protocol was followed during all phases of sample preparation, handling and deployment/collection/analysis. This protocol included the rigorous acid cleaning of all analytical equipment (e.g., petri dishes and Teflon®-coated forceps) to avoid potential contamination of the samples. Clean gloves were worn during all sample-handling activities, including deployment and collection of the samples. Samples were triple-bagged during transport to and from the measurement site to insure sample integrity. Prior to deployment, quartz sample filters were pre-fired in a Class 100 (fewer then 100 particles per cubic foot of air) clean room to insure that no pre-existing mercury was on the filters prior to deployment.

TPM samples were collected by pulling 30 l min^{-1} through a Teflon® open-face filter pack, while PM2.5 samples were collected by pulling 16.7 l min^{-1} through a Teflon® filter-pack. The PM2.5 size separation was achieved using a URG Corp. (Chapel Hill, NC) model URG-2000-30EH Teflon®-coated cyclone impactor. Once again, sample flows were measured using URG Corp. (Chapel Hill, NC) model URG-3000-02C dry gas meters. Sample flows were checked at the start and completion of each sample period to insure accurate and uniform performance through the sampling period and throughout the study. Following collection, all particulate samples returned to their petri dishes, Teflon® taped, triple-bagged and refrigerated until shipment to the laboratory. The samples were then analyzed in a Class 100 clean laboratory using a procedure that involves the passive digestion of the sample filters and the subsequent analysis of the resulting solution using CVAFS.

Direct Measurement of Mercury Dry-Deposition

Direct measurements of total mercury dry-deposition were obtained using a water-based, surrogate surface technique developed by the University of Michigan Air Quality Laboratory (Keeler and Glinsorn, personal communication). To make this measurement, aerodynamic (frisbee-shaped) deposition plates were deployed above the average height of the vegetative canopy. The exception was during the Clarksville Apple Orchard measurements, when the deposition surfaces were placed between trees and slightly below the average canopy height. Each deposition plate, made of Teflon®, contained a removable well that holds 300 ml of ultra-pure water. At the start of each sampling period, ultra pure water was poured into the well from previously filled 500ml Teflon® bottles. The water-filled deposition plates were then left exposed to the atmosphere for the entire sample period (daytime or nighttime). In the event of rainfall, each deposition plate was covered to prevent contamination from rainfall. These plate covers were removed immediately following the completion of the rain event. There were a few instances when precipitation fell overnight when it was not possible to cover the sample plates. For these periods, the dry-deposition samples were considered to be contaminated by the rainfall mercury and thus were not analyzed. At the end of each sampling period, the exposed water was drained from each well and returned to its original bottle, at which time the bottles were Teflon®-taped, triple bagged and refrigerated until transport back the laboratory. All sample handling was performed using particle-free gloves to insure that sample contamination did not occur. All sample equipment and supplies (bottles, wells, etc.) were acid cleaned to insure that they provided no contamination to the samples. Samples were analyzed for total mercury

within a Class 100 cleanroom at the University of Michigan using previously established techniques (Hoyer et al., 1995; Landis and Keeler, 1997).

In addition, measurements of the dry-deposition of ions were also performed in a similar manner, with the exception that sample apparatus associated with the ion sampling procedure were not acid-washed prior to use. Samples were analyzed within a Class 100 cleanroom at the University of Michigan with a Dionex Model DX-600 Ion Chromatography Instrument (Sunnyvale, CA) using a procedure based upon Koutrakis *et al*. (1988) and Keeler *et al*. (1991). Given that the ion dry-deposition was not a primary focus of this study, these results are only presented in Appendix B, Tables B1-B4.

Meteorological Measurements

Micrometeorological measurements were made in the atmospheric surface layer above the canopy (lowest 10's of meters) in an effort to characterize the energy exchanges (and the resulting turbulent transfer environment) over the canopy. As noted earlier, these measurements included: temperature and relative humidity (Campbell Scientific, Inc. CS500 Temp/RH probe), wind direction/wind speed (RM Young Co. Wind Monitor-RE), global radiation (Li-Cor 200-X Pyranometer), net radiation (REBS, Incorporated) and turbulent fluxes of momentum, sensible heat and latent heat (Gill Instruments Solent Ultrasonic Anemometer and Li-COR 7500 Infrared Gas Analyzer). These measurements were made continuously during the course of the study, with the resulting data archived as 30-minute average quantities using a Campbell Scientific, Inc. 21X Micrologger and laptop computer. This data was used in both the overall

interpretation of the chemical data collected during the measurement intensives and as input to the inferential dry-deposition model described in the following section.

Inferential Dry-Deposition Model

Model estimates of the dry-deposition of speciated mercury to the canopy were obtained using a single-layer, inferential dry-deposition model (Hicks *et al*., 1987). This model and similar approaches have been used to investigate the dry-deposition of O_3, SO_2 and several nitrogen species (Baldocchi *et al*., 1987; Wesely *et al*., 1990; Tarnay *et al*., 2002) to varying surface types. To our knowledge, there has been only one previous application of a single-layer inferential model to the study of mercury dry-deposition to an ecosystem (Lindberg *et al*., 1992). This latter study used the model to estimate the dry-deposition of elemental mercury to a hardwood forest in the Walker Branch Watershed, Oak Ridge, TN.

As noted earlier, the present study is the first to apply this model to an ecosystem level study for which the ambient concentrations of all three relevant forms of atmospheric mercury were concurrently measured. The accurate speciation of these forms of mercury is critical, given that the rate and the manner with which mercury deposits to the Earth's surface depends a great deal on chemical form that mercury takes. Due to its high volatility, Hg(0) has a tendency to remain airborne and thus is not thought to make a significant contribution to mercury dry-deposition. Divalent forms of mercury, however, are highly reactive and soluble and thus are believed to be subject to much faster removal from the atmosphere than Hg(0).

The single-layer inferential model is based upon an electrical resistance analogy (Hicks *et al*., 1987). Namely, the delivery of a chemical species from the atmosphere to a given surface is described in terms of a series of "resistances to deposition" which arise due to meteorological, chemical and biological processes that control pollutant delivery, adsorption and capture at natural surfaces (Figure 1). Mathematically, this is described by:

$$V_d = 1 / (R_a + R_b + R_c) \quad (1)$$

where R_a is the is the aerodynamic resistance to transfer (related to atmospheric turbulence), R_b is the near-surface boundary-layer resistance (related to the molecular diffusivity of the depositing species) and R_c is the canopy resistance (related to the various chemical and biological processes associated with the surface to which the species is being delivered). The canopy resistance includes consideration of parallel resistances to the uptake of the chemical species by: (1) the waxy cuticular substance of a leaf, (2) transfer through the stomata of the leaf and uptake by the leaf's internal mesophyll tissues, or (3) transport through the canopy with ultimate deposition to the water or soil surface below. Both the near-surface boundary layer resistance, R_b, and the canopy resistance, R_c, are first calculated on a "per leaf" basis and then divided the canopy leaf area index (LAI) to scale the "per leaf" resistances up to the canopy level.

The resistances considered in this modeling scheme were estimated using relations that have been presented in previous works concerning the development and application of the inferential approach (Baldocchi *et al*., 1987; Wesely, 1989; Walmsley and Wesely, 1996). These relations consider a number of factors related to: (1) the climatological season during which deposition is occurring, (2) the chemical nature of the

depositing species (diffusivity and reactivity), and (3) the type of vegetation to which deposition is occurring. For the work performed in this research effort, the ecosystems studied were considered to be "Mid-summer deciduous forest" for the Pellston Hardwood forest and Clarksville Apple Canopy studies and "Autumn, unharvested land" for the Clarksville Soybean study.

A number of plant species-specific parameters must be provided to the model for use in modeling the plants' response to environmental influences (temperature, solar radiation). These parameters are discussed in detail in Baldocchi *et al*. (1987). For now, the values used in this work are presented in the Table below. The value of r_s *(min)* represents the minimum stomatal resistance, *I* is a radiation parameter, *Topt* is the optimum temperature for the conductance of water vapor through the stomata, *Tmax* and *Tmin* are the maximum and minimum temperatures for stomatal closure.

Plant-specific modeling parameters used during dry-deposition model exercise.

Species	r_s *(min)* *[s/m]*	*I* *(W/m2)*	*Topt* *(ºC)*	*Tmax* *(ºC)*	*Tmin* *(ºC)*
Maple	100	50	25	45	5
Beech	100	50	25	40	5
Apple	100	50	25	45	5(1)
Soybean	35	50	25	45	10

(1) Value estimated based upon Cohen and Naor (2002).

While the reader is directed to previously mentioned works for a detailed description of the model equations and relations used to calculate R_a, R_b and R_c, an

overview of the assumptions required for the model's use in this study are presented below.

Boundary Layer Resistance, R_b

The boundary layer resistance is associated with the transfer of the species in question through the quasi-laminar (non-turbulent) layer of air close to the natural surface and has been shown to be strongly influenced by the diffusivity of the species being transferred (Hicks *et al.*, 1987). Within the model, the "per leaf" boundary layer resistance is determined using the following relation:

$$r_b = \frac{2}{ku_*}\left(\frac{Dv}{Dc}\right)^{\frac{2}{3}} \tag{2}$$

where k is the von Karman constant (0.4), u_* is the friction velocity (m/s), Dv is the diffusivity of water vapor and Dc is the diffusivity of the depositing species. The friction velocity is calculated within the model using a bulk relation based upon the standard meteorological measurements (wind speed and standard deviation of the wind direction). Considerable uncertainty exists regarding the accepted values for the diffusivities of both Hg(0) and RGM. Two values for the diffusivity of Hg(0) have been suggested in the literature: D_{Hg}=0.15 cm^2/s (Browne and Fang, 1978) and D_{Hg}=0.12 cm^2/s (Massman, 1999)). The latter estimate was derived using the Chapman-Enskog approach for the diffusion of Hg(0) through air. The more recent value of D_{Hg}=0.12 cm^2/s was chosen for use in this modeling study based upon sensitivity analysis was performed prior to the performance of modeling runs.

While some uncertainty still exists, it is generally believed that RGM consists primarily of gaseous $HgCl_2$. To our knowledge, extensive studies of the diffusivity of $HgCl_2$.have not been performed and thus values for D_{HgCl2} have not been reported in peer-reviewed literature. For this reason, we followed the methodology of the previous work by using the Chapman-Enskog approach to calculate the molecular diffusivity for gaseous $HgCl_2$ in air. These calculations resulted in an estimated value of D_{HgCl2} = 0.09 cm^2/s.

Canopy Resistance, R_c

The canopy resistance is computed within the model using the following expression:

$$\frac{1}{R_C} = \left[\frac{1}{(R_S + R_M)} + \frac{1}{R_{CUT}} + \frac{1}{R_{SOIL}} \right] \tag{3}$$

where R_S is the resistance to uptake by through the leaf stomata, R_M is the resistance to uptake by the mesophyll surfaces within the leaves, R_{CUT} is the resistance to uptake at the waxy cuticular surface of the leaves, and R_{SOIL} is the resistance to uptake by the underlying soil or water surface. The values for these resistances were computed from the general relations presented in the aforementioned literature. These relations typically incorporate measures of both the solubility and chemical reactivity of the depositing species.

The solubility is considered through the use of species-specific "effective" Henry's law coefficients (H^*), which take into account the effects of acid-base equilibria at a pH of 7. While it is believed that acid-base equilibria impact the uptake of RGM in

cloud droplets, we were not able to find that acid-base equilibria impact the uptake of either Hg(0) or RGM within the leaves. As a result, we modified these relations to use only the standard Henry's Law Coefficient (*H*) for these mercury species. The values for *H* used for this modeling study were 0.11 M atm^{-1} and 1.4 x 10^6 M atm^{-1} for Hg(0) and RGM, respectively (Lin and Pehkonen, 1999).

The "reactivity factor", fo, accounts for the likelihood that a given species will be involved in the oxidation of S(IV) to S(VI) and thus be incorporated into the plant, rather than being re-emitted. The value of this factor ranges from 0 (unreactive) to 0.1 (somewhat reactive) to 1.0 (highly reactive). Hg(0) does not will not participate in the oxidation of S(IV), which would suggest a value of fo=0 would be appropriate. However, as discussed earlier, measurement studies have suggested that there is considerable uptake of Hg(0) via foliage. As a non-polar species, Hg(0) should be able to pass through the non-polar "lipid bilayer" which makes up the outer cell wall of mesophyll tissue. Once inside the mesophyll cell, Hg(0) could be oxidized to Hg^{+2} by other species known have aqueous reactions with Hg(0) (e.g., O_3). Once it its ionic form, there are several pathways for mercury to be incorporated into the plant material. Patra and Sharma (2000) note that mercury may replace the central atom in mesophyll cell chlorophyll, magnesium, thus preventing photosynthetic light harvesting and resulting in a breakdown of photosynthesis. For this reason, we chose to assign a value of fo=0.1 to Hg(0) reactivity for use in the calculation of the model resistances. Due to its high reactivity, a value fo=1.0 was used in calculations of resistance of uptake by RGM.

The canopy stomatal resistance, R_S, is believed to be the path of least resistance for most trace gas species assuming that the canopy is dry and fully transpiring

(Baldocchi *et al*., 1987). The inferential model computes this resistance using a relationship developed to describe the plant-specific stomatal resistance to water vapor transport. In its fullest form, the relation considers the expected maximum stomatal conductance of water vapor (at minimum stomatal resistance) and the effect of a number of potential modifying factors: incident photosynthetically active radiation (PAR), leaf temperature stress, leaf water potential and water vapor pressure deficit between the inner cellular spaces within the leaf and the ambient atmosphere. These modifying factors take on values ranging from 0 to 1, depending on the extent to which this factor limits the stomatal conductance of water vapor. For this modeling effort, only the effects of PAR and leaf temperature stress (with ambient temperature as a surrogate) were considered, using the relation:

$$g_S = g(PAR) \cdot g(T) \cdot \left(\frac{D_{Hg}}{D_V} \right) \tag{4}$$

where g_S is the stomatal conductance for the leaf, g (PAR) is the response of the stomatal conductance to incident PAR and g(T) is the modifying influence of temperature. The final multiplicative term accounts for differences in the diffusivities of water vapor and the depositing chemical species.

The response of the stomatal conductance to PAR is considered to be the inverse of the stomatal resistance to incident PAR. This latter quantity is described using the following relation:

$$r_S(PAR) = {}^{1}\!/_{g_S(PAR)} = r_S(\min) + b_S r_S(\min) / PAR \tag{5}$$

where r_S(min) is the minimum stomatal resistance to water vapor transport, b_S is a species specific constant equal to the PAR flux density at twice the minimum stomatal resistance and *PAR* is the PAR flux density. For the plant species studied, the values used for the minimum stomatal resisance were obtained from Meyers *et al.* (1998).

The relation for the temperature modification factor is given by:

$$g(T) = \left[(T - T_{MIN})/(T_{OPT} - T_{MIN})\right] \cdot \left[(T_{MAZ} - T)/(T_{MAZ} - T_{OPT}\right]^{b_T} \tag{6}$$

where T is ambient temperature (degrees centigrade), T_{MIN} and T_{MAX} are the minimum and maximum temperatures at which stomata will be open, T_{OPT} is the optimum temperature and b_T = [(T_{MAX}-T_{OPT})/(T_{MAX}-T_{MIN})]. Again, for the plant species studied, the values used for the minimum stomatal resisance were obtained from Meyers *et al.* (1998).

Due to the high solubility of RGM, the mesophyll resistance to the uptake of RGM is assumed to be zero in this study. In contrast, the relative insolubility of Hg(0) requires that a non-zero value for this resistance be incorporated into the model. Previous work on the uptake of Hg(0) by wheat (Browne and Fang, 1978) and sorghum (Du and Fang, 1982) suggest that the mesophyll resistances to the uptake of Hg(0) by these species are controlled by temperature dependent reactions involving the enyzyme catalase. A series of laboratory based studies were performed by these authors resulting in the development of two temperature-dependent relations for describing this process:

For wheat:

$$r_M = 111.2 \cdot T - 1.9 \tag{7}$$

For sorghum:

$$r_M = 1208.5 e^{-0.109T} \tag{8}$$

where T in each relation is taken to be the ambient temperature in degrees centigrade. While these two relations show good agreement at elevated temperatures (T>25ºC), the relations diverge considerably at lower temperatures. Given that no such relations have been developed for the species studied in our project, we calculated a "compromise" relation by determining the predicted values of r_M over a range of typical temperatures (10 to 40ºC) using Equations (7) and (8), and then determining a "best fit" curve to the combined set of predicted values. This procedure resulted in the following compromise relation:

$$r_M = 443e^{-0.1T} \tag{9}$$

where T is once again the temperature in degrees centigrade.

Prior performing our model exercise, a sensitivity analysis was performed to determine the variability in calculated dry-deposition velocities using a variety of descriptions of the mesophyll resistance (including Equation 9). These results are presented in Figure 2 and were computed using the data form our Clarksville Soybean study, with the individual model runs defined below:

Model Run	**Value of "fo" used in determination of all resistances for Hg (0)**	**Relation used to determine mesophyll resistance**
SOY	0.0	Equation (9)
SOY_1	0.0	Fixed at 9999 (infinite)
SOY_2	0.1	Wesely (1989)
SOY_3	0.1	Equation (9)

The average Hg(0) dry-deposition velocities calculated for the test data set were 0.08 ± 0.06 cm/sec, 0.07 ± 0.04 cm/sec, 0.59 ± 0.67 cm/sec and 0.13 ± 0.06 cm/sec for soy, soy_1, soy_2 and soy_3, respectively. Of the latter two sensitivity runs performed (using fo=0.1), the results from soy_2 are unrealistically high based upon the early results suggested by Lindberg *et al*. (1992). As a result, the relations used in sensitivity run "soy_3" were used for all model results presented in this report.

Surface Layer Hg(0) Flux Measurements

Dynamic Flux Chamber

During the month of June 2002, a limited number of measurements were made of surface flux of Hg(0) over bare soil Clarksville site using a polycarbonate dynamic flux chamber (DFC). The details to this method have been presented in earlier works by the authors (Zhang et al., 2001). In brief, flushing air is drawn by vacuum through the DFC at a constant flow rate. Concentrations of gas-phase mercury are drawn are measured at both the inlet and outlet of the DFC by a Tekran® Model 2537 Mercury Vapor Analyzer. The steady state flux is calculated using the equation:

$$F = \left(C_o - C_i\right) Q / A \tag{10}$$

where F is the mercury emission flux (ng/m^2/hr), C_o and C_i are the outlet and inlet mercury concentrations (ng/m^3), respectively, Q is the flushing flow rate (m^3/hr) and A is the emission area (m^3) covered by the chamber.

Prior to the start of each chamber measurement run, sample line biases (outlet-inlet) were obtained and used in the correction of the collected data. Also, DFC blanks were

obtained by placing the DFC over an inert foil surface in order to assure that the measured fluxes were not significantly different than zero when no mercury flux was present.

Gradient Transport Theory

Thirty-minute average fluxes of Hg(0) mercury were obtained using gradient transport theory, which describes the flux of a given species using the relation:

$$F_C = -K_Z \frac{\Delta C}{\Delta Z} \tag{11}$$

where F_C is the flux of some quantity, C, K_Z is the vertical eddy-transfer coefficient and $\Delta C/\Delta Z$ is the time-averaged vertical gradient of C. The vertical eddy-transfer coefficient can be obtained using the following relation and Monin-Obukhov similarity theory (Arya, 1999):

$$K_H = \frac{k(z-d)u_*}{\phi_H} \tag{12}$$

where k is the von Karmon constant (0.4), z is the level of the measurement, u_* is the friction velocity, ϕ_H is the similarity function for the dimensionless potential temperature gradient in the surface layer, and d is the displacement height (a measure of the effective height of the canopy). The empirical relation, ϕ_H , is based upon data collected during the 1968 Kansas Field Program (Businger *et al*., 1971). This relation accounts for the effects of stability on the resulting eddy-transfer coefficient. Using the assumption that all scalar quantities are mixed in a similar fashion within the surface layer, K_H can be used to

compute the flux of other passive scalar species such as water vapor or, in our case, Hg(0) (Businger, 1986).

The valid use of gradient transport theory requires that: (a) the observed surface flux be in equilibrium with the observed surface gradient of the species of interest and (b) the atmospheric turbulence field reaching the sensors is horizontally homogeneous and stationary (i.e., statistical properties do not change) over the period that is averaged (in our case, 30 minutes). These conditions can typically be achieved if the turbulent air being sampled has traveled for an adequate upwind distance (or fetch) over which the underlying surface characteristics do not change. As a rule of thumb, this distance can be approximately 100 times the measurement height. During our field measurements at the MSU CHES, the surface wind directions were quite variable and there were times during which the over-canopy fetch was below the minimum value required for the existence of horizontally homogeneous and stationary flow at our sensor. For this reason, the results of this part of our study should be viewed with caution and when speaking in quantitative terms.

Statistical Analysis

Where performed within this report, statistical computations and tests were performed using the SPSS Statistical Software Package, V11.0.1 (Chicago, Illinois).

3. PRESENTATION AND DISCUSSION OF RESULTS

Pellston, Michigan Intensive (June 2001) – Hardwood Forest Canopy

Meteorological Summary

Surface weather maps for Pellston and Clarksville measurement intensives may be found in Appendix A. A quiescent synoptic meteorological pattern persisted over the Great Lakes during much of the measurement period (06 to 16 June 2001). At the start of the period, a large area of high-pressure was located across North Central, while a near stationary front was stretched from the Central Plains to the Mid Atlantic states. This resulted in generally northerly winds during the first few days of the study. The area of high pressure gradually pushed southward toward the Ohio Valley, with isolated showers developing on 09 June, with 2.9 mm of rain reported at the Pellston Airport (within a few miles of the measurement site). Winds were variable during this time, with a primarily southerly flow present. By 10 June, a weak low- pressure system began to form in the Northern Plains. This system moved through the area late on 10 June resulting in scattered light rain (Total Rainfall: 8.9 mm). During the period 11-12, a second low-pressure system moved across the Great Lakes, resulting in a varying wind flow pattern and scattered light rain on 12 June. By 13 June, a large area of low-pressure was developing across the Central Plains. As this low-pressure area strengthened and moved through the Western Great Lakes and into Canada, strong southerly winds developed across the Great Lakes, resulting in warmer and more humid conditions across the region. On 15 June, a strong cold front associated with this low-pressure moved through the area resulting in scattered light rain and thunderstorms (Total Rainfall: 18.8mm). Wind speeds through the measurement period ranged from calm to five m/sec.

Ambient Chemical Measurements

The average PM2.5 mass concentration during the study period was 11.8 ± 10 $\mu g/m^3$. Relatively low PM2.5 mass concentrations (< 10 $\mu g/m^3$) were observed at the site during the first six days of the measurement intensive (Figure 3) during which time the wind-flow during was variable and thus persistent transport from urban/industrialized areas was not observed. Following this period, a large area of high-pressure moved from the Great Lakes to the Atlantic Coast, resulting in a sustained southerly flow pattern during 12-15 June. This flow pattern resulted in elevated levels of PM2.5 at our measurement site, with a peak average concentration observed for the nighttime period of 14-15 June (~45 $\mu g/m^3$). The broadness of this peak in PM2.5 mass concentrations suggests that the site was impacted by a broad area of regional urban/industrial sources, as opposed to a single source. This trend is mirrored in Figure 4, which presents the concentrations of ozone and carbon monoxide that were observed at the site during this same period.

Ambient levels of PM2.5 mercury and Total Particulate Mercury (TPM) during the measurement period are presented in Figure 5, with average concentrations of 5.8 ± 4.8 pg/m^3 and 10.5 ± 5.0 pg/m^3, respectively, observed during the measurement period. Overall, the PM2.5 (fine) fraction contributed to approximately 50% of the TPM. The correlation between the trends in PM2.5 mercury and TPM are significant at the P=.01 level. The overall trends in particulate mercury are not as distinct as those observed for overall PM2.5 mass concentrations, however, visual evidence suggests that there was some increase in both PM2.5 mercury and TPM during the period of 12-15 June, as well, when four of the highest six PM2.5 mercury and TPM concentrations were observed. It

is interesting to note that the highest reported values of PM2.5 mercury and TPM were observed during the day on 06 June, when PM2.5 mass concentrations did not see a simultaneous peak. A 24-hour back trajectory showing the transport history of the air arriving at our site on 06 June (Figure 6) suggests that the air likely had passed over several mercury sources located along the north shoreline of the North Channel of Lake Huron (Environment Canada, 2003). Thus, while the overall PM2.5 mass concentrations were not exceptionally high for that sample period, the relatively short distance between these potential sources and our measurement site resulted in elevated levels of PM2.5 mercury and TPM.

Reactive gaseous mercury (RGM) concentrations are presented in Figure 7. The study average concentration was 14.1 ± 15.3 ng/m^2/period. Two peaks in RGM concentrations are observed. The first broad peak in RGM concentrations occurs during the period of 06 to 08 June. Again, this peak in mercury concentrations may be associated with wind-flow from several industrial source areas along the northern shores of Lake Huron that have reported emissions of mercury. However, given that a similar extended trend was not observed in the PM2.5 mercury and TPM concentrations, an alternative explanation may be linked to the in-situ production of RGM within the forest canopy. This suggests the possibility of either the formation of methylmercury on the surface of canopy leaves and/or deposition of methylmercury on canopy foliage following formation within forest soils (Grigal 2003). A more detailed study on the speciation of mercury within the various forest compartments would be needed to verify this hypothesis with respect to our study. A second broad peak in concentrations is noted during the latter half of the study and may be associated with the southerly transport

pattern of during 12-15 June. Due to its high reactivity, RGM will deposit within 100 km of its source. The fact that we sea a broad peak associated with the southerly transport flow suggests that possibility the formation of RGM via oxidation of Hg(0), during transport from the southern Great Lakes to our site.

A second trend in the observed RGM concentrations is that concentrations are typically lower during periods for which the canopy is wetted by either rain or dew. This is particularly true during the latter part of our measurement period, when a number of nighttime periods experienced considerable dew upon the canopy foliage. Average daytime RGM concentrations were 18.9 ± 17.4 pg/m^3, while average nighttime concentrations were 8.2 ± 10.5 pg/m^3. These observations are consistent with those of Malcolm and Keeler (2002), who found that mercury concentrations within dew were related to ambient RGM concentrations. Additionally, these authors used continuous measurements of RGM to show that RGM concentrations decreased with the onset of dew.

Dry-Deposition Measurements

Measurements of the dry-deposition of mercury to the forest, based upon surrogate water surface measurements, are presented in Figure 8. Again, it is important to note that due to the small solubility of Hg(0), these measurements primarily represent the dry-deposition of RGM and TPM to the surrogate water surfaces. The average mercury dry-deposition for daytime and nighttime periods was estimated to be 21.6 ± 10.8 ng/m^2/period and 16.8 ± 7.3 ng/m^2/period, respectively. Despite some distinct daytime/nighttime differences in the ambient chemical data (i.e., RGM), such consistent differences are not evident in the observed dry-deposition estimates. This lack of a

distinct daytime/nighttime trend in the measured mercury dry-deposition underscores the important fact that a number of factors influence the resulting dry-deposition to the forest canopy: Hg(0), RGM, Hg(p) concentrations, as well as the meteorological conditions and plant physiological processes which control the nature of the air-surface exchange environment above (and within) the forest canopy. These latter processes are addressed in the modeling section of this Final Report.

Clarksville, Michigan Intensive (August 2002) – Apple Orchard Canopy

Meteorological Summary

Another quiet synoptic weather pattern was found across the Great Lakes during the start of the second measurement period (20 to 30 August 2002). An area of high-pressure was centered over the Lower Peninsula of Michigan, providing mild temperatures and light winds. As the area of high-pressure moved eastward, an area of low-pressure developed in the Northern Plains resulting in warm and humid southerly flow across the area on 21 June. The low-pressure area and its associated fronts moved across the Great Lakes on 22 June, producing significant rainfall at our site (Total Rainfall: 23.9 mm). A few isolated showers lingered into the morning hours of 23 June (Total rainfall: 0.5 mm). Winds behind this system were northerly with speeds from 0 to 3 m/sec. A weak area of high pressure moved into the Great Lakes after the passage of the storm, resulting in relatively quite conditions with partly cloudy skies and northwest to northeasterly winds. On 26 August, a cold front moved across the Great Lakes, followed by the approach of a large area of high-pressure from Canada. The area of high-pressure lingered across the Great Lakes for several days, while skies remained clear to partly cloudy, with northeasterly winds for the balance of the study period.

Ambient Chemical Measurements

The temporal variation in PM2.5 and TPM mass concentrations is presented in Figure 9. The study average PM2.5 and TPM mass concentrations were 10.2 ± 6.3 $\mu g/m^3$ and 19.0 ± 7.4 $\mu g/m^3$, respectively. The fine fraction (PM2.5) represented 52 percent of the TPM, with the two PM fractions being highly correlated ($r = 0.67$ at $p=0.01$). During the initial days of the study, a large area of high-pressure moved through the Great Lakes into the New England states resulting in southerly flow across south Michigan. PM levels slowly increased during the period from 20-23 June, with the lone exception being during the daytime hours of 22 August. On this day, a cold front moved through the area resulting in 23.9 mm of rainfall. This precipitation likely scavenged a considerable amount of PM from the atmosphere resulting in the relatively low observed PM levels for this sample period. As another area of high-pressure moved into the Great Lakes behind the cold front, initial easterly winds lead to a peak in PM concentrations, likely from sources in southeast lower Michigan. In the days that followed, 24-26 August, northerly flow conditions resulted in transport from a region with relatively few PM sources compared to the southern Great Lakes. As a result, PM levels were fairly low and constant. Another area of high-pressure moved into the Great Lakes on 27 August, resulting in an easterly flow patter for the balance of the study period. Under these easterly flow conditions, PM levels gradually increased as this flow regime likely allowed sources in southeast Michigan to impact our site.

The temporal variation in PM2.5 mercury and TPM mercury concentrations is presented in Figure 10. The average PM2.5 mercury and TPM mercury concentrations during this study period were 5.0 ± 2.6 pg/m^3 and 10.8 ± 5.0 pg/m^3, respectively. The

fine fraction (PM2.5) represented 44 percent of the TPM, with the two PM fractions being highly correlated ($r = 0.89$ at $p=0.01$). The highest observed concentrations occurred at the start of the study, when winds were east to southeasterly. As winds gradually become more southerly on 21-22 August, the observed PM2.5 mercury and TPM mercury concentrations decreased. The lowest concentrations for both fractions were observed on 23 August, the day in which significant rains fell across the area. Following the end of the precipitation, mercury PM levels increased once again with the highest levels occurring under easterly flow conditions. This mirrored the overall PM mass concentration trend and thus was likely a result of the transported air having passed through the industrial areas of southeast Michigan.

The temporal variation in RGM concentrations is presented in Figure 11. Overall, RGM levels were quite low during this period with a period average RGM concentration of 3.9 ± 2.7 pg/m^3. Despite the low absolute concentrations, the concentration trends were consistent with expectations. At the start of the period, we experienced a number of problems with our denuder measurement system, resulting in a loss of data from 21-22 August. One of the highest observed concentrations occurred during the daytime of 23 August, when wind flow was from the northwest, potentially resulting in the impact from local sources. Other periods with relatively high observed RGM concentrations were the daytime periods on 26, 28 and 29 August, when wind flow was from the east on each of these days. This flow could have potentially resulted in impact form mercury sources in southeast Michigan. Inspection of Figure 11 also shows once again that low concentrations occurred for periods in which the canopy was reported to be wet. It is interesting to note that while some light dew was observed on the night of 27-28 August,

the surface winds remained significant through much of the night (>2 m/sec), resulting in a late dew formation that night. As a result, RGM levels were reported to be higher that night relative to other clear nights when very light winds and early dew were reported.

Dry-Deposition Measurements

The temporal variation in mercury dry-deposition is presented in Figure 12. Overall, the measured dry-deposition values were quite low, with an estimated daytime and nighttime mercury dry-deposition 4.6 ± 2.5 ng/m^2/period and 6.6 ± 5.3 ng/m^2/period, respectively. These relatively low values (compared with those obtained in the Pellston study) are consistent with the relatively low ambient RGM concentrations observed during this study. It is interesting to note that unlike the Pellston study, the average nighttime deposition was greater than that observed during the daytime hours. This trend is likely related, in part, to the fact that some of the highest particulate mercury concentrations were also observed during the nighttime periods. Samples during the period 21-22 August were contaminated due to precipitation falling into the water collection plates.

Clarksville, Michigan Intensive (September 2002) – Soybean Canopy

Meteorological Summary

The final measurement period (10 to 19 September 2002) began with a cold front moving across the measurement site on 10 September resulting in partly cloudy skies across the area. The front moved rapidly to the south and east, with a large area of Canadian high-pressure moving into the Central Plains in its wake. As the area of high-pressure pushed to the south and east, winds across the Great Lakes shifted from the northwest to the southwest under partly cloudy skies. High-pressure persisted across the

Great Lakes through 14 September, westerly winds observed across the area. The approach of a cold front late on 14 September resulted in more southerly winds, which gave way to a northerly wind flow as the cold front moved across the Great Lakes during the morning of 15 September. Considerable cloudiness was associated with the front, but no precipitation was reported at our site. An area of high-pressure moved into the Great Lakes on 16 September and persisted through the day on 17 September. With the area of high-pressure moving eastward, and a low-pressure system developing in the Central Plains States, southerly winds developed for the balance of the study bring warmer and more humid air into the Great Lakes. As a result of the warm and humid conditions, scattered shows and thunderstorms were observed at the measurement site on both 18 September (Total rainfall: 2.5 mm) and 19 September (Total rainfall: 8.6 mm).

Ambient Chemical Measurements

The temporal variation in the observed PM2.5 and TPM mass concentrations is presented in Figure 13. The study average PM2.5 and TPM mass concentrations were 10.9 ± 6.3 μg/m^3 and 23.9 ± 13.9 μg/m^3, respectively. For the period, PM2.5 accounted was positively correlated with TPM ($r = 0.63$, $p=.01$) and, on average, accounted for 58 percent of the total particulate mass. Two broad peaks in PM2.5 and TPM mass concentrations can be seen during the periods 13-14 September and 16-18 September. At the start of the period, winds were from the northwest, leading to relatively load PM values. The first peak in PM was associated with southwesterly winds that developed ahead of an approaching cold front. Figure 16 presents the 24 hour back-trajectory/history of the airmass that moved across the site during the afternoon of 14 September. This suggests that the likely source of the elevated PM observed at our site

had its origins in the southern Lake Michigan Basin. In the 24-36 hours following the frontal passage, surface winds became north to northeasterly, leading to a sharp decrease in PM concentrations. As high-pressure moved through the Great Lakes and into the New England states, southwesterly flow redeveloped across the Great Lakes leading to a second peak in the observed PM concentrations at the site. PM levels decreased during the final 24-36 hours with the onset of scattered showers and thunderstorms.

The temporal variation of PM2.5 and TPM mercury concentrations is presented in Figure 14. The study average PM2.5 and TPM mercury concentrations were 7.1 ± 4.4 pg/m^3 and 11.3 ± 7.8 pg/m^3, respectively. For the period, PM2.5 accounted was highly positively correlated with TPM ($r = 0.91$, $p=.01$) and, on average, accounted for 63 percent of the total particulate mass. It is obvious from inspecting this figure that the general trends in PM mercury were very similar to those observed in overall PM mass. There are slight differences of 12-24 hours in the maximum values associated with each of the two broad peaks, but this is not to be unexpected. While the two broad peaks in PM mass and PM mercury were both observed during sustained southwesterly flow, slight variations in wind flow would likely result in our site being impacted from varying types of PM and mercury sources, leading to differences in the PM mass to mercury relations.

Once again, temporal variations in the observed RGM concentrations (Figure 15) were closely linked to both the impacting source region and the occurrence of dew and rain wetted canopy conditions. The lowest concentrations were observed on those nights when the canopy was wet. In contrast, on the night of 14 September, southwesterly flow and the dry canopy conditions resulted in the highest observed nighttime RGM

concentrations. The peak daytime concentrations were associated with the same southwesterly flow pattern that lead to elevated PM mass and mercury concentrations.

Dry-Deposition Measurements

The general trends observed in the mercury dry-deposition measurements for this period mirrored those of the observed ambient RGM and PM mercury concentrations (Figure17). Namely, the highest observed mercury dry-deposition occurred during periods of southwesterly flow, with likely transport from the southern Lake Michigan Basin. Overall, the average daytime and nighttime mercury dry-deposition values were quite similar, being 8.1 ± 7.3 ng/m2 and 6.0 ± 4.7 ng/m2, respectively. The highest observed dry-deposition occurred in the relatively turbulent environment in advance of an approaching cold front. The subsequent nighttime sample, which included the passage of the front itself, also likely had a very turbulent environment that would have enhanced both particle and gas deposition to our surrogate water surfaces. It should be noted that overall, the mercury dry-deposition observed during this portion of the study was greater than that observed during our measurements above within the apple orchard. The reasons for these differences were likely related to both differences in observed ambient chemical conditions (higher PM and RGM concentrations during the latter measurement period) and differences in plant canopy structure and physiology.

Dry-Deposition Modeling

Following the conclusion of the measurement phase of this project, the NOAA Inferential Model (Hicks *et al*., 1986) was used to predict the dry-deposition of mercury to each of the three ecosystems studies: mixed-hardwood forest, apple canopy and soybean canopy. The NOAA Inferential Model was developed for use with species that

have a unidirectional flux (i.e., deposition). As a result, in its current configuration the model is valid for use with both RGM and particulate mercury. However, the flux of Hg(0) has been shown to be bi-directional, with the direction of flux varying based upon soil Hg concentration, ambient Hg(0) concentrations and other environmental and plant physiological conditions. Due to the bi-directional nature of this flux, it is not currently possible to verify the unidirectional component of the flux (i.e., downward) that could be predicted by the sum of the ambient Hg(0) concentrations and the modeled dry-deposition velocities. In fact, as noted earlier, preliminary test during the development of our surrogate water surfaces samplers showed that Hg(0) was not taken up by the surfaces due to its relative insolubility. As a result, while the model dry-deposition velocities obtained for Hg(0) will be presented and discussed, the comparison of model vs. measured mercury dry-deposition will be include only that dry-deposition associated with RGM and particulate Hg components of the downward flux.

As noted earlier, given the distinct differences in atmospheric stability during the daytime and nighttime periods, the following data has been separated into daytime and nighttime periods. The periods of transition (day to night, night to day) are typically characterized by rapidly changing conditions. Under such transitional conditions, many of the assumptions used in the development of the equations used in the model are not valid. Therefore, data associated with these transition periods (when the net radiation changes sign) were removed before statistical analyses were performed.

Figures 18-20 present the temporal variation of modeled mercury dry-deposition velocities for each of the above three studies. It should be noted that when precipitation was reported during a given 30-minute period, that data was removed from the dataset

(both in the figure presented and in the determination of descriptive statistics). As can be seen, a general diurnal pattern is evident for each species. This diurnal nature is driven to a large extent by the effect of atmospheric stability. As noted, during the nighttime hours, the surface radiates thermal energy toward space, cools the surface and the adjacent layer of the atmosphere and thus works to stabilize the lower atmosphere. Under these stable conditions, turbulence is greatly suppressed and the aerodynamic resistance to deposition increases significant. As a result of this suppression of turbulence (and thus turbulent transport of the mercury species to the surface), the resulting dry-deposition velocities decrease sharply after sunset. For rough canopy surfaces, such as those typically associate with trees (forests and/or orchards), mechanically generated turbulence (due to wind sheer above the surface of the vegetation) can maintain a higher level of nighttime turbulence than that experienced over the "smoother" soybean canopy. As a result, while the RGM dry-deposition velocity has a strong diurnal pattern over the soybean canopy, the rougher surfaces over the mixed hardwood forest and apple orchard result in stronger turbulence over the canopy at night, thus reducing the extremes in the otherwise strong diurnal pattern. This is especially true for the results associated with the apple orchard, which has a very complex physical structure as described earlier.

The resulting average speciated mercury dry-deposition velocities are presented below in Table I. For all three studies (and thus ecosystems), the estimated dry-deposition velocity for RGM [or Hg(+2)] was consistently the largest, with the modeled dry-deposition velocities for Hg(0) and Hg(part) often an order of magnitude lower than that of RGM. This was expected given the relatively high solubility of RGM and its

tendency to be highly reactive, especially with respect to its affinity for organic matter of soil and/or vegetation (Patra and Sharma, 2000; Grigal 2003). While, the values obtained for RGM and Hg(part) are consistent with those suggested by other researchers (e.g., Shannon and Voldner, 1995; USEPA, 1997), the values obtained in this modeling exercise for Hg(0), however, are much greater than those typically suggested for Hg(0). The reason for the higher estimated Hg(0) dry-deposition velocities obtained in our study is related to our assumption that Hg (0) would be slightly reactive within the leaf, as opposed to have a very low reactivity based upon the NOAA Inferential model's typical parameterization scheme. We feel that the model results for Hg(0) dry-deposition velocity are within reason, given that several observational studies have suggested that ambient Hg(0) uptake by vegetation foliage is likely an important and significant process (Lindberg *et al*., 1992; Hanson *et al*., 1995; Leonard *et al*., 1998; Grigal 2003). Several species typically found in leaf water (e.g., O_3) have known aqueous reactions with Hg (0) (Lin and Pehkonen, 1999) and thus could serve to oxidize Hg(0) to Hg(+2), resulting in a higher likelihood of being more permanently incorporated in the leaf structure. The modeled Hg(0) dry-deposition velocities obtained in this study represent the higher end of estimates for Hg(0) uptake by deciduous trees made by Lindberg *et al* (1992) and Ericksen *et al*. (2003).

Table I. Model Derived Dry-Deposition Velocities (cm/sec)

	Dry-Deposition Velocities (cm/sec)		
	Hg (0)	**Hg (+2)**	**Hg (part)**
Forest Canopy[1]	0.17 ± 0.07 (D) 0.06 ± 0.02 (N)	1.96 ± 0.57 (D) 1.05 ± 0.91 (N)	0.38 ± 0.24 (D) 0.05 ± 0.04 (N)
Apple Canopy[2]	0.19 ± 0.07 (D) 0.07 ± 0.02 (N)	1.06 ± 0.36 (D) 0.82 ± 0.49 (N)	0.16 ± 0.10 (D) 0.03 ± 0.02 (N)
Soybean Canopy[2]	0.18 ± 0.05 (D) 0.09 ± 0.03 (N)	1.56 ± 0.51 (D) 0.75 ± 0.58 (N)	0.21 ± 0.12 (D) 0.03 ± 0.02 (N)

[1] Pellston, Michigan, [2] Clarksville, Michigan, (D) =Daytime and (N) = Nighttime

For each day, the daytime and nighttime average speciated mercury dry-deposition velocities were combined with their respective measured ambient concentrations in order to obtain estimates of the dry-deposition of speciated mercury to the surrogate water surfaces (and thus the respective canopies). The results from these calculations are presented in Table II. As can be seen, the average modeled dry-deposition fluxes are approximately 50 percent of the measured values. As an example of results, Figure 21 presents time series comparison of the daily modeled versus measured mercury dry-deposition. Overall, the model is able to track the general trends of the measured mercury dry-deposition. However, the tendency for the modeled estimates of mercury dry-deposition to be systematically lower than the measured levels stems from the models under-prediction of the mercury dry-depositional flux at night. In fact, for every period modeled, the nighttime modeled flux was less than its corresponding measured flux.

Table II. Comparison of Modeled versus Measured Dry-Deposition Fluxes for RGM and Hg(part)

	Modeled (ng/m2/pd)	Measured (ng/m2/pd)
Forest Canopy[1]	9.3 ± 10.3	18.9 ± 10.0
Apple Canopy[2]	1.9 ± 1.6	5.6 ± 4.4
Soybean Canopy[2]	4.5 ± 4.6	7.1 ± 6.1

[1] Pellston, Michigan, [2] Clarksville, Michigan

There are a number of possible factors that may contribute to such a systematic bias in modeled estimates of mercury dry-deposition at night. One of the most likely possibilities is related to the manner in which the model characterizes the impact of atmospheric stability on the turbulent exchange over each of the canopies studied. In short, the popularity of this model for use in dry-deposition studies and monitoring programs stems from the model's use of simplified bulk relationships to describe turbulent exchange processes. These relationships require time-averaged meteorological quantities as input and thus the researcher can use rather inexpensive instrumentation to monitor the meteorological quantities necessary for input into the model. However, the mathematical description is turbulent exchange and quite complex. However, the desire/need to use easily measured meteorological quantities resulted in the use of a number of simplifying assumptions that may not adequately describe the impact of varying stability on the turbulent exchange process at night. In the last ten years, the cost of a number of fast-response instruments capable of making direct measurements of turbulent exchange quantities (such as friction velocity) have decreased considerably. With such instruments now more accessible, it may now be possible to replace some of

the parameterized variables with their directly measured counterparts, thus improving overall model performance.

A second potential reason for the model under-prediction of the mercury dry-depositional flux at night may be related to the manner in which the model describes the canopy response to the onset of nightfall. In short, if the canopy remains dry after nightfall, the model sets both the stomatal and mesophyll resistance to large constant values for the nighttime period. However, the existence of nocturnal respiration by some plants indicates that the stomata do not completely close at night and thus uptake may continue (though to a much lesser degree) at night. As a result, the model's assignment of a large value to the nocturnal stomatal and mesophyll resistance may lead to the observed under-prediction in nighttime dry-deposition. Improvement in the overall description of time-varying plant responses to changing environmental conditions (such the response of leaf stomata to varying air-leaf temperature differences) is greatly needed and will be one of the subjects of our future work.

Foliage Uptake of Ambient Mercury

It is generally accepted that there are three major ways in which plant foliage acquire mercury: (1) adsorption of Hg(+2) and/or Hg(0) to onto leaf surfaces [the latter of which requires oxidation of Hg(0) to avoid subsequent loss of Hg(0) back to the atmosphere via volatilization], (2) adsorption of particulate mercury onto leaf surfaces, or (3) uptake of Hg(0) and/or Hg(+2) through the stomata and into the leaf. Iverfeldt (1991) and others have shown that mercury deposited onto leaves via the first two processes may be washed off the leaf surface during precipitation events. These conclusions have been drawn from simultaneous measurements of rainfall and throughfall (rainfall that first

intercepts that plant canopy before falling to the ground) that have shown an increase in the concentration of throughfall relative to the rainfall alone (e.g., Rea *et al*., 1996).

Rea *et al*. (1996) among others have also shown that litterfall, the dropping of senescent leaves, is another important depositional pathway by which atmospheric mercury is delivered to the soil. While some of this "leaf-bound" mercury is a result of the aforementioned adsorption to the leaf surface, a number of studies have suggested that uptake of atmospheric mercury is the major source of mercury to plant foliage (e.g., Fleck *et al*., 1999; Erickson *et al*. 2003). While a number of studies have investigated the uptake of atmospheric mercury by deciduous and coniferous trees, few studies have looked at the uptake of atmospheric mercury in cash crops such as the apple orchard and soybean canopies studied as part of this research effort. For this reason, we collected foliage samples from throughout the growing season for each of the ecosystems studied as part of this research effort. The methodology used in this part of our research was described earlier in this report. Figures 22 and 23 present the result of the foliage sample collection at our Pellston (2001) and Clarksville (2002) measurement sites, respectively.

As can be seen, each of the species sampled showed a marked increase in the mercury content of the leaves through the course of the growing season. In 2001, leaves were collected from a stand of Maple and Birch trees once in late June and once in mid-September. The total mercury content of Maple leaves (expressed on a per dry weight basis) increased from an average of 25.5 ng/g-dry weight in June 2001 to 50.8 ng/g-dry in September 2001. The total mercury content of Birch leaves increased from an average of 12.5 ng/g-dry weight in June 2001 to 31.8 ng/g-dry in September 2001. These results are consistent with those obtained in a sampling study in another northern hardwood forest

Lake Champlaign, VT by Rea *et al*. (1996). In that study, Rea *et al*. (1996) suggested that leaf mercury (deposited to the forest floor as litterfall) accounted for up to 50 percent of the total mercury deposited to the forest floor.

In 2002, leaves were collected from the apple and soybean canopies at three different times during the growing season. First, each type of vegetation was sampled within two weeks of leaf out and then again once each in the months of August and October. The October samples were actually litterfall samples. The average total mercury content of Apple leaves (expressed on a per dry weight basis) was found to be 4.2 ± 0.4, 4.2 ± 0.4 and 4.2 ± 0.4 ng/g-dry weight during May, August and September 2002, respectively. The average total mercury content of Soybean leaves (expressed on a per dry weight basis) was found to be 6.5 ± 1.7, 10.1 ± 1.8 and 52.0 ± 6.3 ng/g-dry weight during June, August and September 2002, respectively.

Mercury in Soils

A series of soil samples were collected at the Clarksville Horticulture Experiment Station in Clarksville, Michigan in October 2002. Two sets of samples (0 to 2 cm and 10 to 15 cm below surface level) were collected at two locations within each of air-surface exchange study areas (Apple and Soybean canopies). The results of these measurements are presented in Figure 24. The total mercury content of the soils was fairly consistent both with depth and across locations within the Clarksville Horticulture Experiment Station property, ranging from 10-25 ng/g-dry weight, which is well within the range typically assigned to “background” soils: <500 ng/g-dry weight (Schroeder and Munthe, 1998. These concentrations are similar to those measured in the Upper Peninsula (Chippewa and Luce Counties) of Michigan by Zhang et al. (2001), where the total

mercury content of surface soils were found to range from 16 ng/g-dry weight in an open grassy field to 69-98 ng/g-dry weight in forest soils. The relatively higher mercury content found in the forest soils is likely due to the affinity of mercury for binding with reduced sulfur groups associated with organic soil matter (Grigal, 2003). For the sake of further comparison, total mercury soil content for other locations include: ~110 ng/g-dry weight for U.S. agricultural soils (Steinnes, 1990), ~5000 ng/g-dry weight in contaminated soils within the Walker Branch, Tennessee watershed (Lindberg, 1995), 1200 to 14,600 ng/g-dry weight in the Steamboat Springs Geothermal Area of Nevada (Gustin *et al*., 1999), and up to $9x10^6$ ng/g-dry weight within the Almaden Mining District, Spain (Higueras *et al*., 2003).

Surface Layer Fluxes of Hg(0) over Soils

During the period 26-28 June 2002, a short-term study was conducted at the Clarksville Horticulture Experiment Station in an effort to quantify the surface layer fluxes of Hg(0) agricultural soils. The measurements were conducted solely during the daylight periods of the aforementioned dates using the dynamic flux chamber system described earlier. The chamber was placed in a number of locations within the field, some which contained soil only (between row) and some which contained both soil and immature soybean plants (within row). The soybean plants had just broken ground within the past week, with plant heights in the range of 4-6 cm. The measurement chamber used is shown below during one of the "between row" measurement periods. At this particular site, "no tillage" practices were being studied and thus the detritus (i.e., dead plant matter) from the previous growing season can be seen between the rows.

For this period, the average flux of Hg(0) over these soils was measured to be 0.9 ± 0.7 ng/m^2/hr. Using a one-sample T-test, the average of these measured fluxes was found to be statistically different from zero at P=0.01. This result would suggest that during this three day period, the surface soils were acting as a weak source of Hg(0) to the atmosphere during the daylight hours. Nighttime measurements were not performed. It should be noted that there were no apparent differences in the characteristics of the measured fluxes for the between row and within row locations. An example of the temporal variation of the Hg(0) flux over the soil on 27 June 2002 is presented in Figure 25. As can be seen, the Hg(0) flux over the soil exhibits a diel trend, with a peak in emission near the solar maximum. Zhang *et al.* (2001) has shown that Hg(0) fluxes over the soils are positively correlated with the incident solar radiation and with soil temperature. Our results were consistent with these previous findings.

Surface Layer Fluxes of Hg(0) over a Mature Canopy

During both measurement intensives performed at the Clarksville Horticulture Experiment Station, measurements of the air-surface exchange of Hg(0) were made over

the respective plant canopies (Apple and Soybean) using the methodology described earlier in this report. Unfortunately, during our study over the Apple Canopy, we experienced a number of difficulties with the mercury analyzer/gradient system. After lengthy review of the data, it is our opinion that there is enough uncertainty associated with these measurements such that it is not possible to draw scientifically credible conclusions for the Apple Canopy portion of our study. For this reason, we will only present results of our measurements of the air-surface exchange of Hg(0) over the mature Soybean canopy.

Measurements of the surface flux of Hg(0) over the Soybean Canopy at the Clarksville Horticulture Experiment Station were performed during the period of 09 to 19 September 2002. The time variation of the 30-minute average Hg(0) gradient over the canopy is presented in Figure 26. In this figure, it can be seen that there were several nighttime periods for which a significant positive gradient (concentration increasing with height) in Hg(0) was observed over the canopy. These nights were characterized by clear skies, strong radiational cooling (as evidenced by observed negative net-radiation values) and light winds (speeds less than 0.5 m/sec). These micrometeorological conditions resulted in the development of a stable atmospheric surface layer (lowest tens of meters) just above the canopy. Under such stable conditions, atmospheric turbulence would have been reduced and Hg(0) would have been allowed to become slowly depleted from the layer above the canopy via deposition to the surface without being re-supplied from levels further above the canopy. We hypothesize that this depletion was the result of deposition to the surface, given that there no nocturnal reactions that have been proposed that would result in the depletion of Hg(0) in the surface layer. Also, given that Soybeans

are known to have nighttime respiration, this would suggest that the leaf stomata are not completely closed, allowing for the possibility of a small fraction of the depleted Hg(0) to be taken up within the plant itself.

During the daytime hours, the observed gradients of Hg(0) above the soybean canopy were highly variable with no obvious trend of either deposition to, or emission from, the surface (i.e., canopy and soil). We hypothesize that the small magnitude and high variability in the observed daytime Hg(0) gradients was the result of two factors: (1) fairly strong surface winds (~2.5 m/sec) that likely resulted in the effective mixing of Hg(0) near the surface layer and (2) the apparent decrease in air-plant exchange as a result of the visible water stress (as evidence by the wilting of foliage) affecting the canopy during our measurement period. This water-stress can be attributed, in part, to the fact that no rain was observed at the site between 23 August and 18 September (25 days). Under such conditions, one would expect that the leaf stomata would not be opening fully during the day in an effort to retain leaf water during the dry conditions. Additionally, a rapid yellowing of the canopy foliage signaled the onset of canopy senescence during the measurement period. At the start of our measurements over the Soybean canopy, approximately 20-30 percent of the foliage on these plants had turned yellow, signaling that photosynthetic processes (including air-plant exchange of carbon dioxide/water vapor/trace gas species) were slowing down. By the end of our measurements over the Soybean canopy two week later, approximately 60-70 percent of the foliage had yellowed. The reduction in plant photosynthetic activity was evidenced by the reduction in the exchange of carbon dioxide over the canopy during the course of our measurement study. The temporal variable of carbon dioxide exchange over the

canopy during this period is presented in Figure 27. While the low carbon dioxide fluxes observed on the final two days were due in part to significant cloudiness, overall trend of a decrease in carbon dioxide exchange is evident. As a result of this rapid changes in foliage structure and function, one must be very careful about extending the results of our short-term study to the early and middle parts of the growing season, with typically sufficient soil moisture conditions like result in more active air-plant exchange and thus, perhaps, more consistent trends in daytime Hg(0) gradients and fluxes over the canopy.

4. CONCLUSIONS

This research project sought to obtain a better understanding of the air-surface exchange of speciated mercury over three land-use types/ecosystems that are of importance within the State of Michigan, and within the Great Lakes, as a whole. The land-use types/ecosystems studied were: (1) a mixed-hardwood forest in Pellston, MI [June 2001], (2) an apple canopy in Clarksville, MI [August 2002] and (3) a soybean canopy in Clarksville, Michigan [September 2002]. Short-term (~ 14 days) measurement intensives were conducted within each ecosystem. These measurements included: ambient concentrations of the three relevant mercury forms [Hg(0), RGM and Hg(p)], direct measurements of the dry-deposition of mercury to the ecosystem canopies and micrometeorological quantities to assist in the interpretation of the chemical measurement results and for use as input into a single-layer, dry-deposition model used to predict mercury dry-deposition to the canopies studied. Important results from this project are summarized below:

1. We obtained twice-daily measurements of the ambient concentrations of speciated mercury. When viewed in conjunction with other chemical and meteorological data, we will be able to learn more about these other factors on the ambient levels of the

relevant species of mercury. For example, ambient levels of RGM were found to be lowest during periods of light winds and wetted canopies (typically from dew, but also from rain). These results provide evidence of the rapid uptake of RGM during such conditions.

2. We obtained "event-based" measurements of mercury dry-deposition to three vegetation canopies. For the ecosystems studied, the average mercury dry-deposition per period (~12 hour periods) was found to be: 18.9 ± 10.0 ng/m^2 (hardwood forest), 5.6 ± 4.4 ng/m^2 (apple canopy), and 7.1 ± 6.1 ng/m^2 (senescing soybean canopy). It is important to note that the measurement technique employed (surrogate water surface) collects only RGM and Hg (p) due to the relative insolubility of Hg(0), the obtained dry-deposition values should be considered a "lower limit" under growing season conditions.

3. We were able to predict the magnitudes of the dry-deposition of speciated mercury to these ecosystems to within an overall factor of two using a single layer inferential model that was modified for use with speciated mercury. For the three canopy types studied, average daytime/nighttime predicted dry-deposition velocities ranged from: 0.06 to 0.19 cm/sec for Hg(0), 0.03 to 0.38 cm/sec for Hg(p) and 0.75 to 1.96 cm/sec for RGM. When compared with the directly measured dry-deposition, the model was able to predict the trends in daily mercury dry-deposition. However, when viewed by period, nighttime dry-deposition was consistently under-predicted. These model sensitivity tests and overall results suggest that improvement in model performance will require: (1) improvements in the description of nighttime air-surface exchange processes, (2) a narrowing in the uncertainty surrounding the relative resistance of mesosphyllic tissues to the uptake of Hg(0), a means of incorporating the re-emission of Hg(0) dry-deposited to vegetation such that a realistic "net deposition" of Hg(0) could be determined from the model.

4. Measurements of soil mercury content were performed at the apple canopy and soybean canopy study sites within the Clarksville Horticulture Experiment Station. Soil mercury content varied from 10-25 ng/g-dry weight, which is well within the range typically assigned to "background" soils: <500 ng/g-dry weight. These results correlated with the chamber-based soil mercury flux measurements performed at the soybean canopy study site. Performed over a four day period in June 2002, these latter measurements suggested that (on average) these soils were a weak source of Hg(0) to the atmosphere during the daylight hours.

5. Measurements of surface-layer fluxes of Hg(0) over the mature, senescing soybean canopy (September 2002) suggested that Hg(0) was deposited to the canopy at night, with variable directional fluxes during the daytime.

6. Measurements of foliage at the Pellston (maple and birch) and Clarksville (apple and soybean) study sites suggest that each of these canopies experiences considerable uptake of Hg(0) from the ambient atmosphere. It was beyond the scope of this study to determine the extent to which this sequestered mercury is returned to the local soils.

While each of these measurement studies were short-term in nature, combined they have provided us with valuable information on the speciated and total mercury in a number of ecosystem compartments (soil, foliage, air), as well as the magnitudes of the exchanges of mercury between the air and surface under a variety of meteorological and plant physiological conditions. These results will also provide useful information that can be drawn upon in the development of improved description of the air-surface exchange of speciated mercury.

5. ACKNOWLEDGEMENTS

The authors would first like to thank the Michigan Great Lakes Protection Fund for providing the resources to perform this study. We would like to thank the staffs of the University of Michigan Biological Station and the Michigan State University Clarksville Horticulture Experiment Station for the kindness and endless support of our research activities at their respective sites. We would also like to thank the laboratory staff at the University of Michigan for their "behind the scenes" work, as this project would not have been possible without them. Special thanks to Dr. Jeff Andresen for his invaluable guidance on issues concerning agricultural meteorology and crop plant physiology and Dr. Hong Zhang for his assistance with the soil mercury flux measurements. Finally, the authors would like to thank the NOAA Air Resources Laboratory (ARL) for the provision of the HYSPLIT transport and dispersion model and READY website (http://www.arl.noaa.gov/ready.html) used in the preparation of this report.

6. REFERENCES

Arya, S.P. Air Pollution Meteorology and Dispersion **1999**, Oxford University Press, New York, NY.

Baldocchi, D.D., Hicks, B.B., Camara, P. *Atmos. Environ*. **1987**, 21, No. 1, 91-101.

Bishop, K.E., Lee, Y.E., Pettersson, C. and Allard, B. Biogeochemistry 1998, 40, 101-113.

Browne, C.L., Fang, S.C. *Plant Physiol*. **1978**, 61, 430-433.

Businger, J.A., Wyngaard, J.C., Izumi, Y., Bradley, E.F. *J. Atmos. Sci*. **1971**, 28, 181-189.

Businger, J.A. *J. Climate and Applied Meteorology*. **1986**, 25, 1100-1124

Carpi, A., Lindberg, S.E. *Atmospheric Environment* **1998**, 32, No. 5, 873-882.

Chan, H.M., Scheuhammer, A.M., Ferran, A., Loupelle, C., Holloway, J, and Weech, S. *Human and Ecological Risk Assessment* **2003**, 9, 867-883.

Cho, U-H. and Park, J-O. *Plant Science* **2000**, 156, 1-9.

Cohen, S., and Naor, A. *Plant, Cell and Environment* **2002**, 25, 17-28.

Draxler, R.R. and Rolph, G.D., 2003. HYSPLIT (HYbrid Single-Particle Lagrangian Integrated Trajectory) Model access via NOAA ARL READY Website (http://www.arl.noaa.gov/ready/hysplit4.html). NOAA Air Resources Laboratory, Silver Spring, MD.

Du, S.-H., Fang, S.C. *Environ. and Exper. Botony*. **1982**, 22, 4, 437-443.

Ericksen, J.A., Gustin, M.S., Schorran, D.E., Johnson, D.W., Lindberg, S.E., and Coleman, J.S. **2003**, *Atmos. Environ*., 37, 1613-1622.

Environmental Canada **2003**, NPRI On-Line Mapping, http://gis.ec.gc.ca/npri/root/main.

Fitzgerald, W.F., Engstrom, D.R., Mason, R.P., and Nater, E.A. *Environ Sci. and Technol*. **1998**, 32, No. 1, 1-7.

Fleck, J.A., Grigal, D.F. and E.A. Nater *Water, Air and Soil Pollut*. **1999**, 115, 513-523.

Godbold, D.L. *Water Air and Soil Pollut*. **1991**, 56, 823-831.

Grigal, D.F. *Environmental Review* **2002**, 10, 1-39.

Grigal, D.F. *J. Environ. Qual*. **2003**, 32, 393-405.

Gustin, M. S.; Lindberg, S.; Marsik, F.; Casimir, A.; Ebinghaus, R.; Edwards, G.; Hubble-Fitzgerald, C.; Kemo, R.; Kock, H.; Leonard, T.; London, J.; Majewski, M.; Montecinos, C.; Owens, J.; Pilote, M.; Poissant, L.; Rasmussen, P.; Schaedlich, F.;Schneeberger, D.; Schroeder, W.; Sommar, J.; Turner, R.; Vette, A.; Wallschlaeger, D.; Xiao, Z.; Zhang, H. *J. Geophys. Res.* **1999**, *104* (D17), 21,831-21,844.

Hanson, P.J., Lindberg, S.E., Tabberer, T.A., Owens, J.G. and Kim, K-H. **1995**, *Water, Air and Soil Pollut*., 80, 373-382.

Hicks, B.B., D.D. Baldocchi, D.D. Meyers, T.P, Hosker, R.P., Matt, D.R. *Atmos. Environ*. **1987**, 32: 1317-1322.

Higueras, P., Oyarzun, R., Biester, H., Lillo, J., and Lorenzo, S. *J. of Geochem. Exploration* **2003**, 80, 95-104.

Hoyer, M., Burke, J., Keeler, G.J. *Water, Air and Soil Pollut*. **1995**, 80, 199-208.

Iverfeldt, A. **1991**, *Water, Air and Soil Pollut*., 56, 553-564.

Keeler, G.J., Spengler, J.D. and Castillo, R. *Atmos. Environ*. **1991**, 24A, 2915-2923.

Koutrakis, P., Wolfson, J.M., Slater, J.L., Brauer, M, Spengler, J.D., Stevens, R.K. and Stone, C.L. *Environ. Sci. Technol*. **1988**, 22, 1463-1468.

Kozuchowski, J. and Johnson, D.L. **1978**, *Nature*, 274, 468-469.

Landis, M.S. and Keeler. *Environ. Sci. Technol*. **1997**, 31: 2610-2615.

Landis, M.S., Stevens, R.K., Schaedlich, F. and Prestbo, E. **2002**. *Environ. Sci. Technol*., 36, 3000-3009.

Leonard, T.L., Taylor, G.E., Gustin, M.S., Fernandez, G.C.J. *Environmental Toxicology and Chemistry* **1998**, 17, No. 10, 2072-2079.

Lin, C.-J., Pehkonen, S.O. *Atmos. Environ*. **1999**, 33, 2067-2079.

Lindberg, S.E., Meyers, T.P., Taylor, G.E., Turner, R.R., Schroeder, W.H. *Journal of Geophysical Research* **1992**, 97, No. D2, 2519-2528.

Lindberg, S.E., Meyers, T.P., Munthe, J. *Water, Air and Soil Pollution* **1995**, 85, 2265-2270.

Lindberg, S.E., Hanson, P.J., Meyers, T.P., and K.-H. Kim Atmos. Environ. **1998**, 32, No. 5, 895-908.

Lindberg, S.E., Dong, W. and Meyers, T. **2002**, *Atmos. Environ*., 36, 5207-5219.

Massman, W.J. *Atmos. Environ*. **1999**, 33, 453-457.

Melieres, M-A., Pourchet, M., Charles-Dominique, P., and Gaucher, P. **2003**, *Science of the Total Environ*., 311, 261-267.

Meyers, T.P., Finkelstein, P., Clarke, J., Ellestad, T.G., Sims, P.F. *J. Geophys. Res*. **1998**, 103, D17, 22645-22661.

Myers, G.J., Davidson, P.W., Cox, C., Shamlaye, E., Cernichiari, E. and Clarkson, T. *Environmental Research* **2000**, Section A, 83, 275-285.

Patra, M. and Sharma, A. *The Botanical Review* **2000**, 66, No. 3, 379-422.

Poissant, L., Casimir, A. *Atmospheric Environment* **1998**, 32, No. 5, 883-893.

Rea, A.W., Keeler, G.J., Scherbatskoy, T. *Atmos. Environ*. **1996**, 30, 3257-3263.

Rea, A.W., Lindberg, S.E. and Keeler, G.J. *Environ. Sci. Technol*. **2000**, 34, 2418-2425.

Rodgers, J., Hocker, J., Hanas, R., Nwosu, C., Hanas, J. *Biochemical Pharmacology* **2001**, 61, 1543-1550.

Rolph, G.D., 2003. Real-time Environmental Applications and Display sYstem (READY) Website (http://www.arl.noaa.gov/ready/hysplit4.html). NOAA Air Resources Laboratory, Silver Spring, MD.

Shannon, J.D., Voldner, E.C. *Atmos. Environ*. **1995**, 29, No. 14, 1649-1661.

Steinnes, E., **1990**. *In* Heavy Metals in Soils (B.J. Alloway, Ed.), Wiley and Sons, New York, NY, USA.

Schroeder, W.H., and Munthe, J. *Atmospheric Environment* **1998**, 32, No. 5, 809-822.

Sorensen, J.A., Glass, G.E., and Schmidt, K.W. ***Environ. Sci, Technol.* 1994, *28*,** 2025-2032.

Swain, E., Engstrom , D., Brigham, M. *Science* **1992**, 257, 784-787.

Tarnay, L. Gertler, A, Taylor, G.E. *Atmos. Environ.* **2002**, 36 no20: 3277-3287.

USEPA **1997**, Mercury Study Report to Congress, EPA-452/R-97-005.

Walmsley, J.L., Wesely, M.L. *Atmos. Environ*. **1996**, 30, No. 7, 1181-1188.

Wesely, M.L. *Atmos. Environ*. **1989**, 23, No. 6, 1293-1304.

Zhang, H., Lindberg, S.E., Marsik, F.J., Keeler, G.J. *Water, Air and Soil Pollution* **2001**, 126, 151-169.

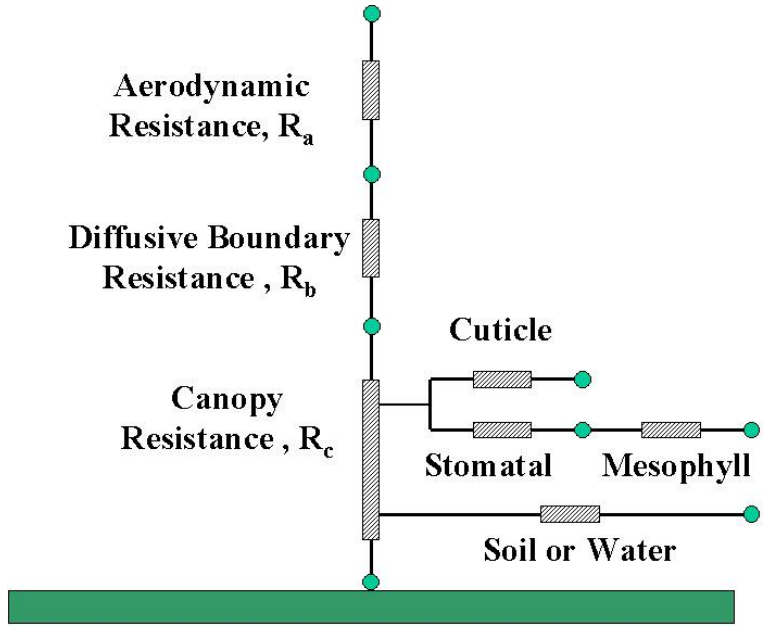

Figure 1. Resistances to deposition considered by the Hicks *et al*. (1987) inferential dry-deposition model.

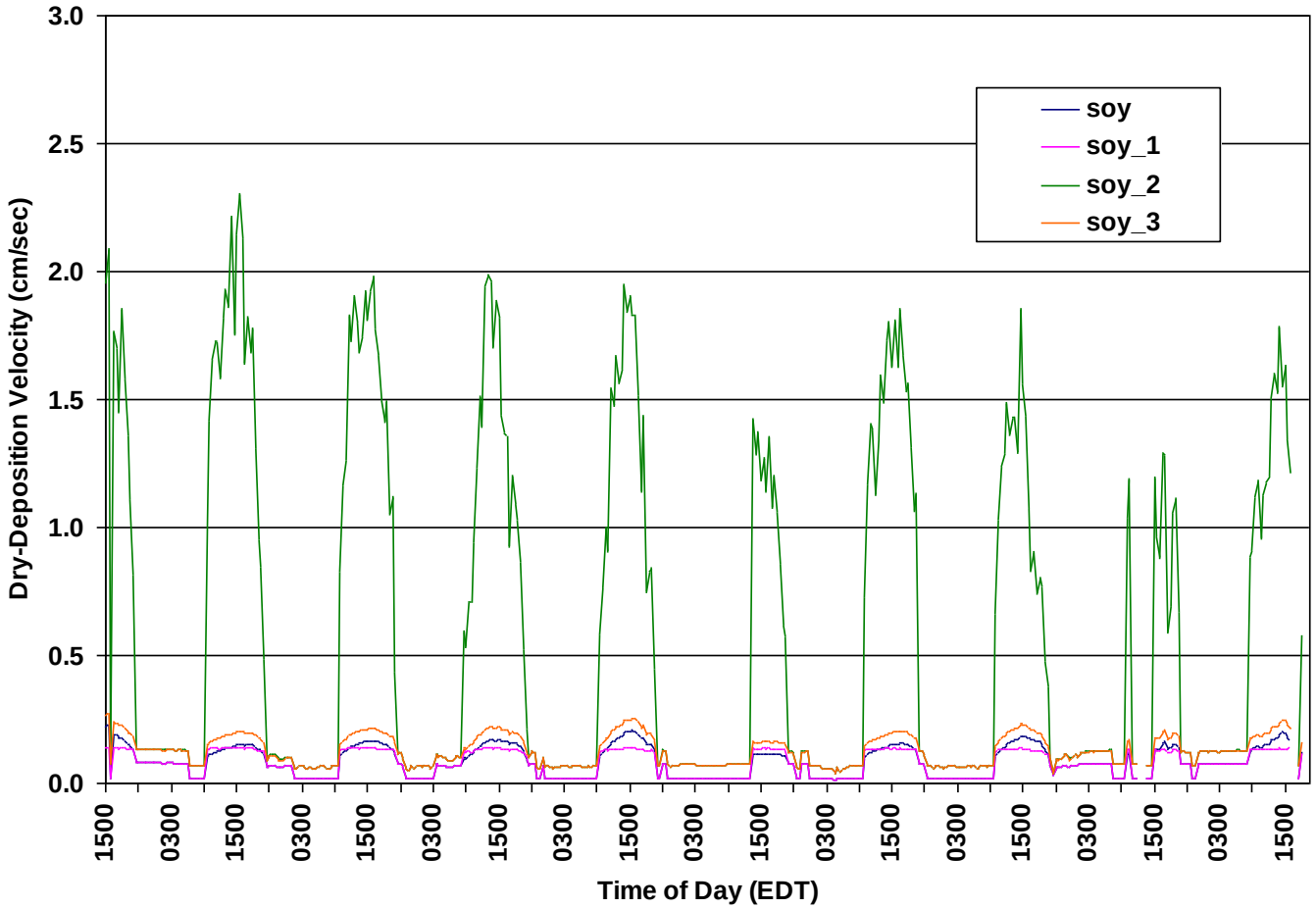

Figure 2. Comparison of Modeled Mercury Dry-Deposition Velocities using differing values of Mesophyll Resistance to Hg(0) Uptake.

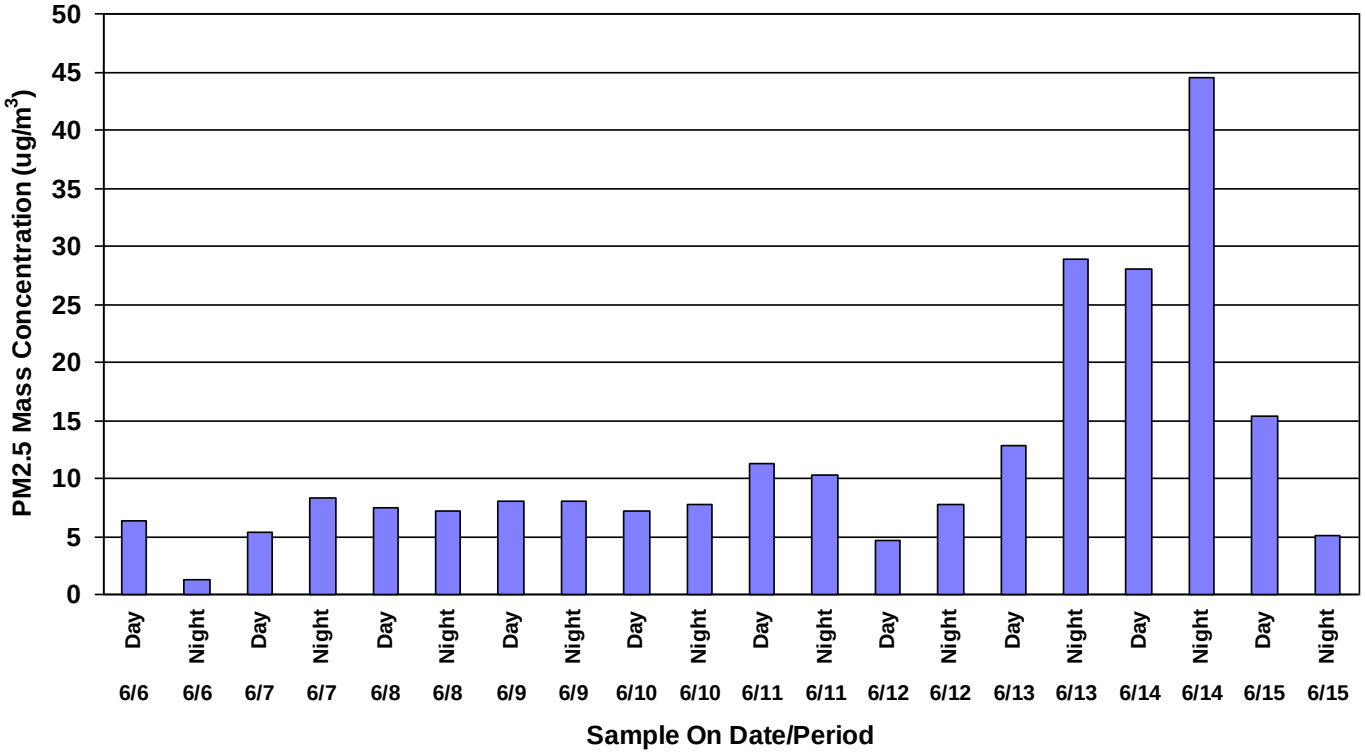

Figure 3. Temporal variation of PM2.5 Mass Concentration at Pellston, Michigan during the 2001 MACE Study.

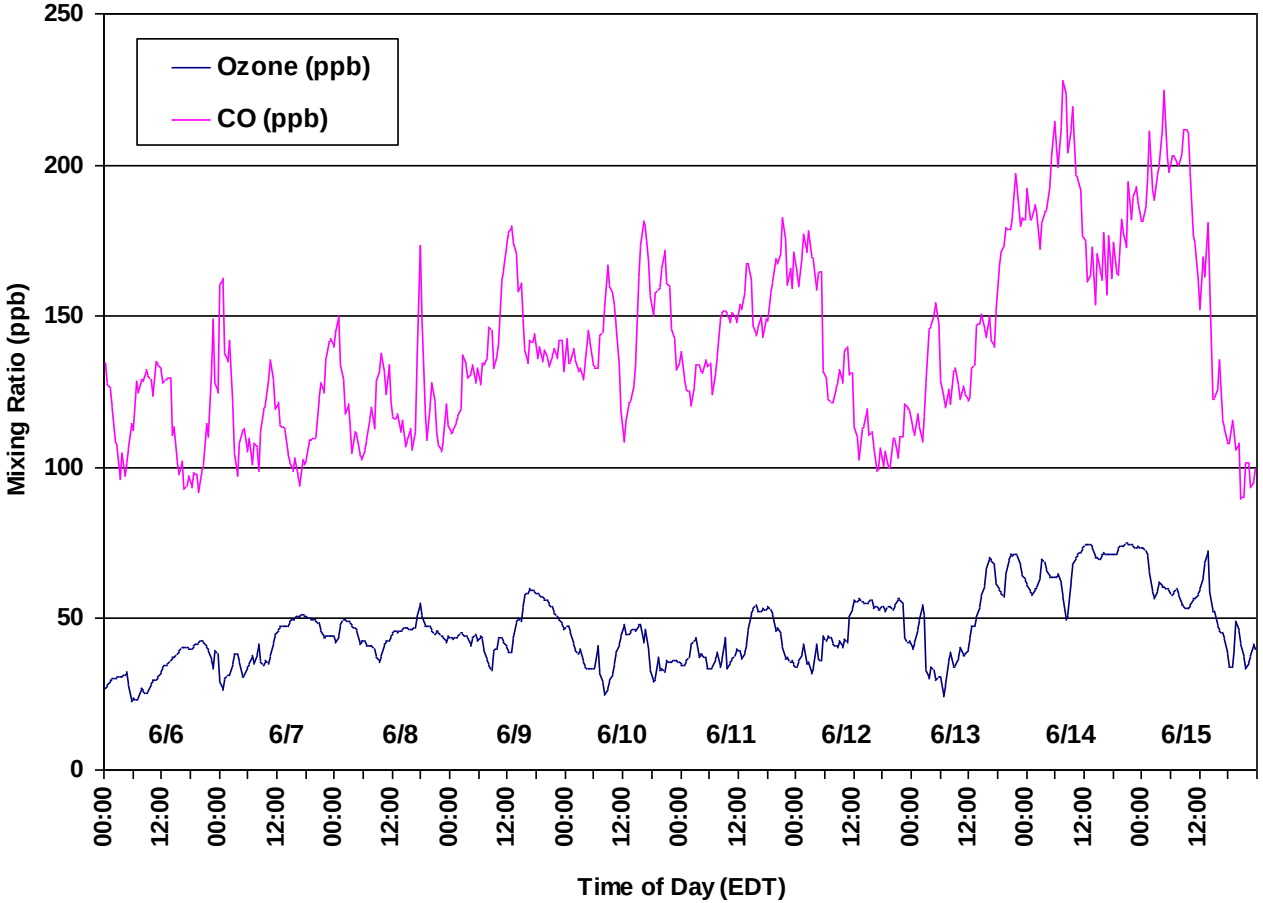

Figure 4. Temporal variation of Ozone and Carbon Monoxide Mixing Ratios at Pellston, Michigan during the 2001 MACE Study. Data provided by Dr. Mary Anne Carroll, University of Michigan.

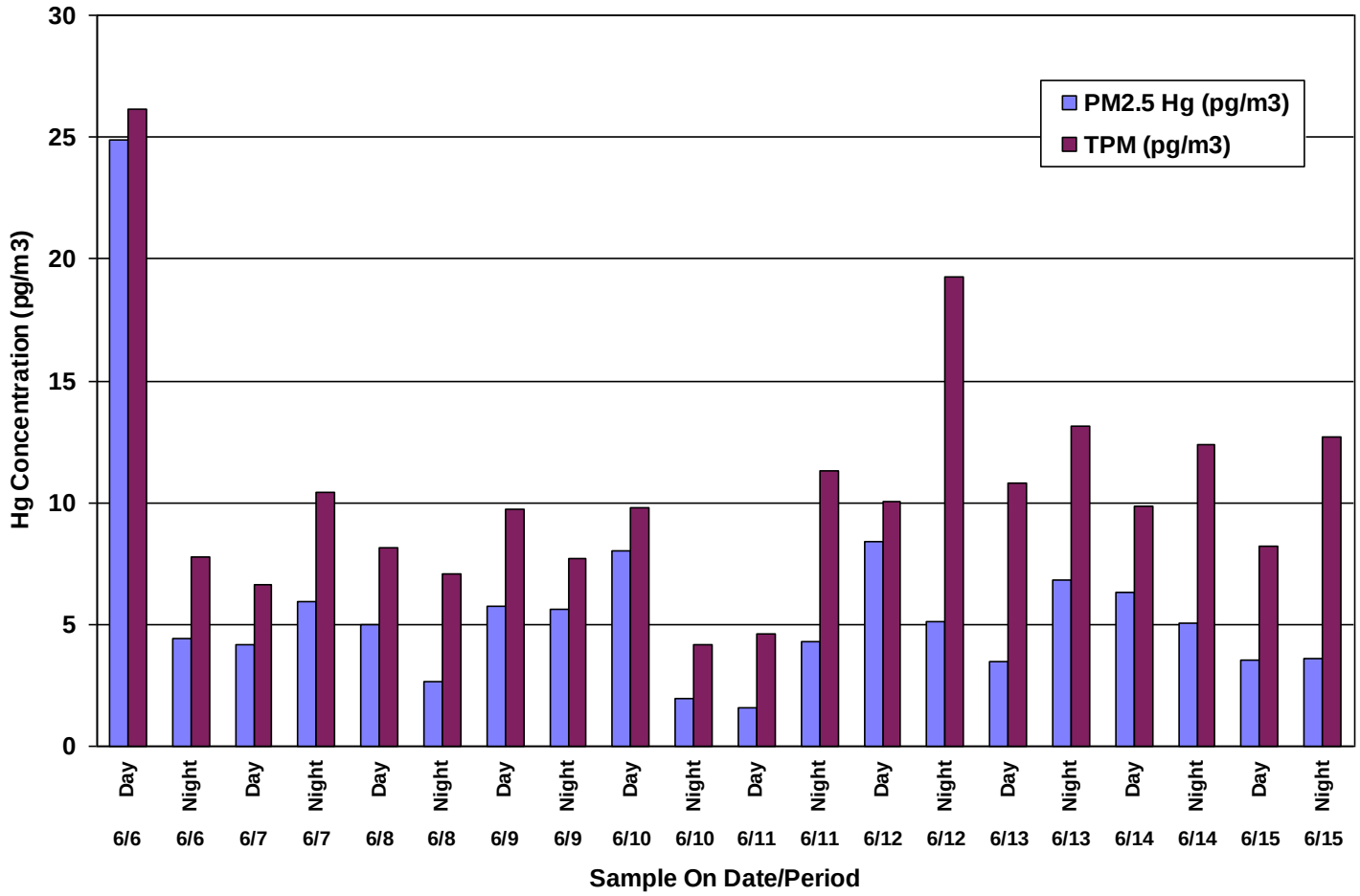

Figure 5. Temporal variation of PM2.5 and Total Particulate Mercury concentrations at Pellston, Michigan during the 2001 MACE Study.

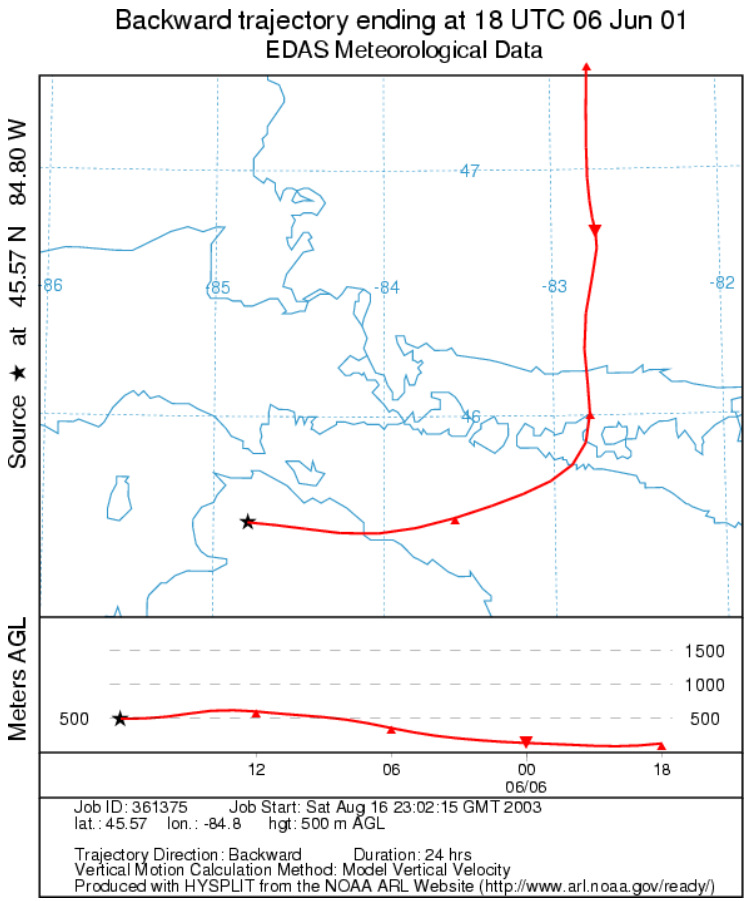

Figure 6. Twenty-four hour back trajectory (transport history) for airmass arriving in Pellston, Michigan at 1400 EDT on 06 June 2001.

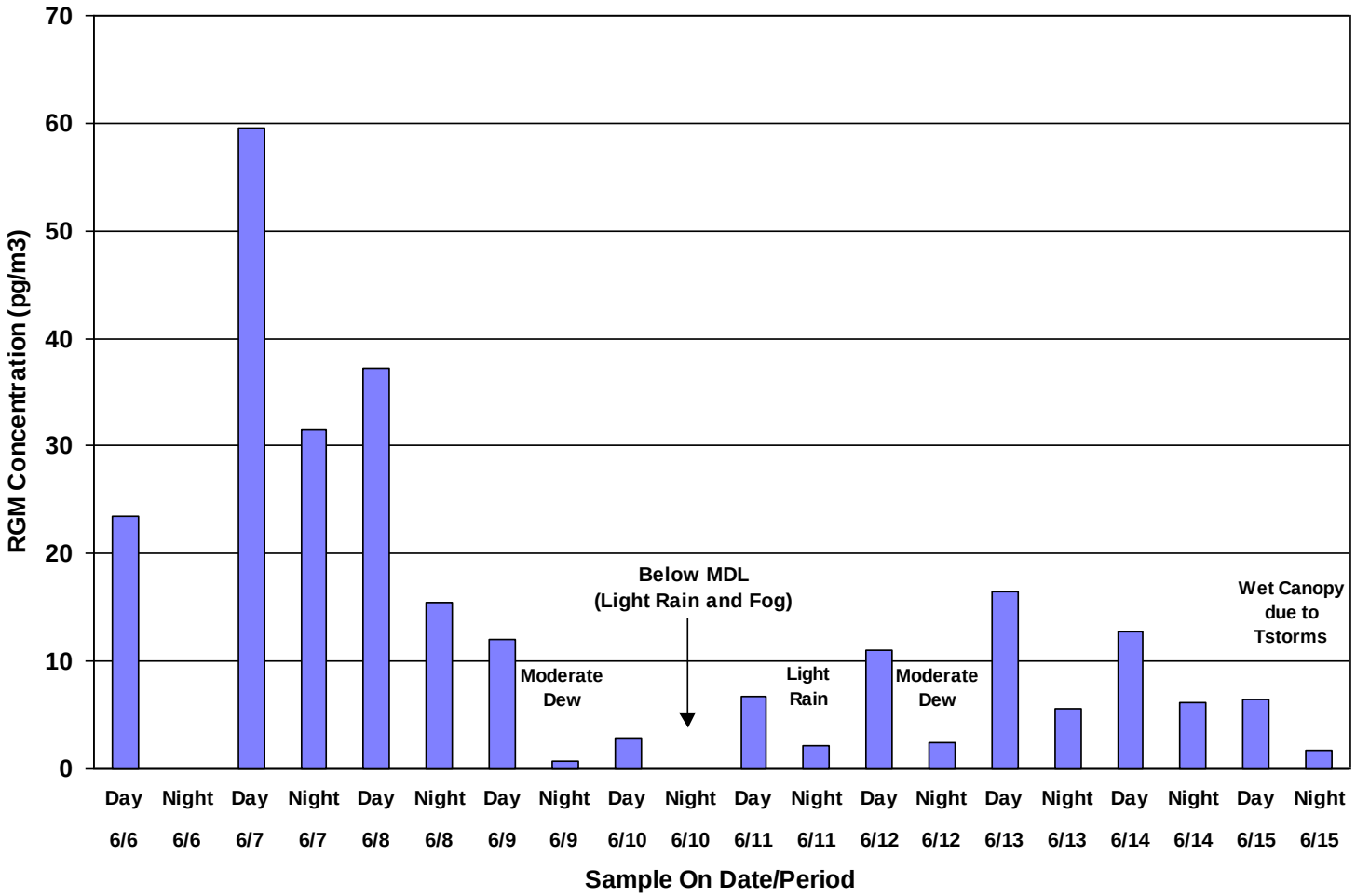

Figure 7. Temporal variation of Reactive Gaseous Mercury concentrations at Pellston, Michigan during the 2001 MACE Study.

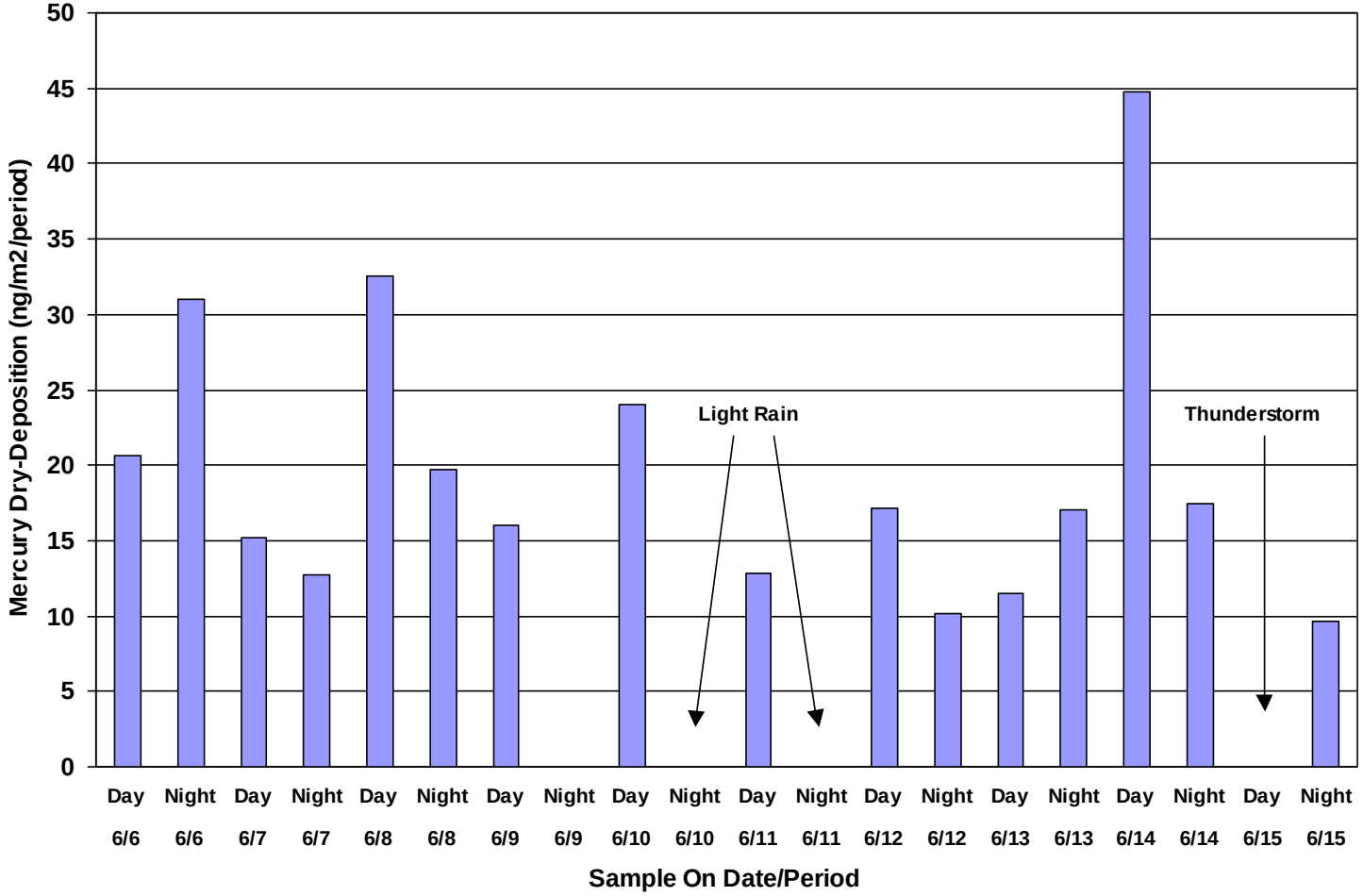

Figure 8. Temporal variation of tower-based Total Mercury dry-deposition at Pellston, Michigan during the 2001 MACE Study.

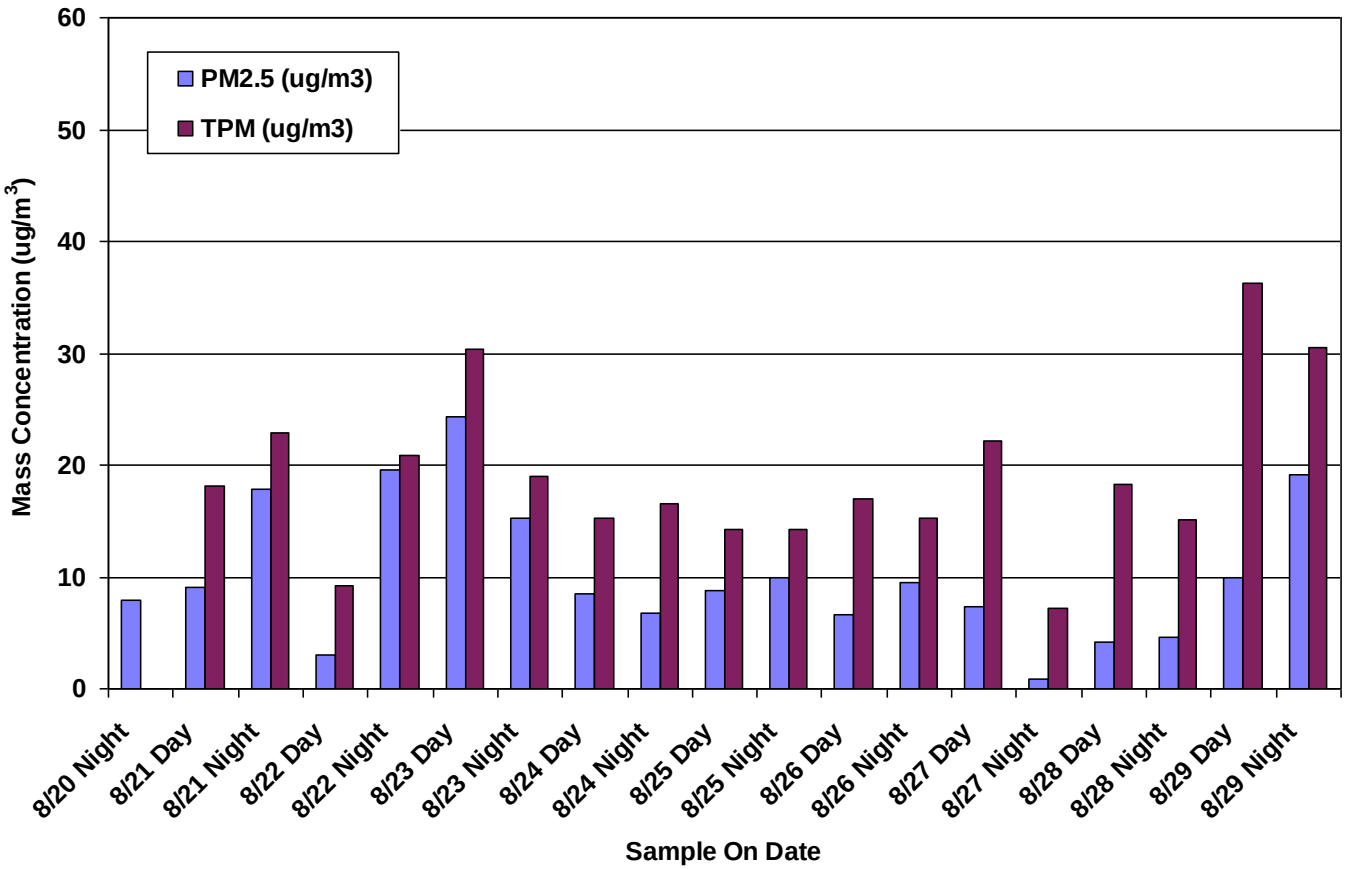

Figure 9. Temporal variation of PM2.5 and Total Particulate Mass concentrations at Clarksville, Michigan during the 2002 MACE Apple Canopy Study.

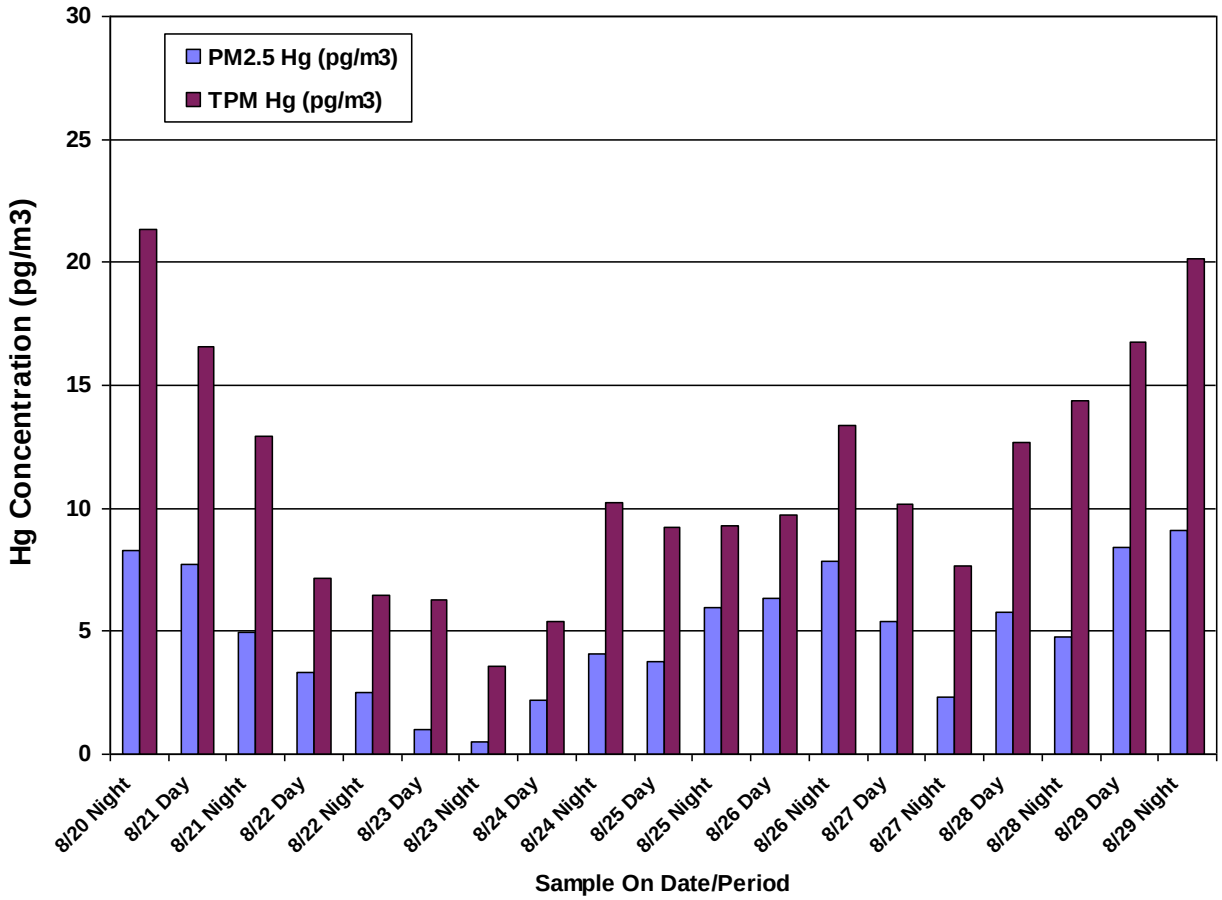

Figure 10. Temporal variation PM2.5 and Total Particulate Mercury concentrations at Clarksville, Michigan during the 2002 MACE Apple Canopy Study.

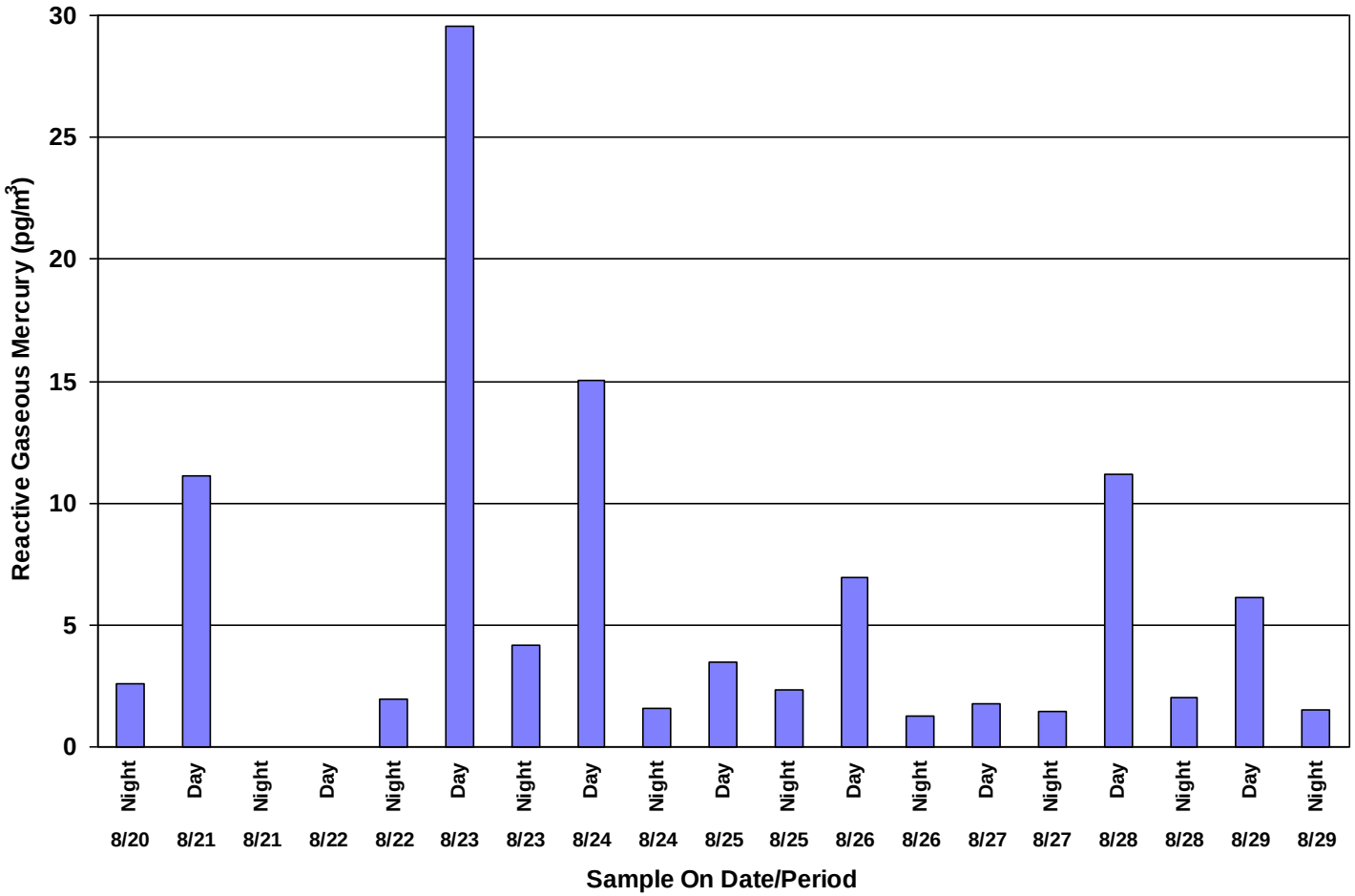

Figure 11. Temporal variation of Reactive Gaseous Mercury at Clarksville, Michigan during the 2002 MACE Apple Canopy Study.

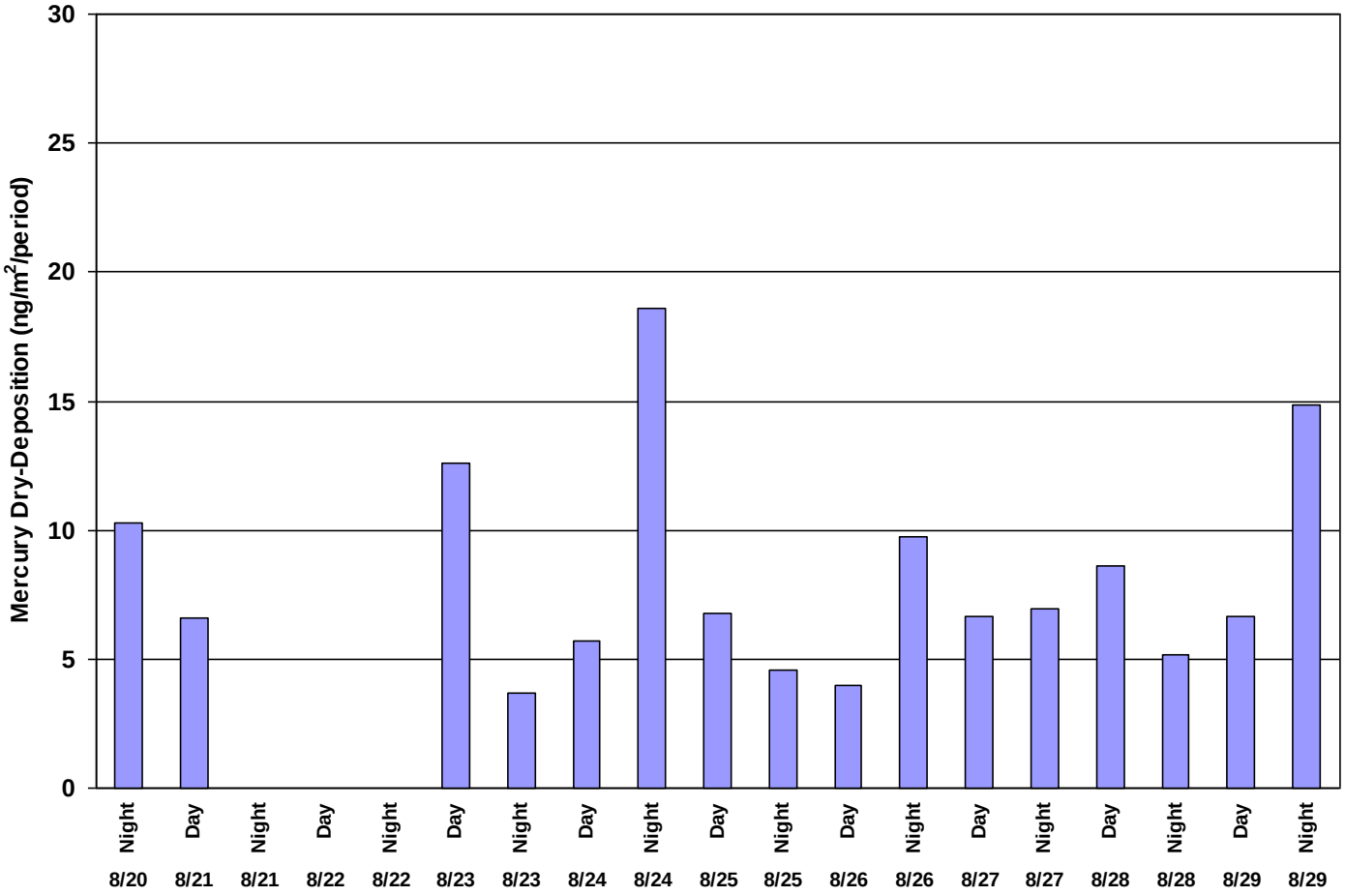

Figure 12. Temporal variation of Total Mercury dry-deposition at Clarksville, Michigan during the 2002 MACE Apple Canopy Study.

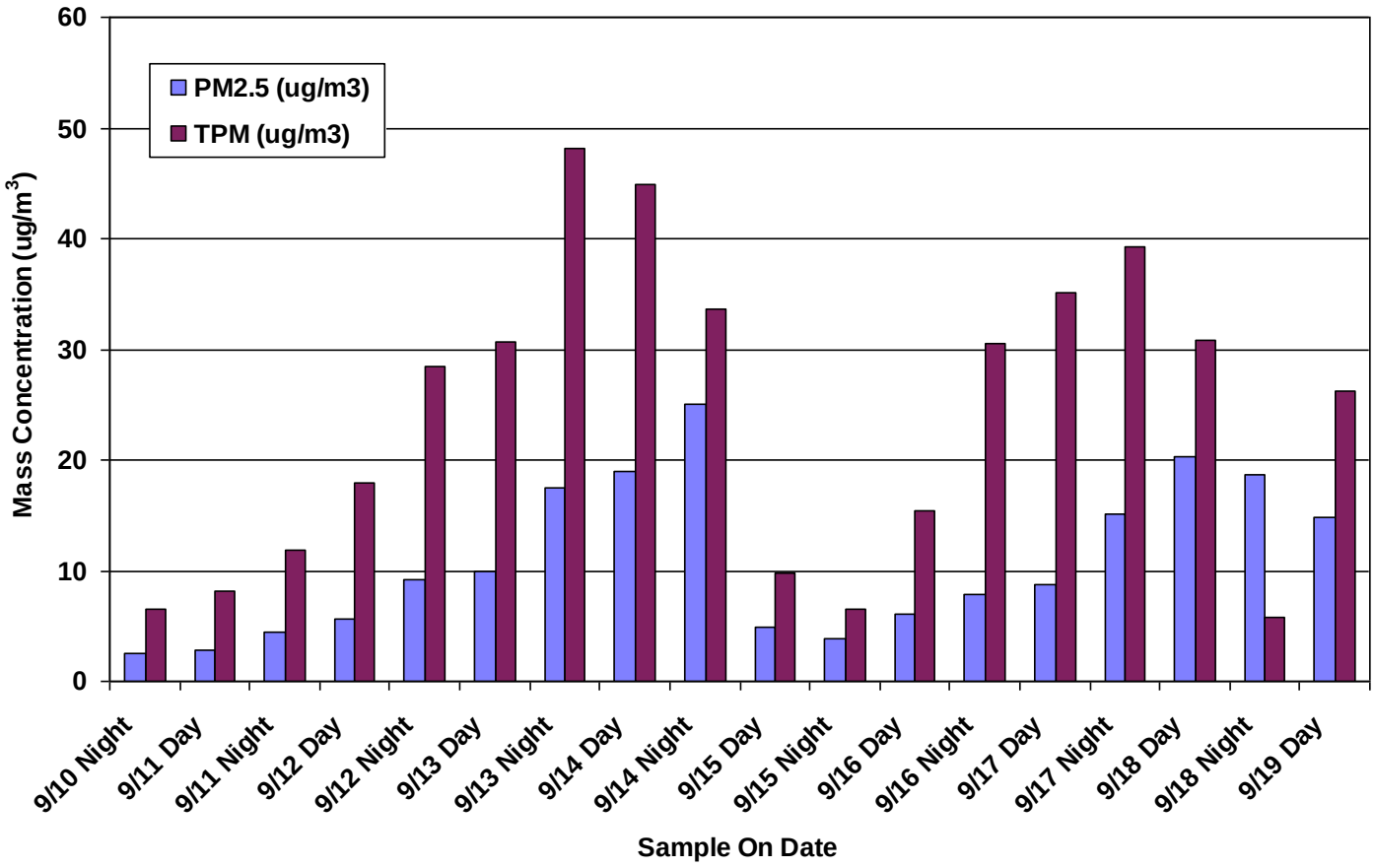

Figure 13. Temporal variation PM2.5 and Total Particulate Mass concentrations at Clarksville, Michigan during the 2002 MACE Soybean Canopy Study.

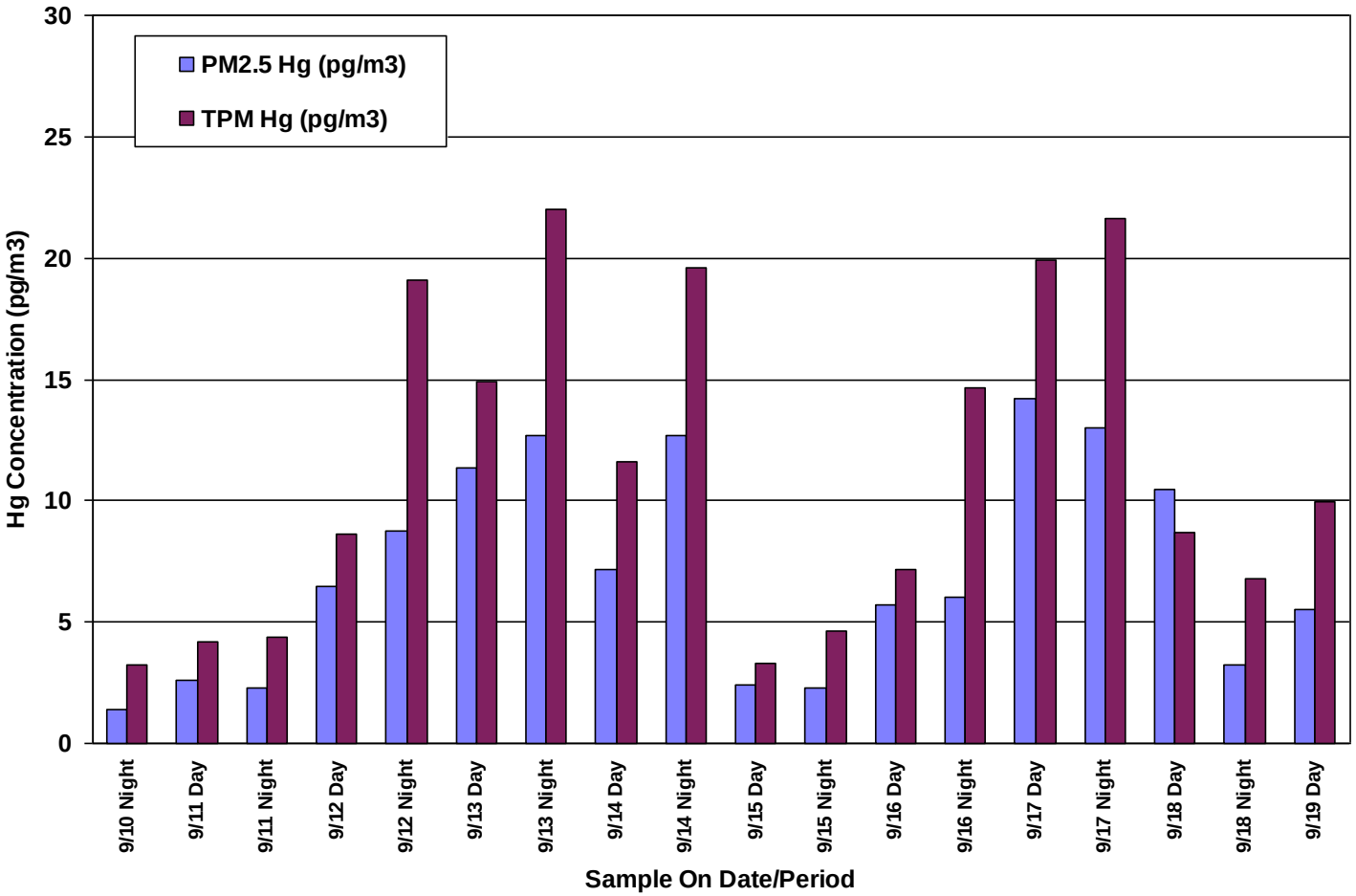

Figure 14. Temporal variation PM2.5 and Total Particulate Mercury concentrations at Clarksville, Michigan during the 2002 MACE Soybean Canopy Study.

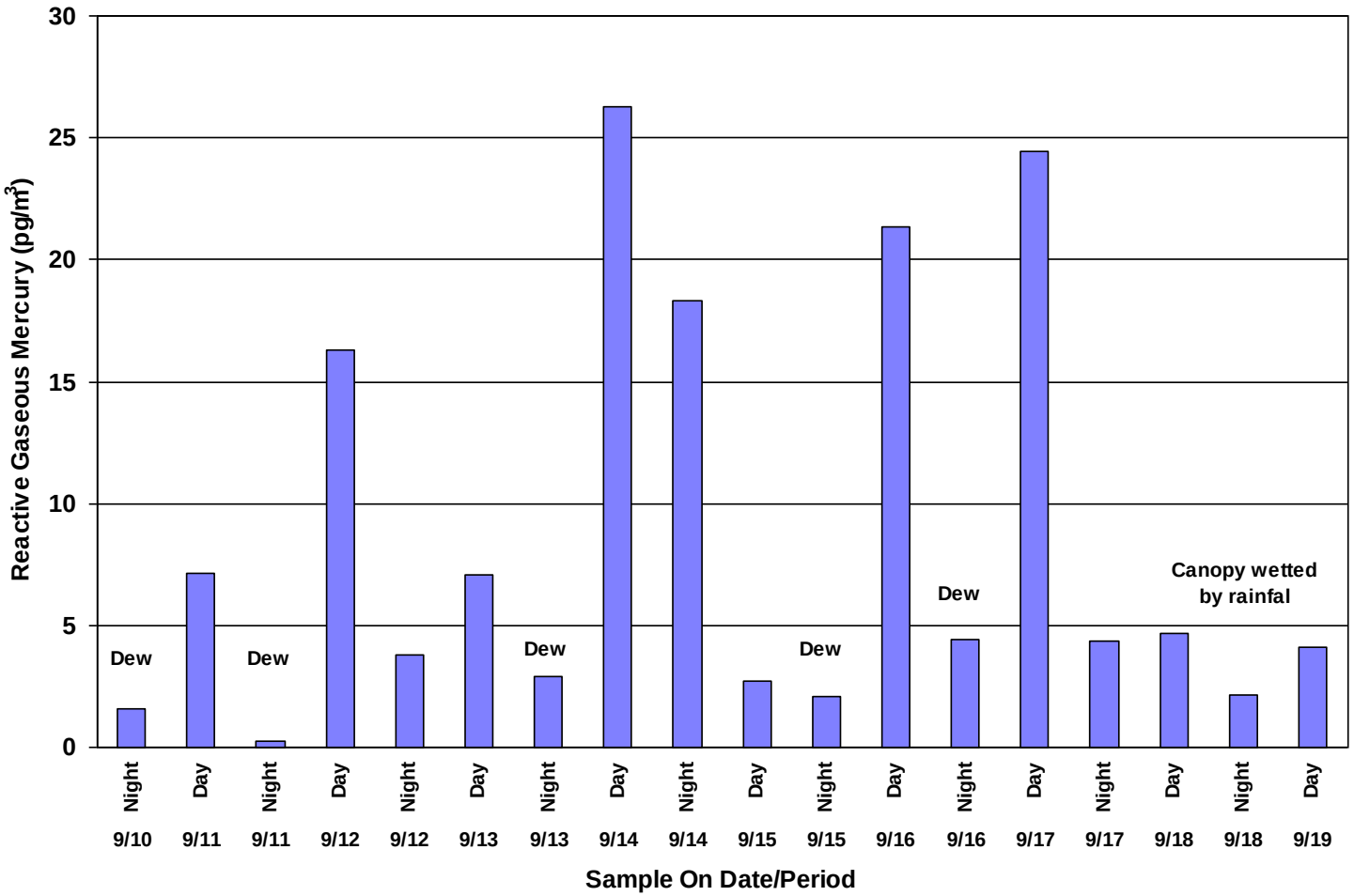

Figure 15. Temporal variation of Reactive Gaseous Mercury concentrations at Clarksville, Michigan during the 2002 -MACE Soybean Canopy Study.

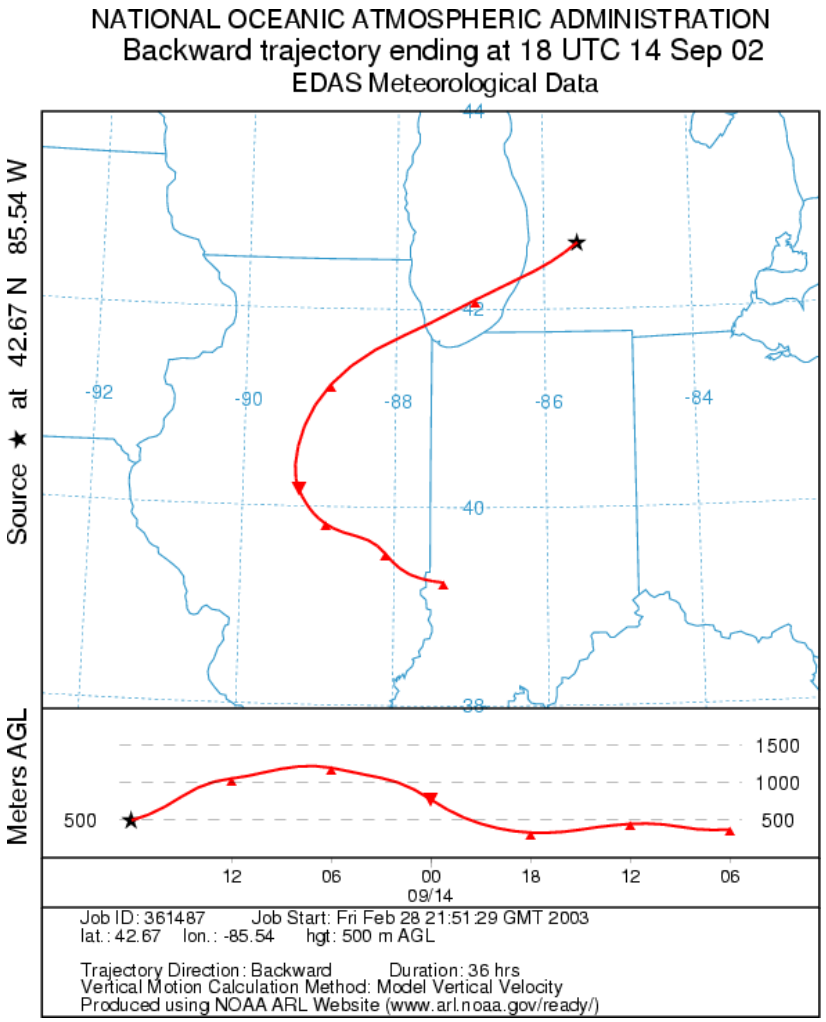

Figure 16. Twenty-four hour back trajectory (transport history) for airmass arriving in Clarksville, Michigan at 1400 EDT on 14 September 2002.

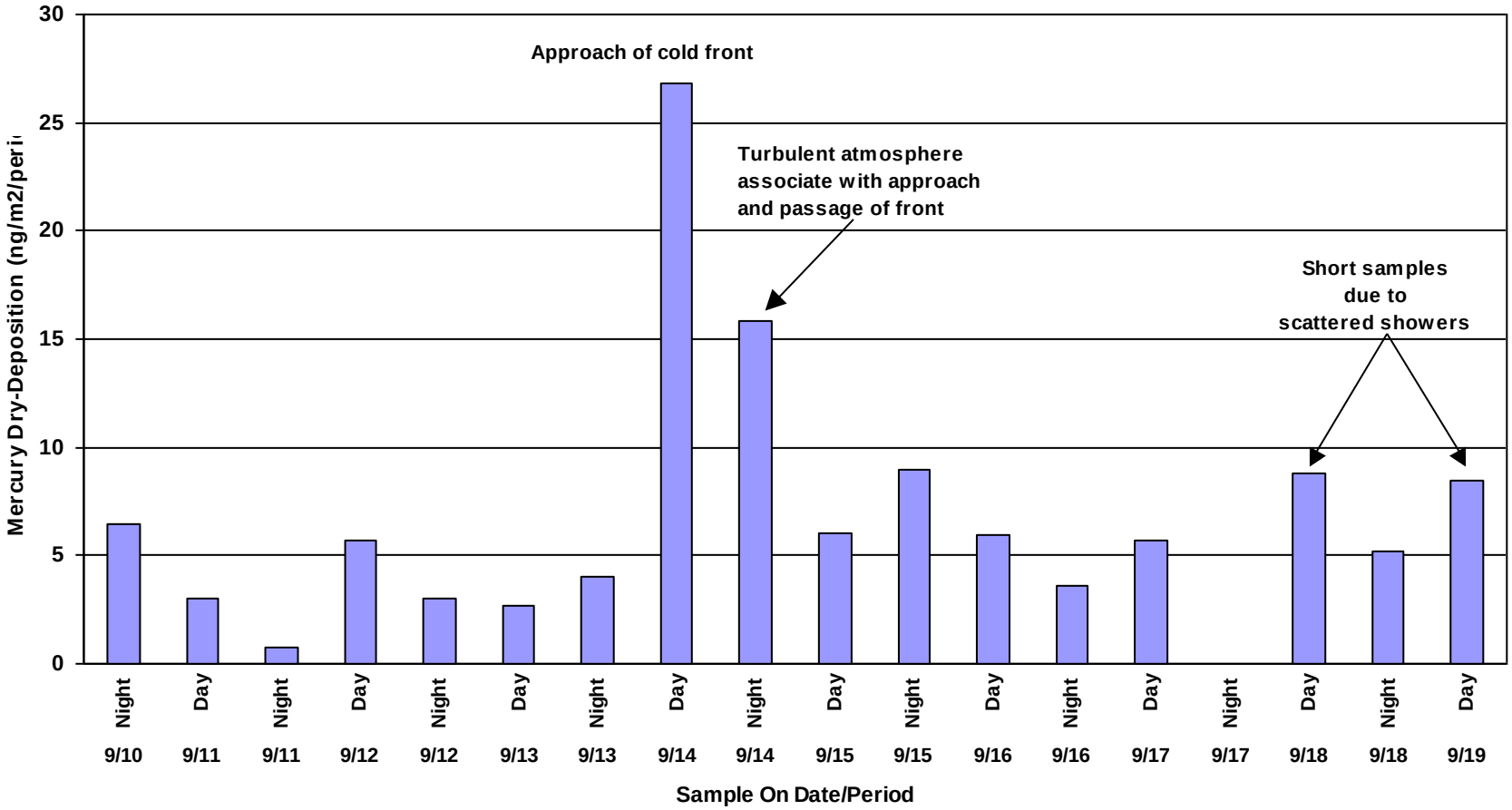

Figure 17. Temporal variation of Total Mercury dry-deposition at Clarksville, Michigan during the 2002 MACE Soybean Canopy Study

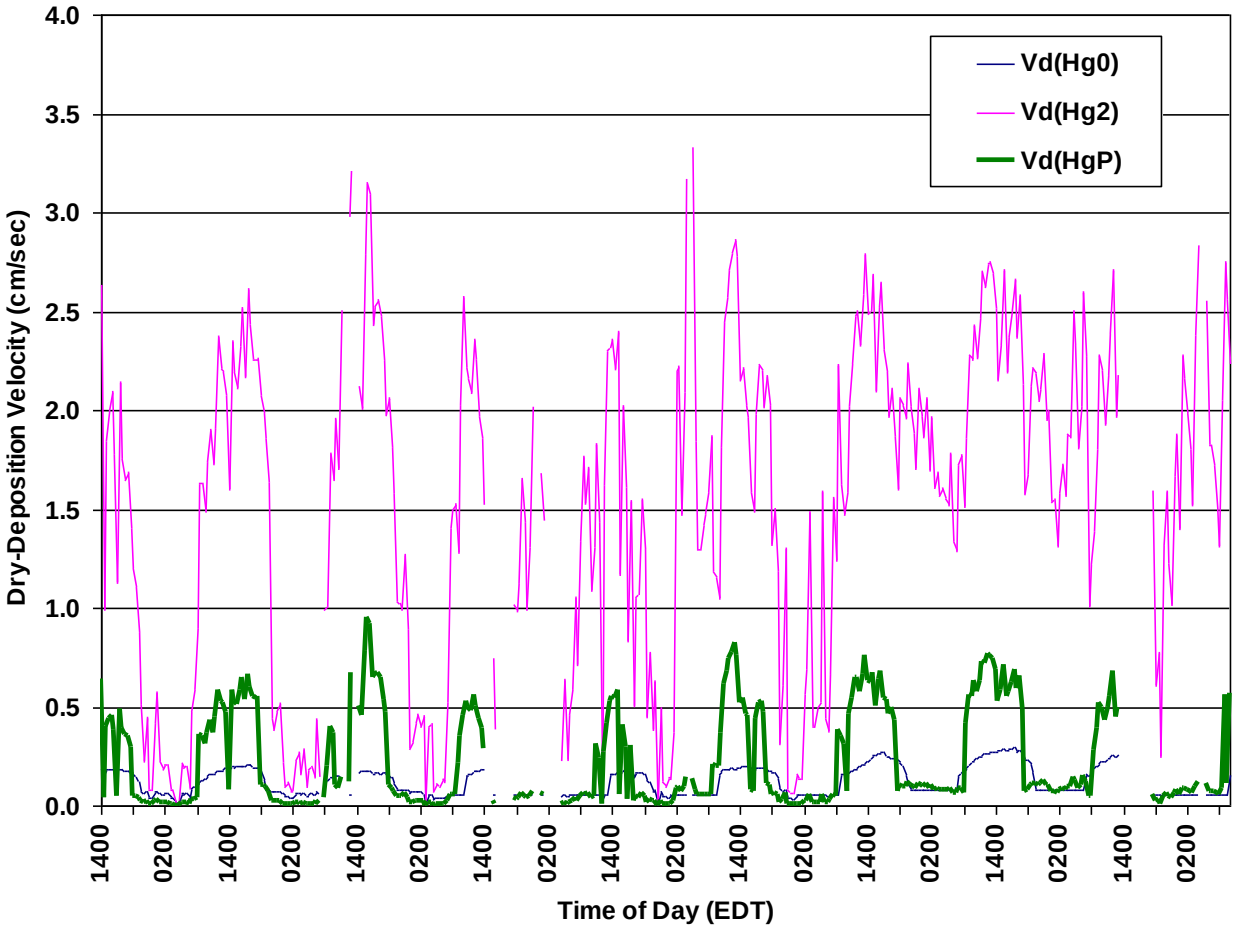

Figure 18. Temporal Variation of Speciated Mercury Dry-Deposition Velocities over a Mixed Deciduous Forest Canopy, Pellston, Michigan - 07 to 16 June 2001.

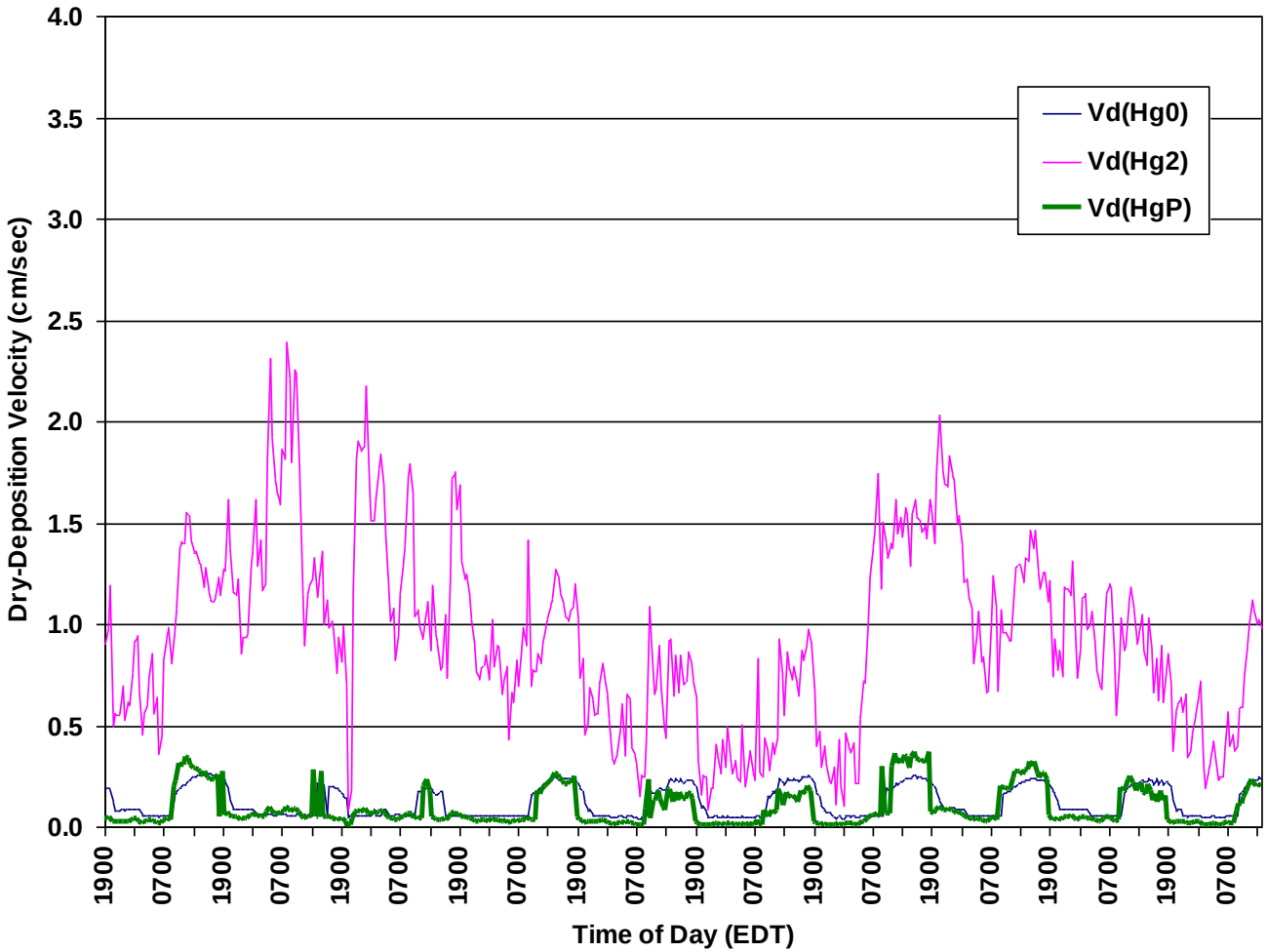

Figure 19. Temporal Variation of Speciated Mercury Dry-Deposition Velocities over Apple Canopy, Clarksville, Michigan - 23 to 29 August 2002.

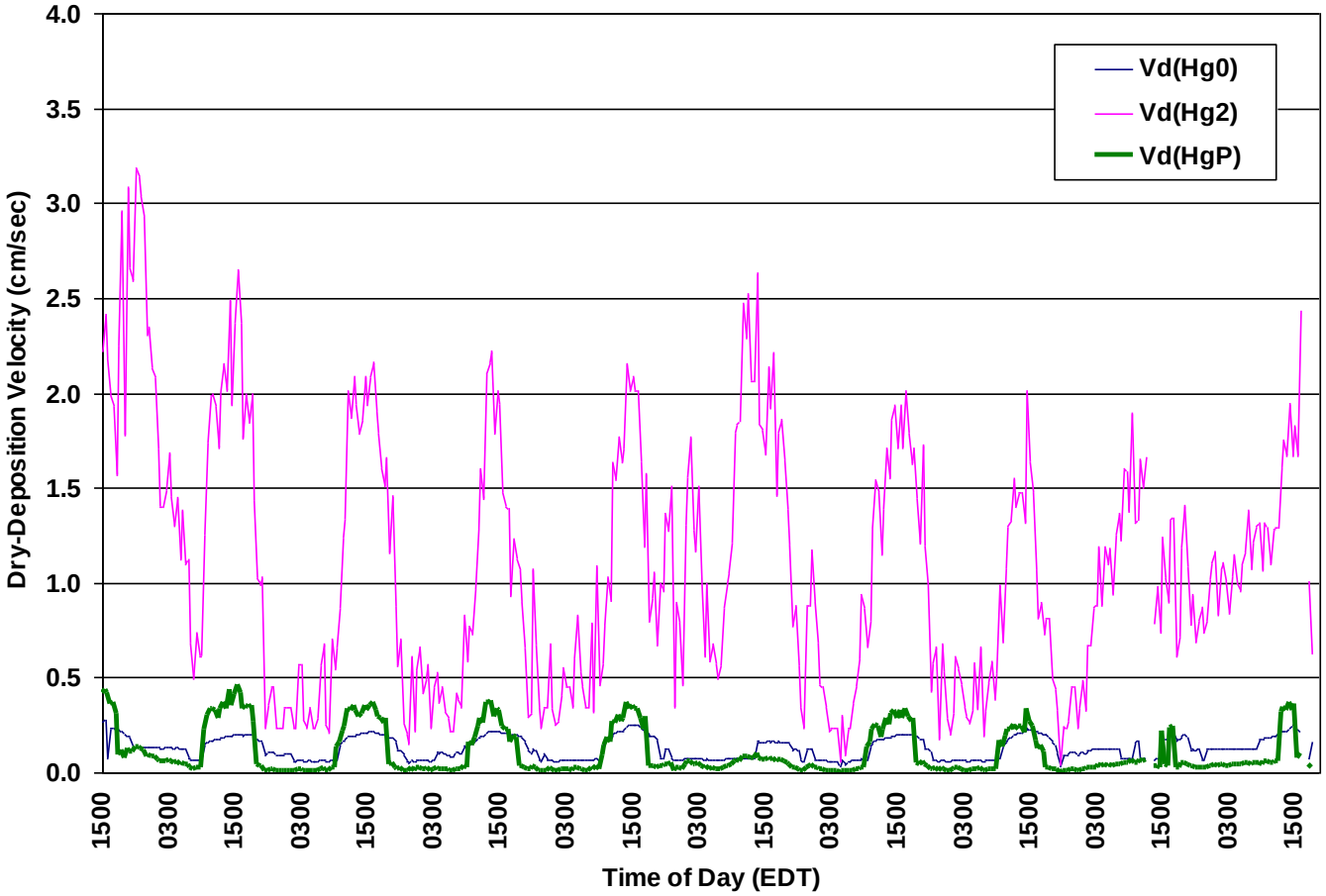

Figure 20. Temporal Variation of Speciated Mercury Dry-Deposition Velocities over a Soybean Canopy, Clarksville, Michigan - 10 to 19 September 2002.

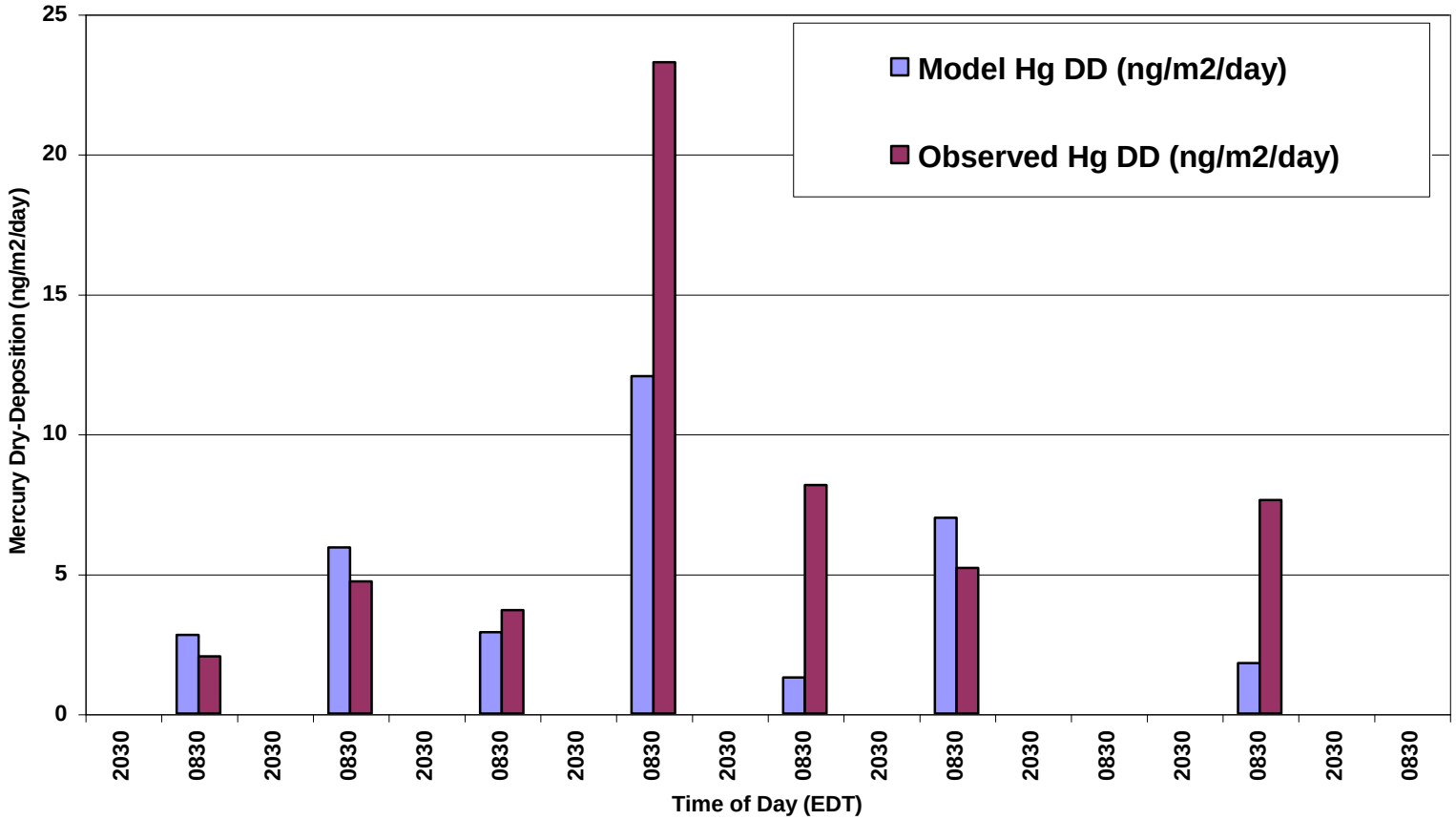

Figure 21. Comparison of Modeled versus Measured Daily Dry-Deposition of Mercury to Soybean Canopy, Clarksville, Michigan, 10-19 September 2002.

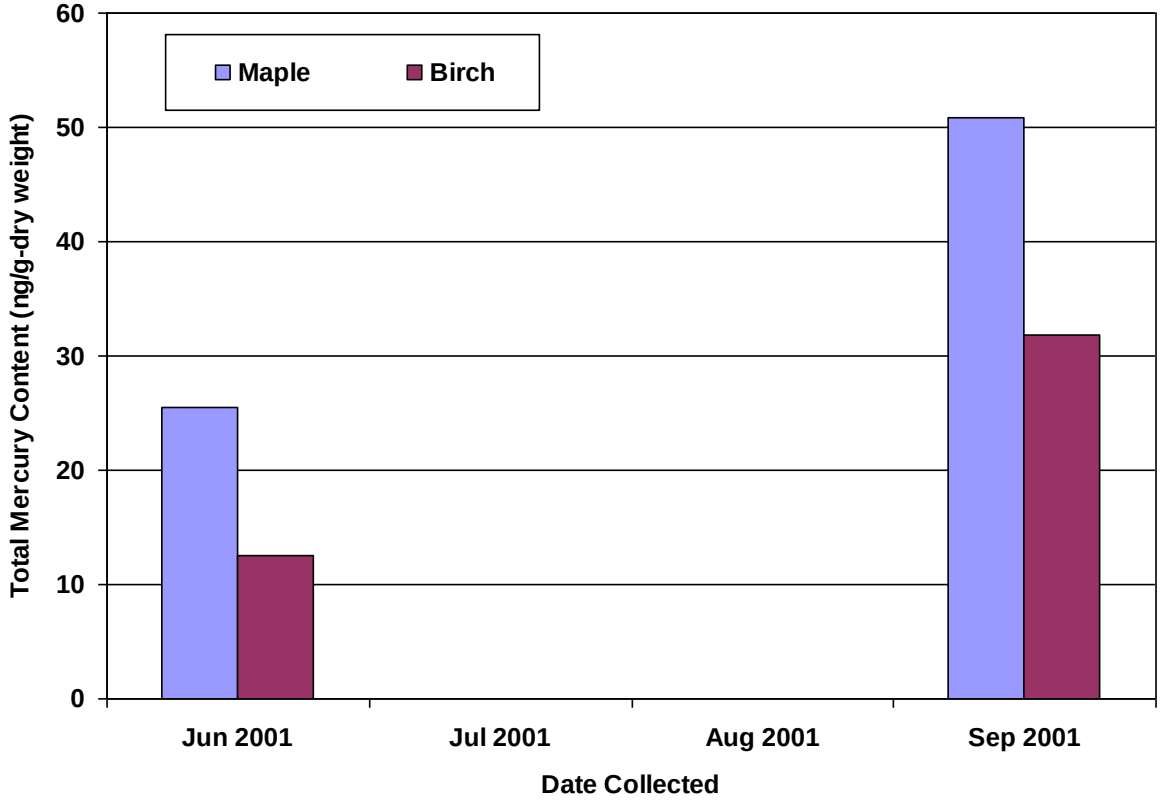

Figure 22: Average total mercury content of foliage sampled during the 2001 growing season at the University of Michigan Biological Station, Pellston, Michigan.

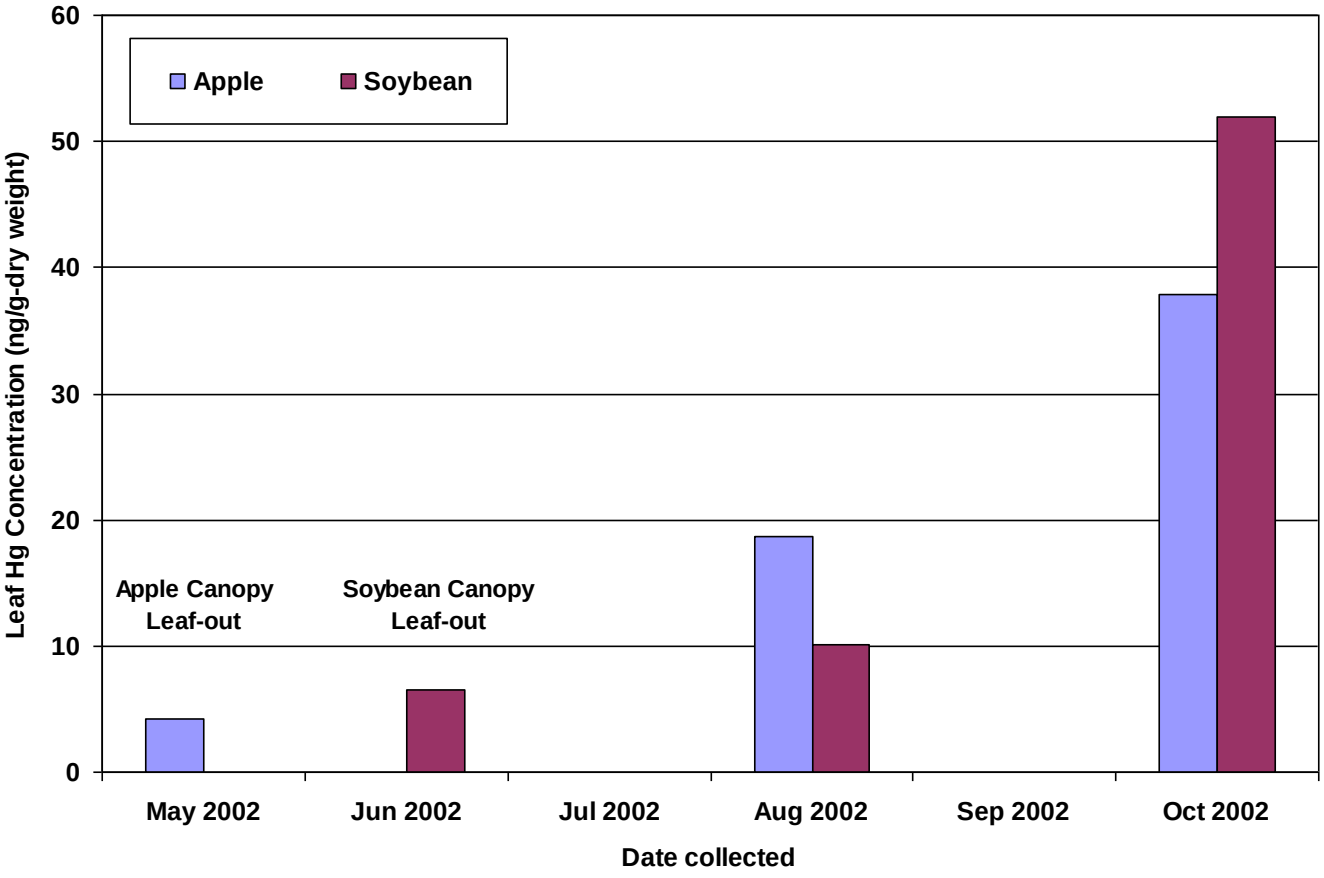

Figure 23. Average total mercury content of foliage sampled during the 2002 growing season at the Clarksville Horticulture Experiment Station, Clarksville, Michigan.

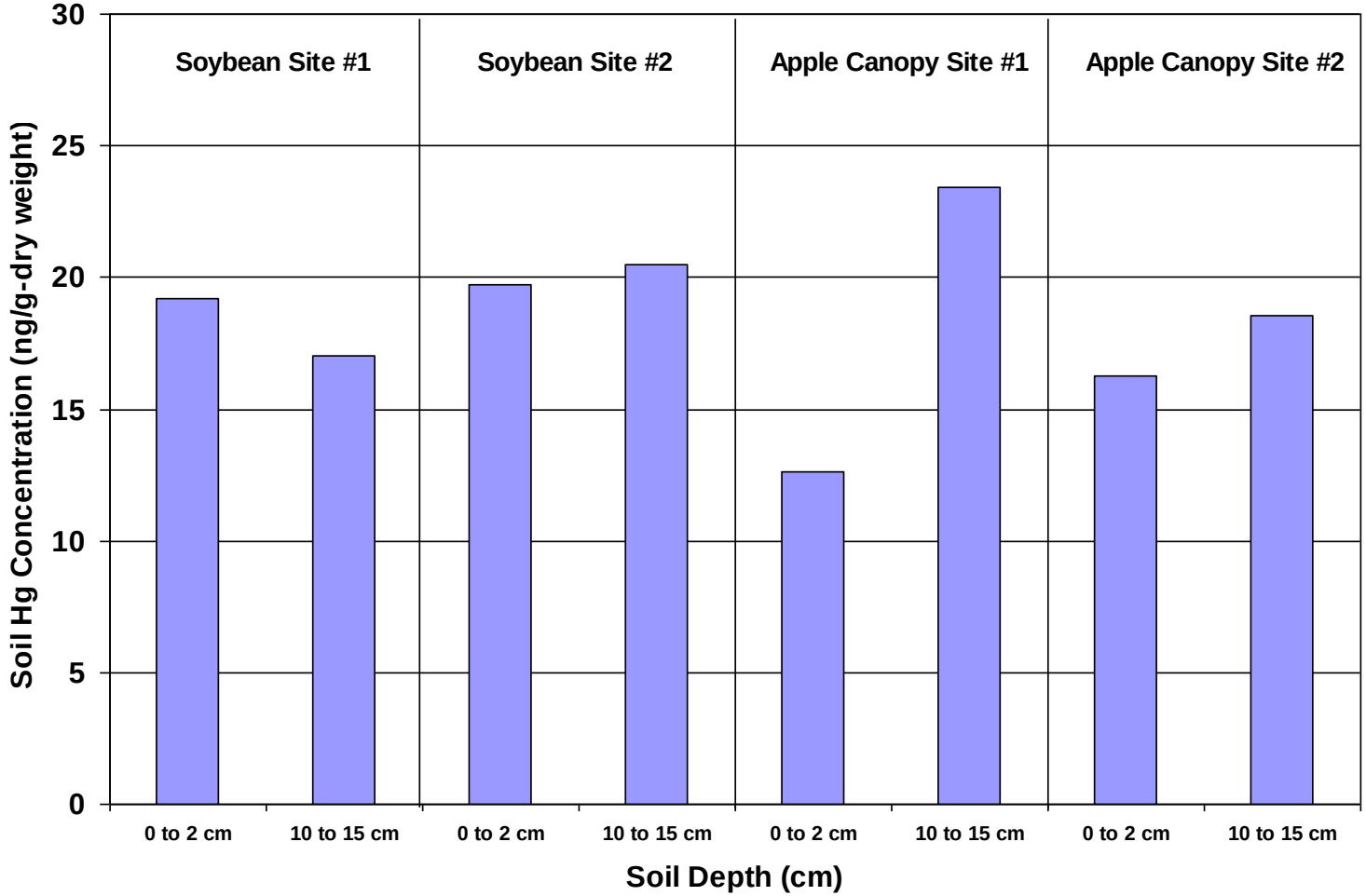

Figure 24. Total mercury in soils at the Clarksville Horticulture Experiment Station, Clarksville, Michigan (October 2002)

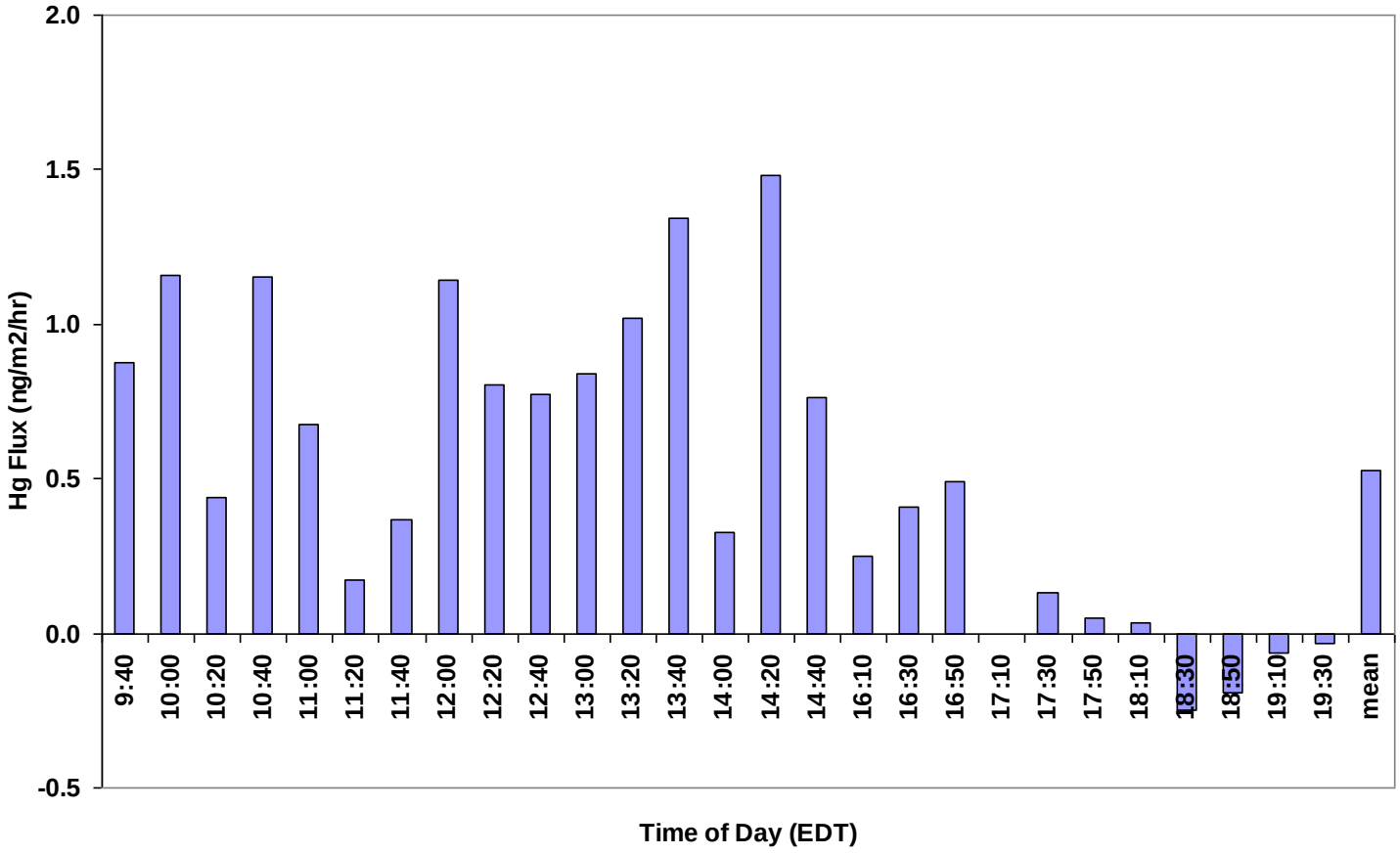

Figure 25. Measured surface layer fluxes of Hg (0) over the soil of a Soybean field at the Clarksville Horticulture Experiment Station on 27 June 2002.

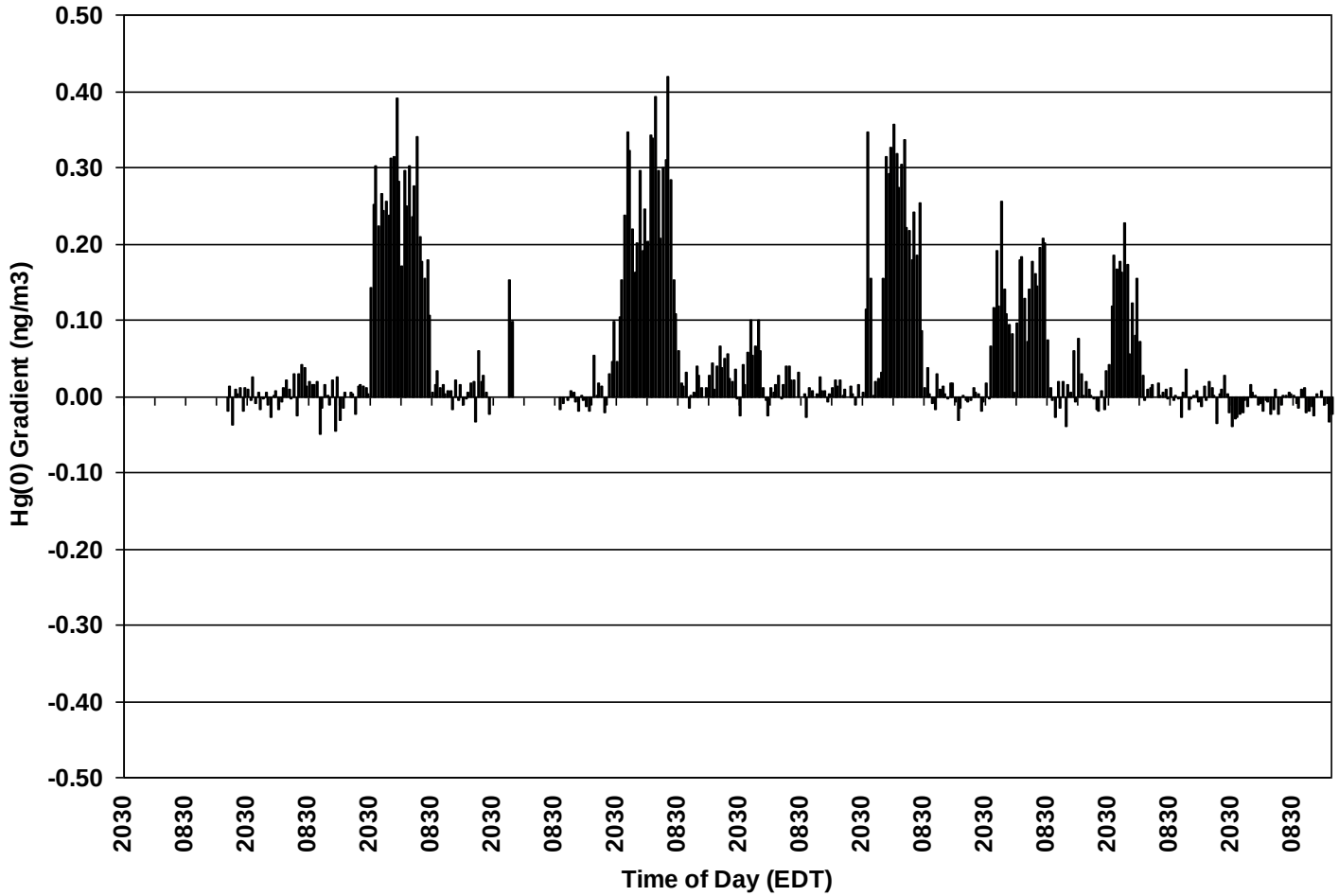

Figure 26. Temporal Variation of the gradient in Hg(0) over the Soybean Canopy at Clarksville Horticulture Experiment Station for the period 09 to 19 September 2002.

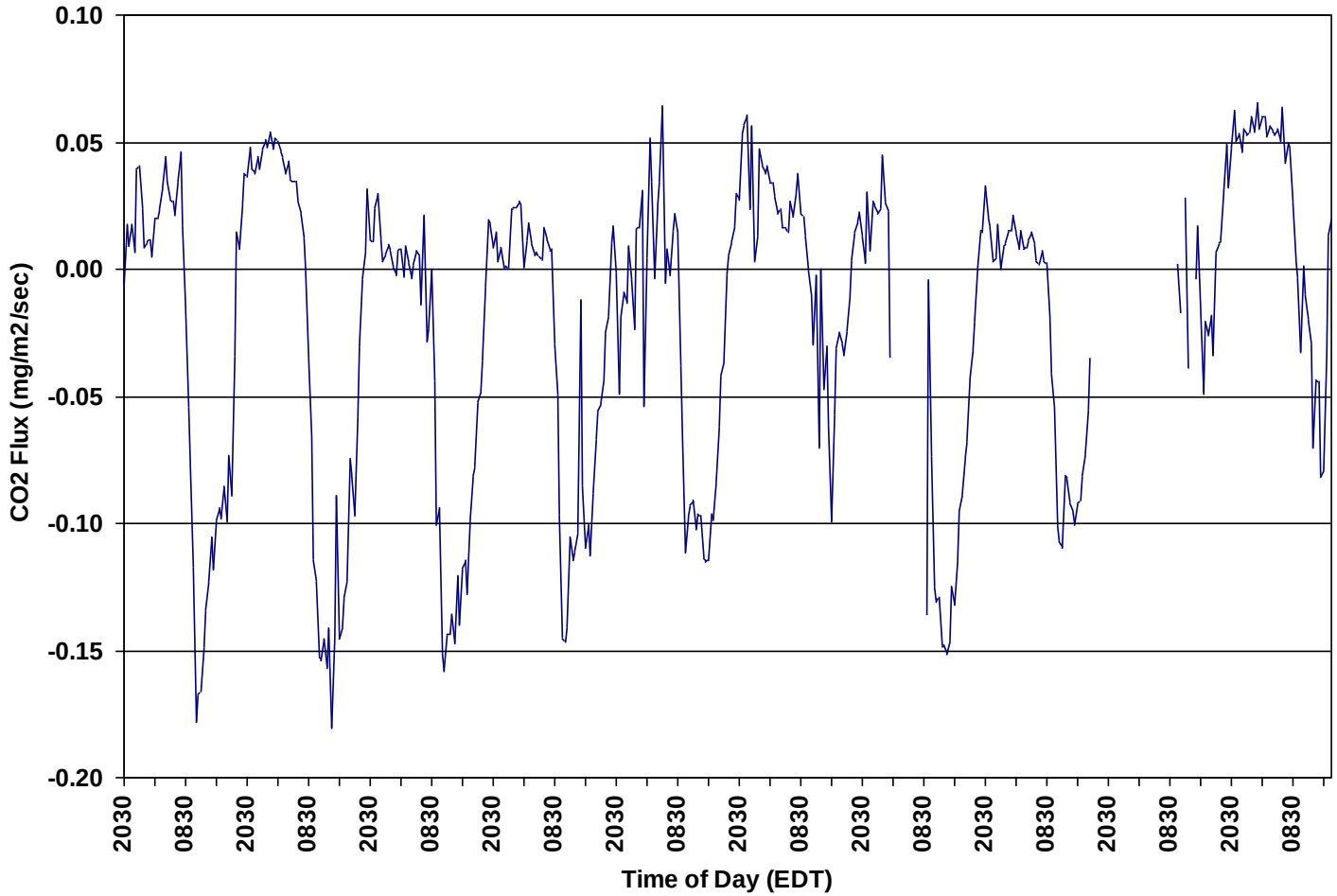

Figure 27. Temporal variability of the surface layer flux of carbon dioxide over the Soybean Canopy at Clarksville Horticulture Experiment Station in Clarksville, Michigan - 09 to 19 September 2002.

APPENDIX A

METEOROLOGICAL SURFACE MAPS

(Source: NOAA/National Center for Environmental Prediction)

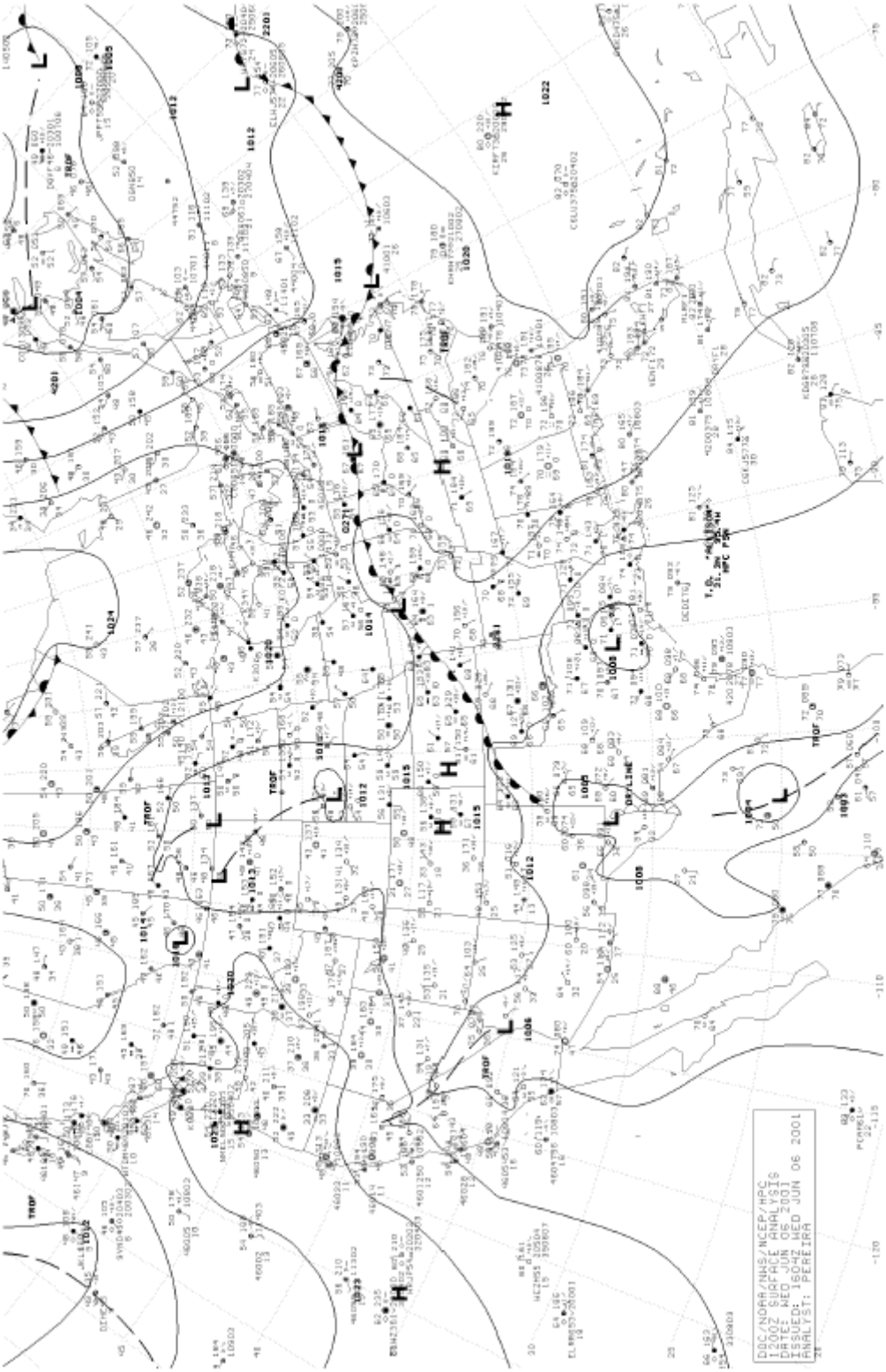
DOC/NOAA/NWS/NCEP/HPC
12002 SURFACE ANALYSIS
DATE: WED JUN 06 2001
ISSUED: 1604Z WED JUN 06 2001
ANALYST: PEREIRA

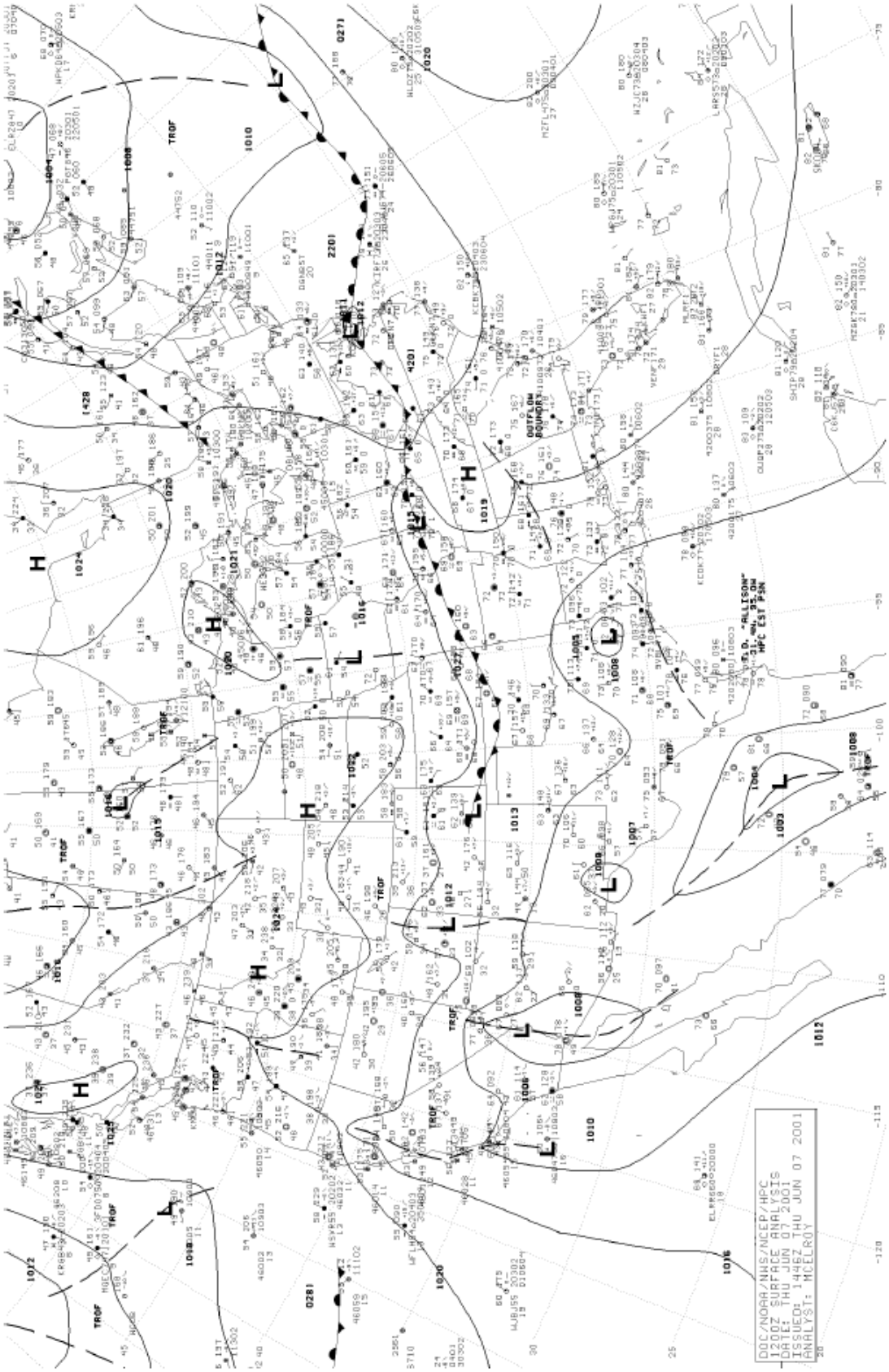
DOC/NOAA/NWS/NCEP/HPC
1200Z SURFACE ANALYSIS
DATE: THU JUN 07 2001
ISSUED: 1446Z THU JUN 07 2001
ANALYST: MCELROY

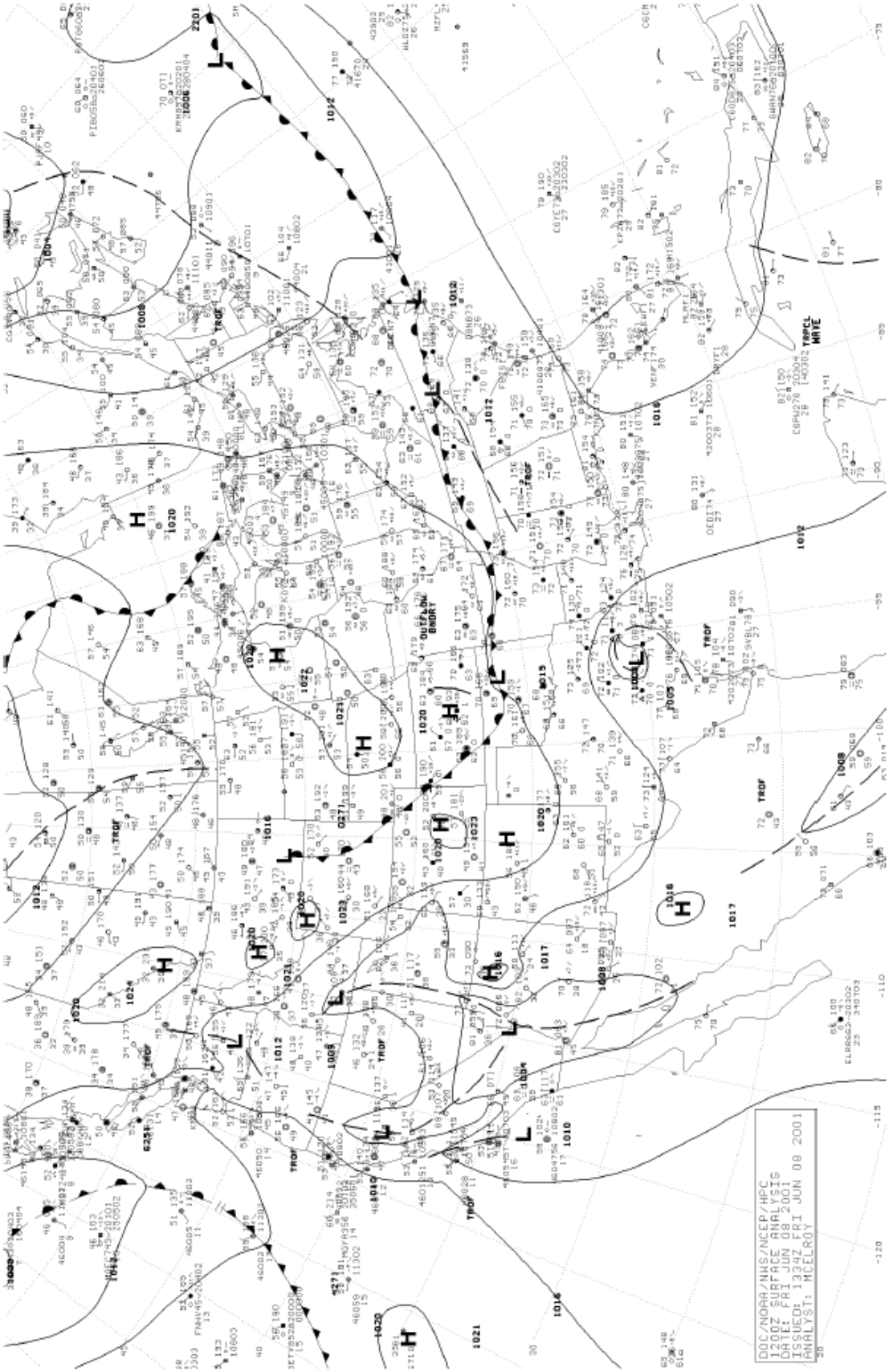
DOC/NOAA/NWS/NCEP/HPC
1200Z SURFACE ANALYSIS
DATE: FRI JUN 08 2001
ISSUED: 13HZ FRI JUN 08 2001
ANALYST: MCELROY

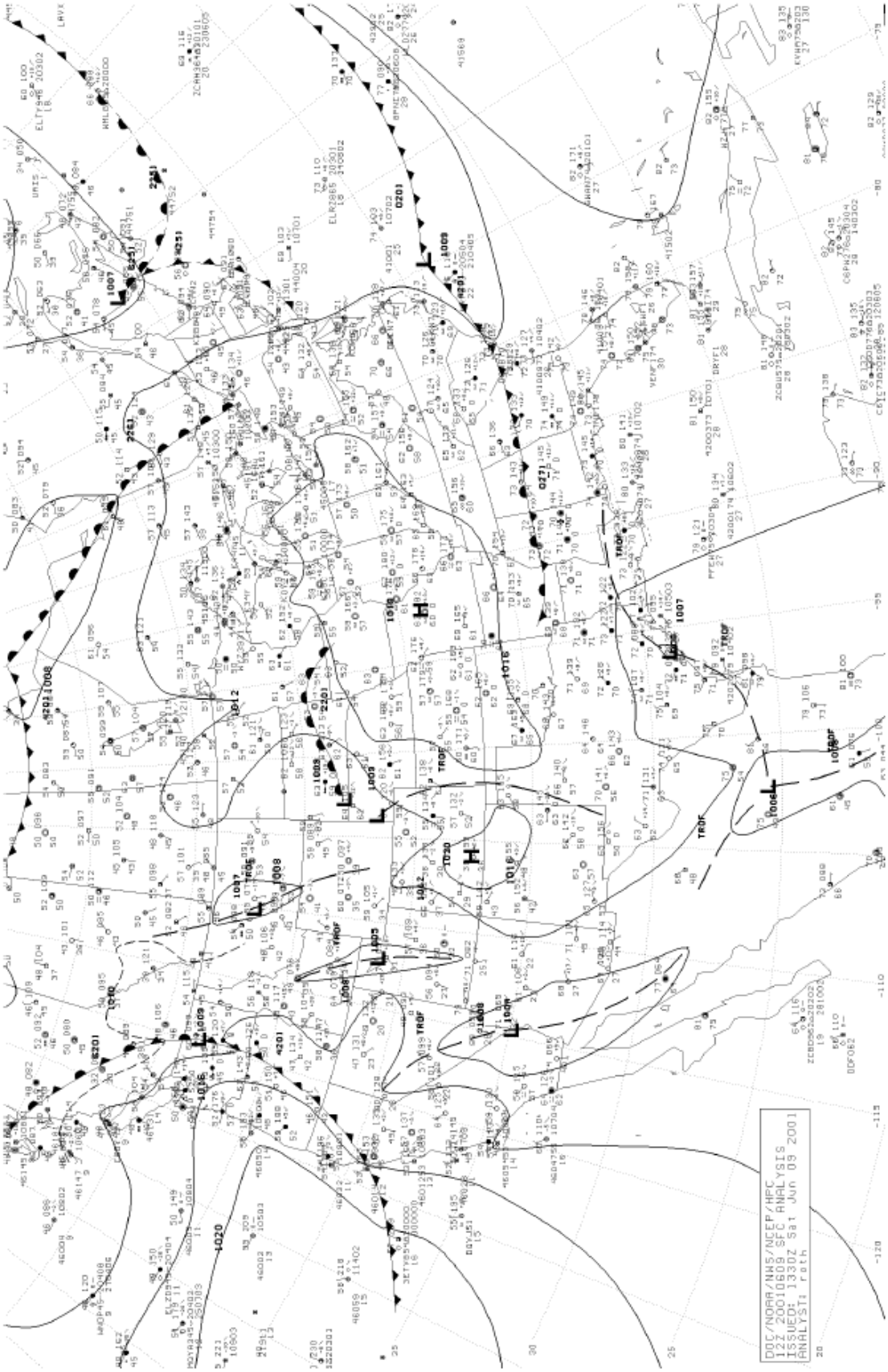
DOC/NOAA/NWS/NCEP/HPC
12Z 20010609 SFC ANALYSIS
ISSUED: 1330Z Sat Jun 09 2001
ANALYST: roth

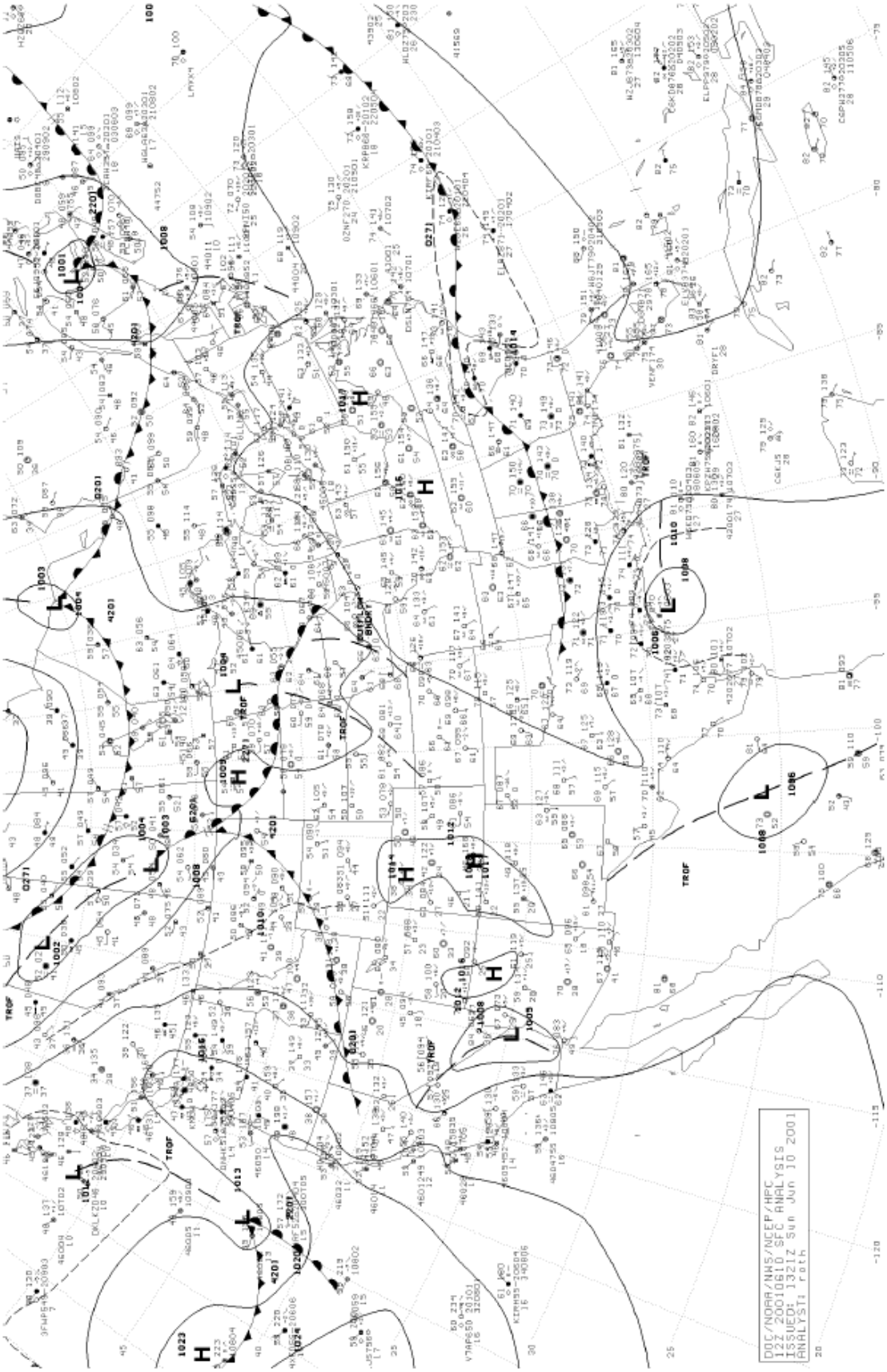
DOC/NOAA/NWS/NCEP/HPC
12Z 20010610 SFC ANALYSIS
ISSUED: 1321Z Sun Jun 10 2001
ANALYST: rath

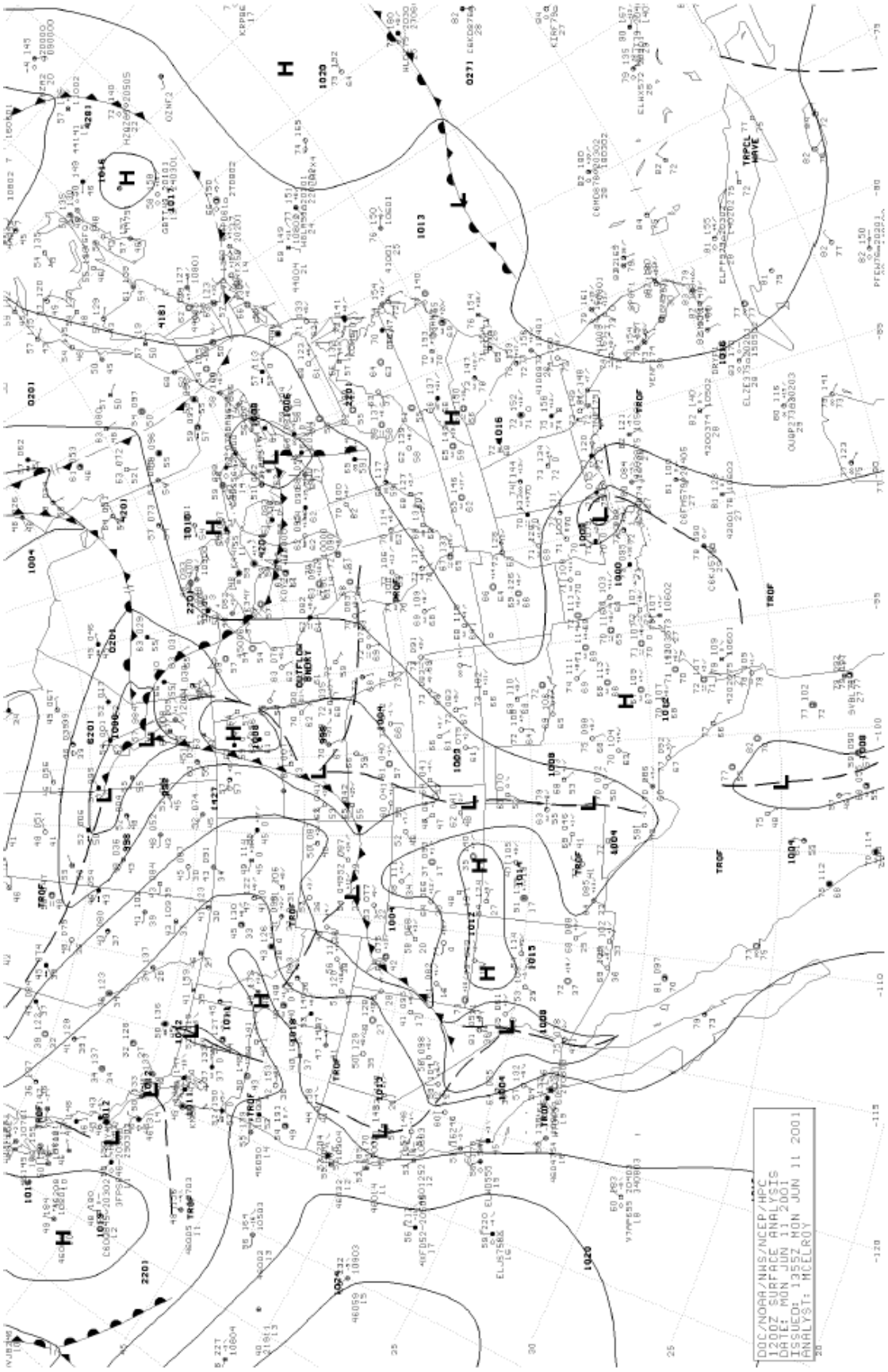
DOC/NOAA/NWS/NCEP/HPC
1200Z SURFACE ANALYSIS
DATE: MON JUN 11 2001
ISSUED: 1355Z MON JUN 11 2001
ANALYST: MCELROY

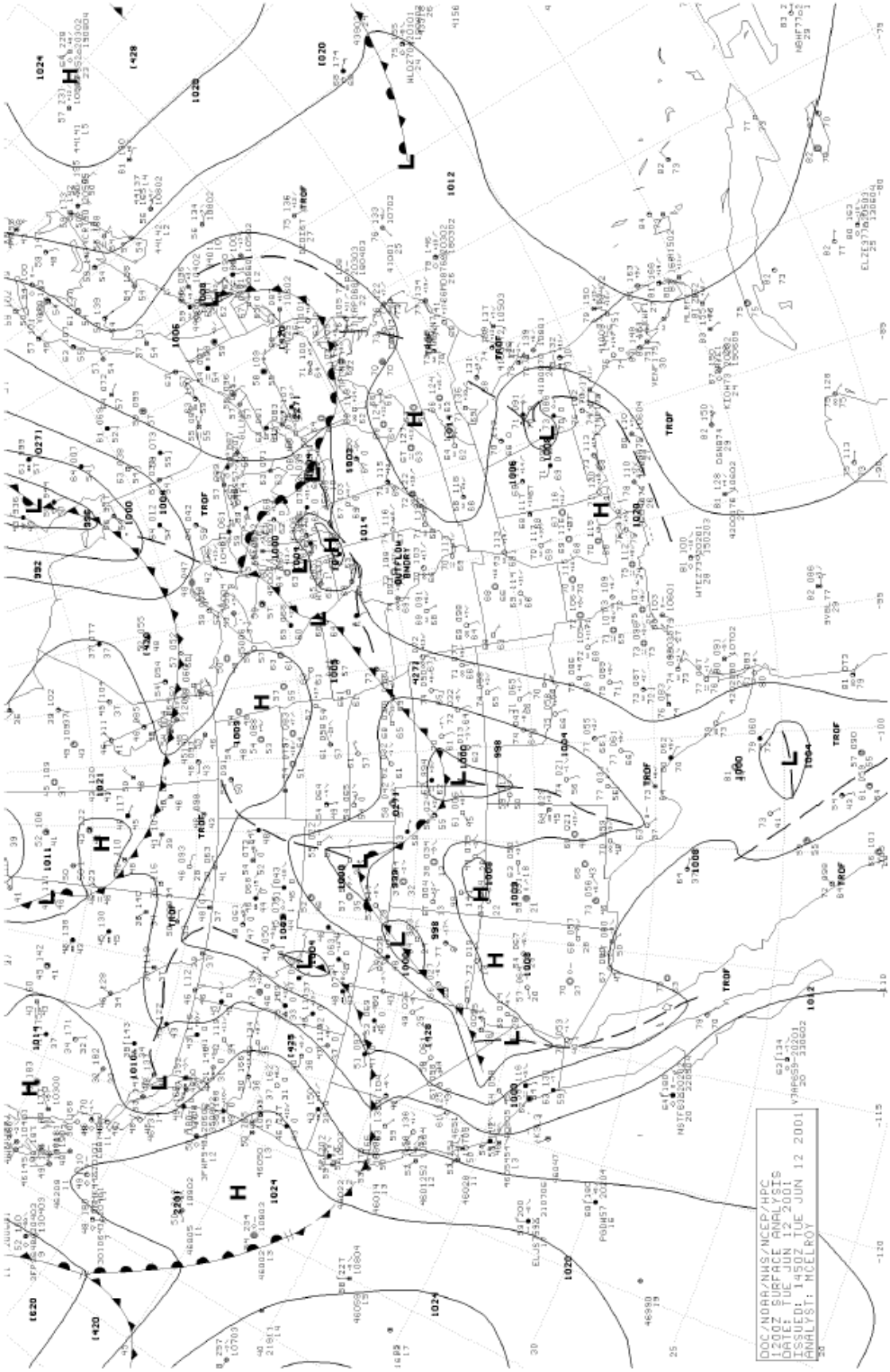
DOC/NOAA/NWS/NCEP/HPC
12002 SURFACE ANALYSIS
DATE: TUE JUN 12 2001
ISSUED: 1450Z TUE JUN 12 2001
ANALYST: MCELROY

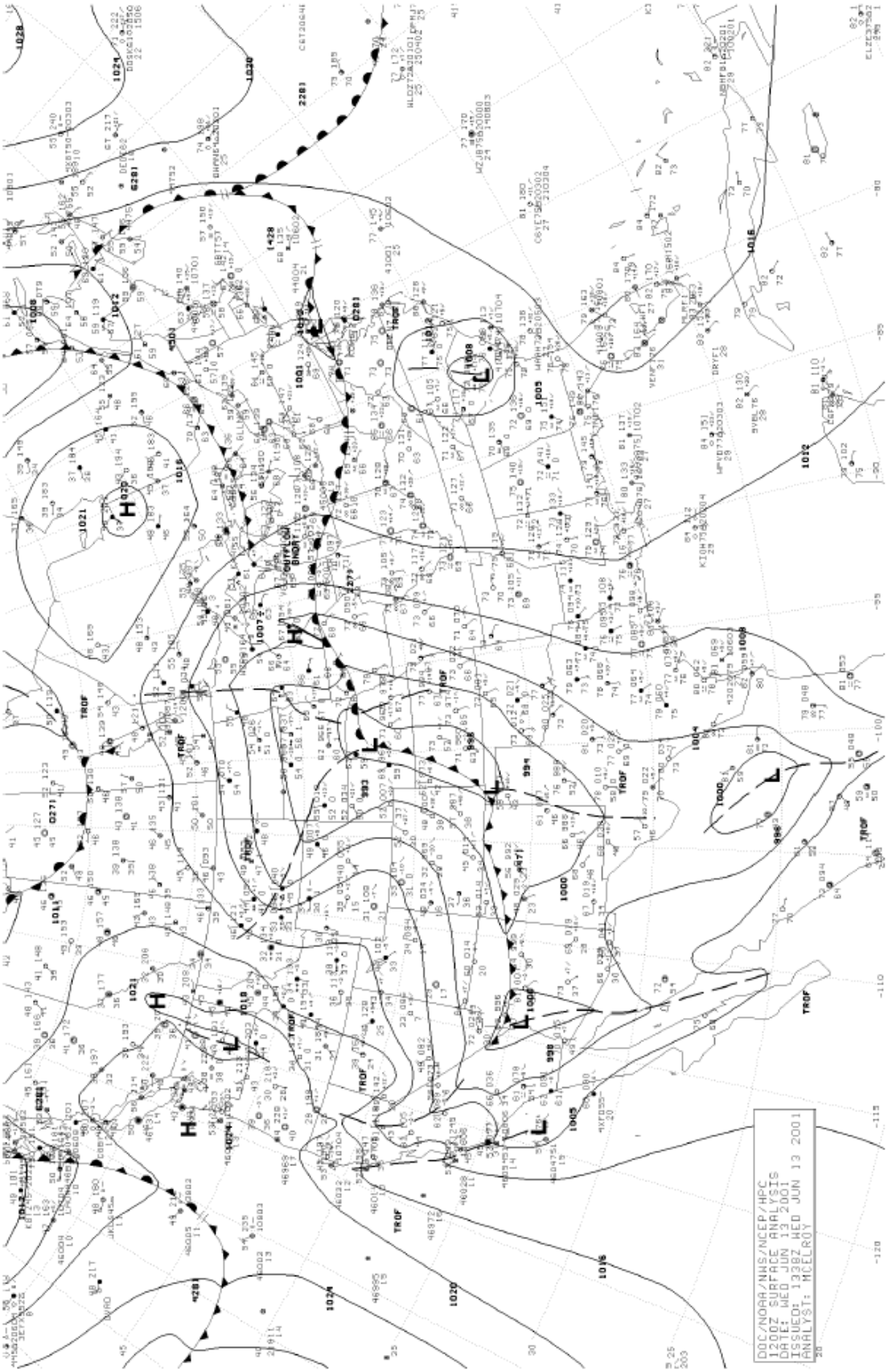
DOC/NOAA/NWS/NCEP/HPC
1200Z SURFACE ANALYSIS
DATE: WED JUN 13 2001
ISSUED: 1338Z WED JUN 13 2001
ANALYST: MCELROY

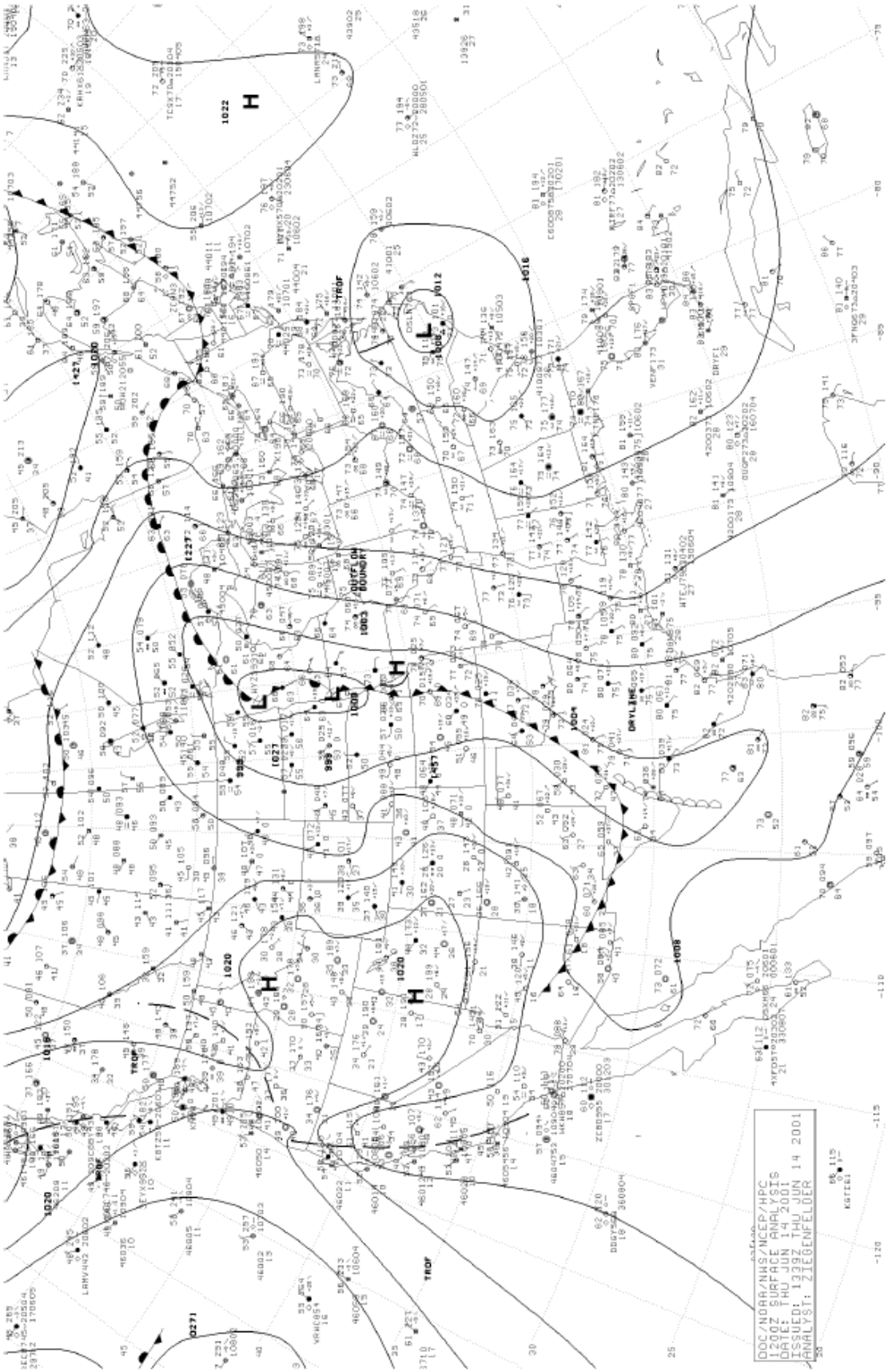
DOC/NOAA/NWS/NCEP/HPC
12002 SURFACE ANALYSIS
DATE: THU JUN 14 2001
ISSUED: 1339Z THU JUN 14 2001
ANALYST: ZIEGENFELDER

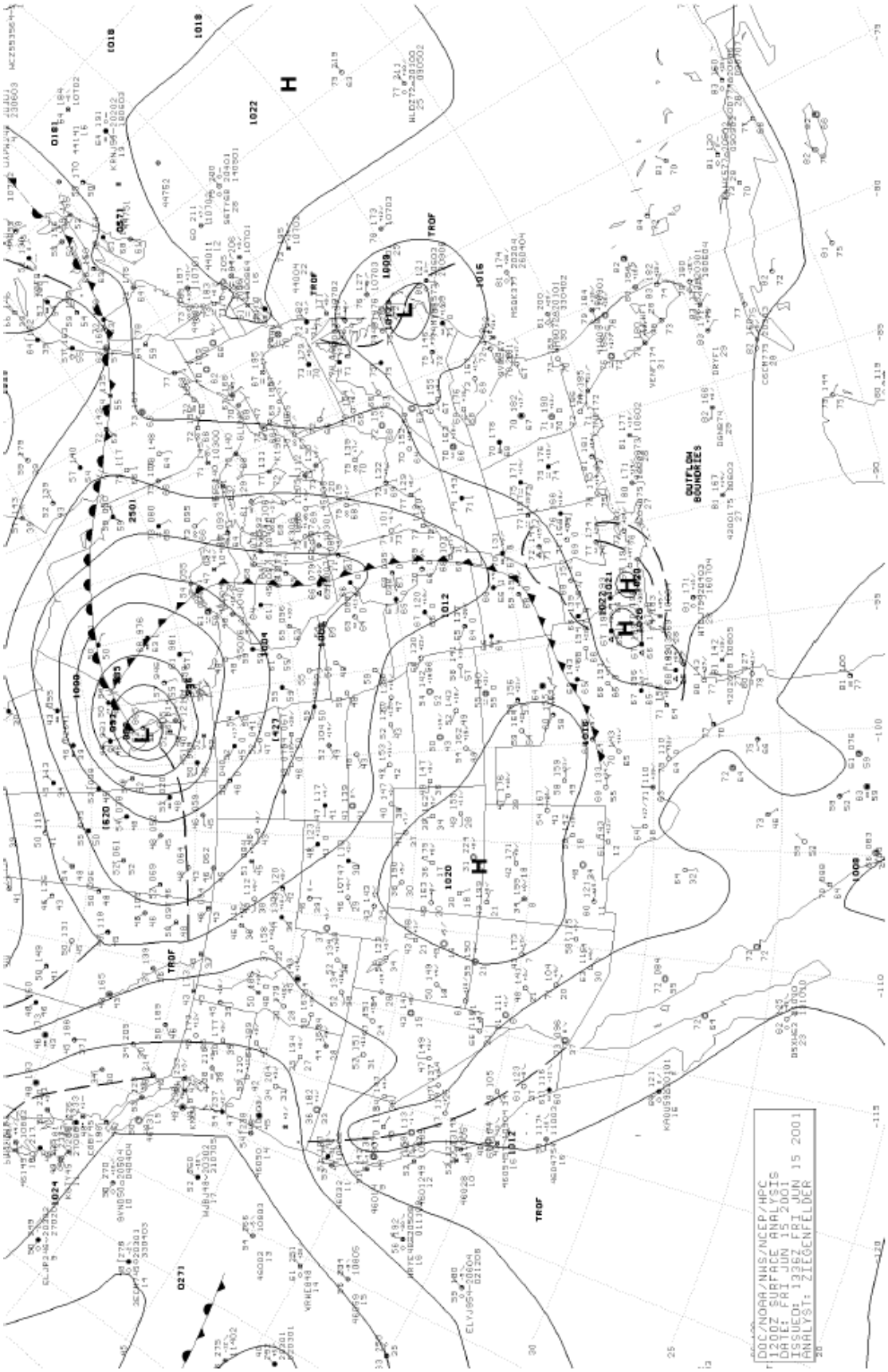
DOC/NOAA/NWS/NCEP/HPC
1200Z SURFACE ANALYSIS
DATE: FRI JUN 15 2001
ISSUED: 1336Z FRI JUN 15 2001
ANALYST: ZIEGENFELDER

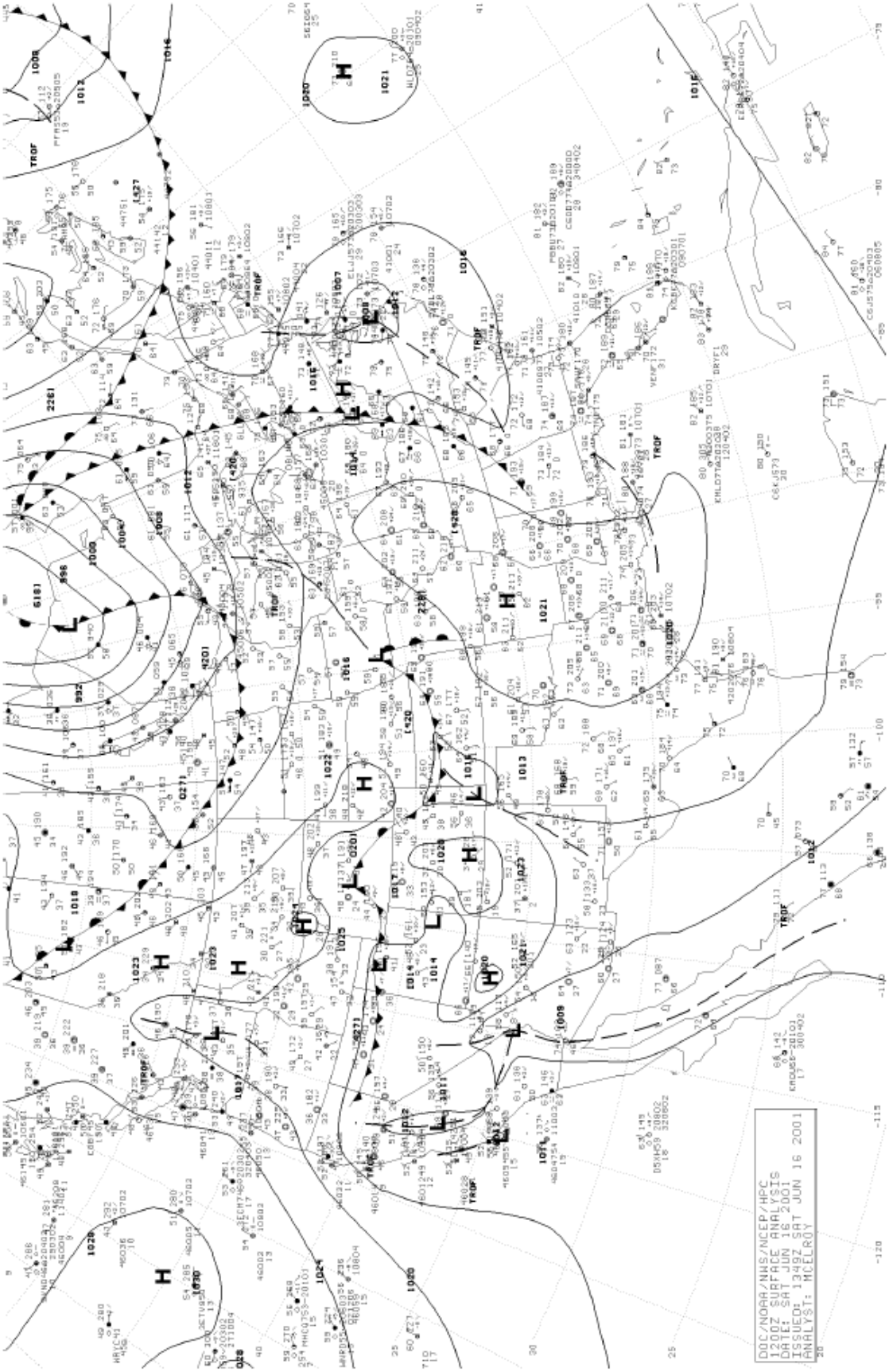
DOC/NOAA/NWS/NCEP/HPC
1200Z SURFACE ANALYSIS
DATE: SAT JUN 16 2001
ISSUED: 1349Z SAT JUN 16 2001
ANALYST: MCELROY

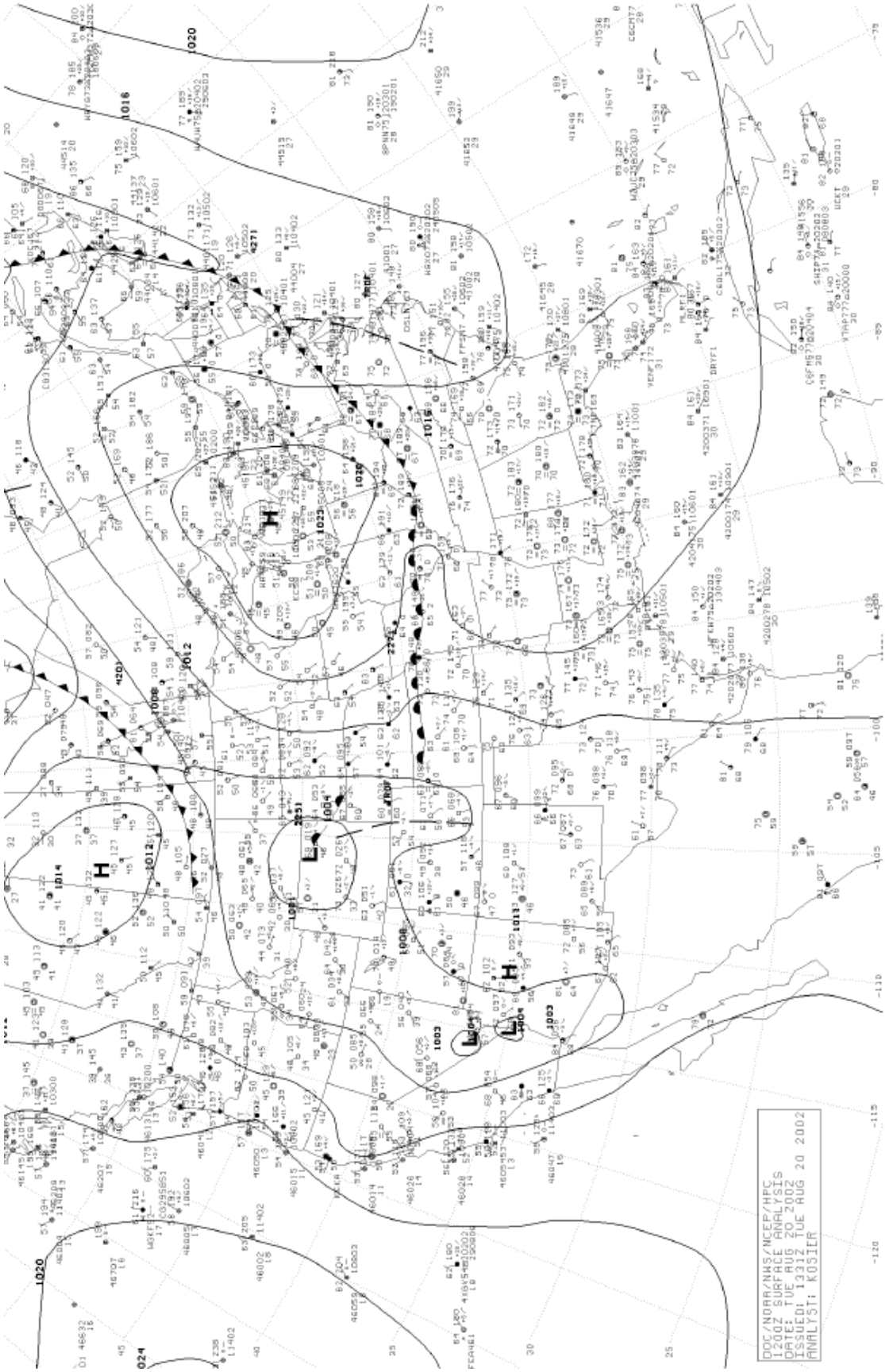
DOC/NOAA/NWS/NCEP/HPC
1200Z SURFACE ANALYSIS
DATE: TUE AUG 20 2002
ISSUED: 1331Z TUE AUG 20 2002
ANALYST: KOSIER

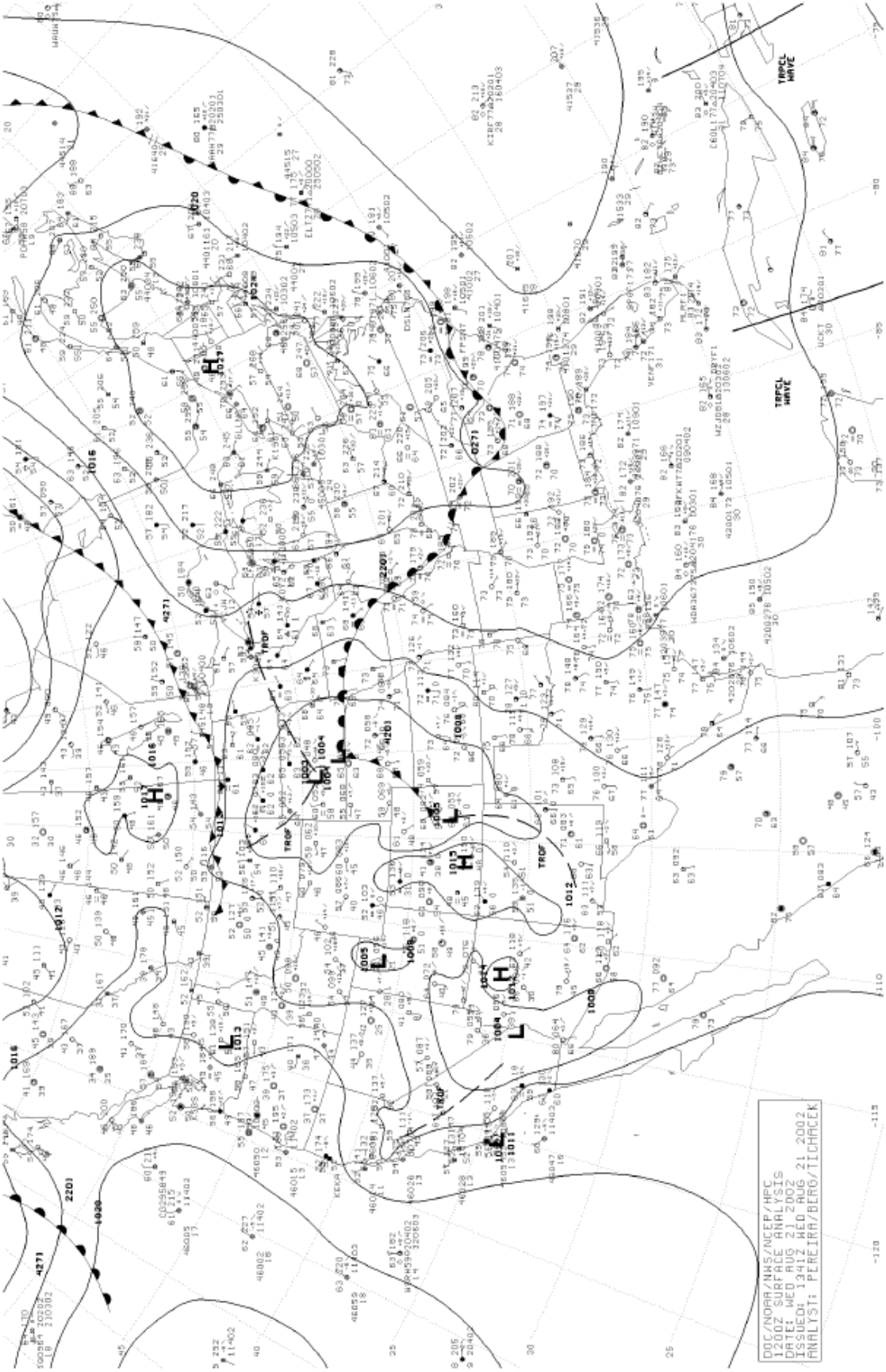
DOC/NOAA/NWS/NCEP/HPC
12002 SURFACE ANALYSIS
DATE: WED AUG 21 2002
ISSUED: 1417 WED AUG 21 2002
ANALYST: PEREIRA/BERG/TICHACEK

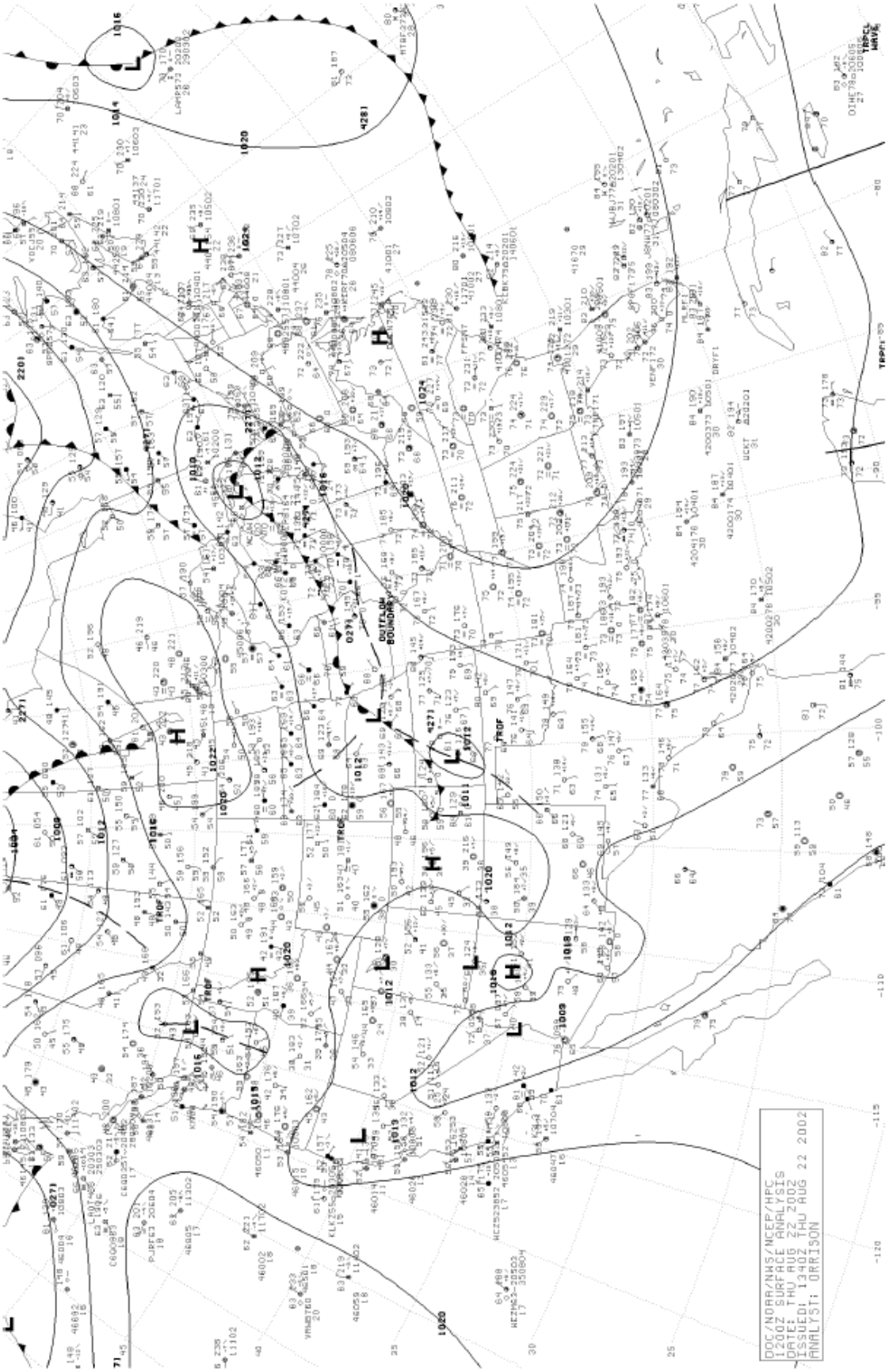
DOC/NOAA/NWS/NCEP/HPC
1200Z SURFACE ANALYSIS
DATE: THU AUG 22 2002
ISSUED: 1340Z THU AUG 22 2002
ANALYST: GRAISON

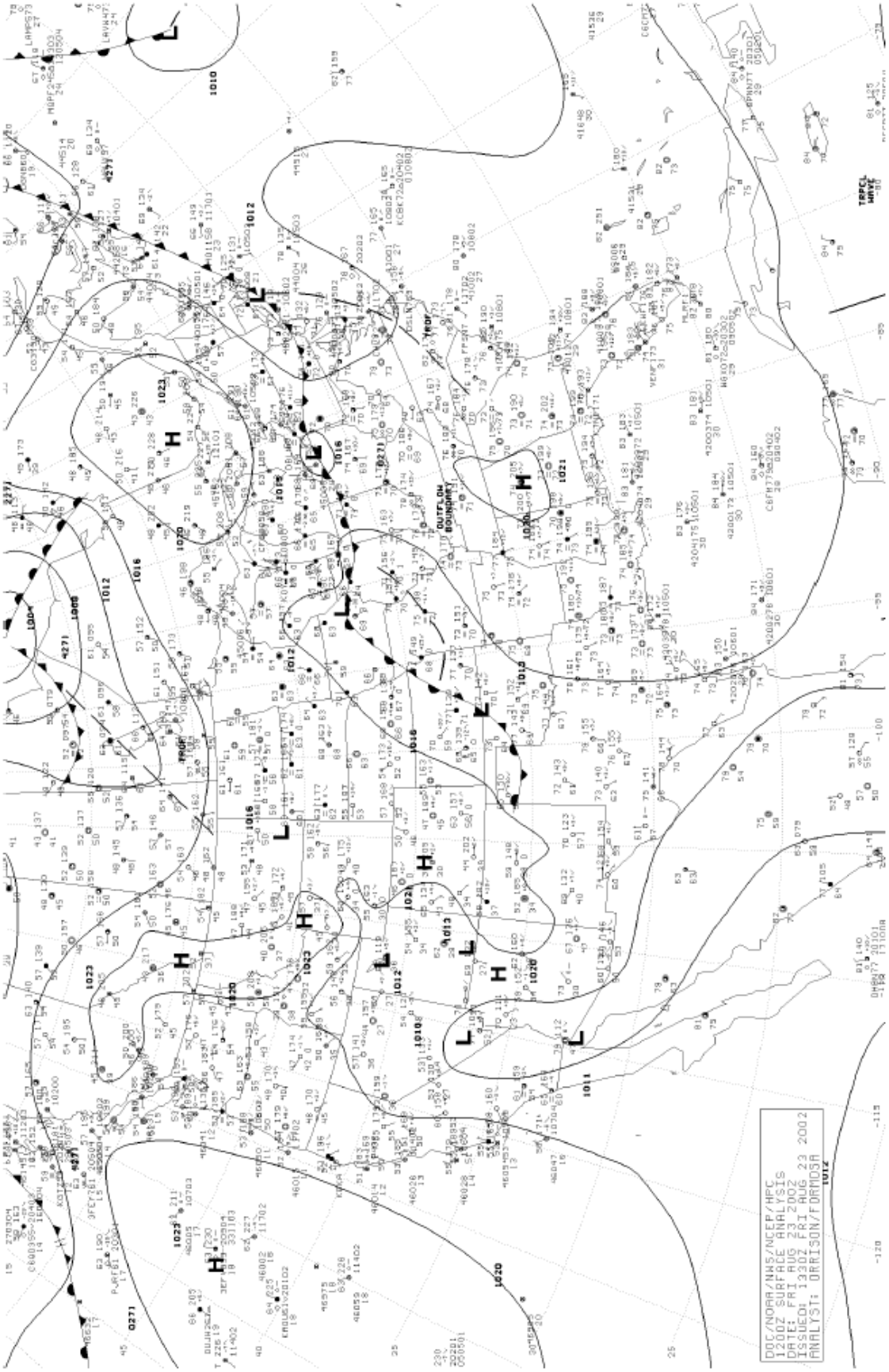
DOC/NOAA/NWS/NCEP/HPC
1200Z SURFACE ANALYSIS
DATE: FRI AUG 23 2002
ISSUED: 1300Z FRI AUG 23 2002
ANALYST: ORRISON/FORMOSA

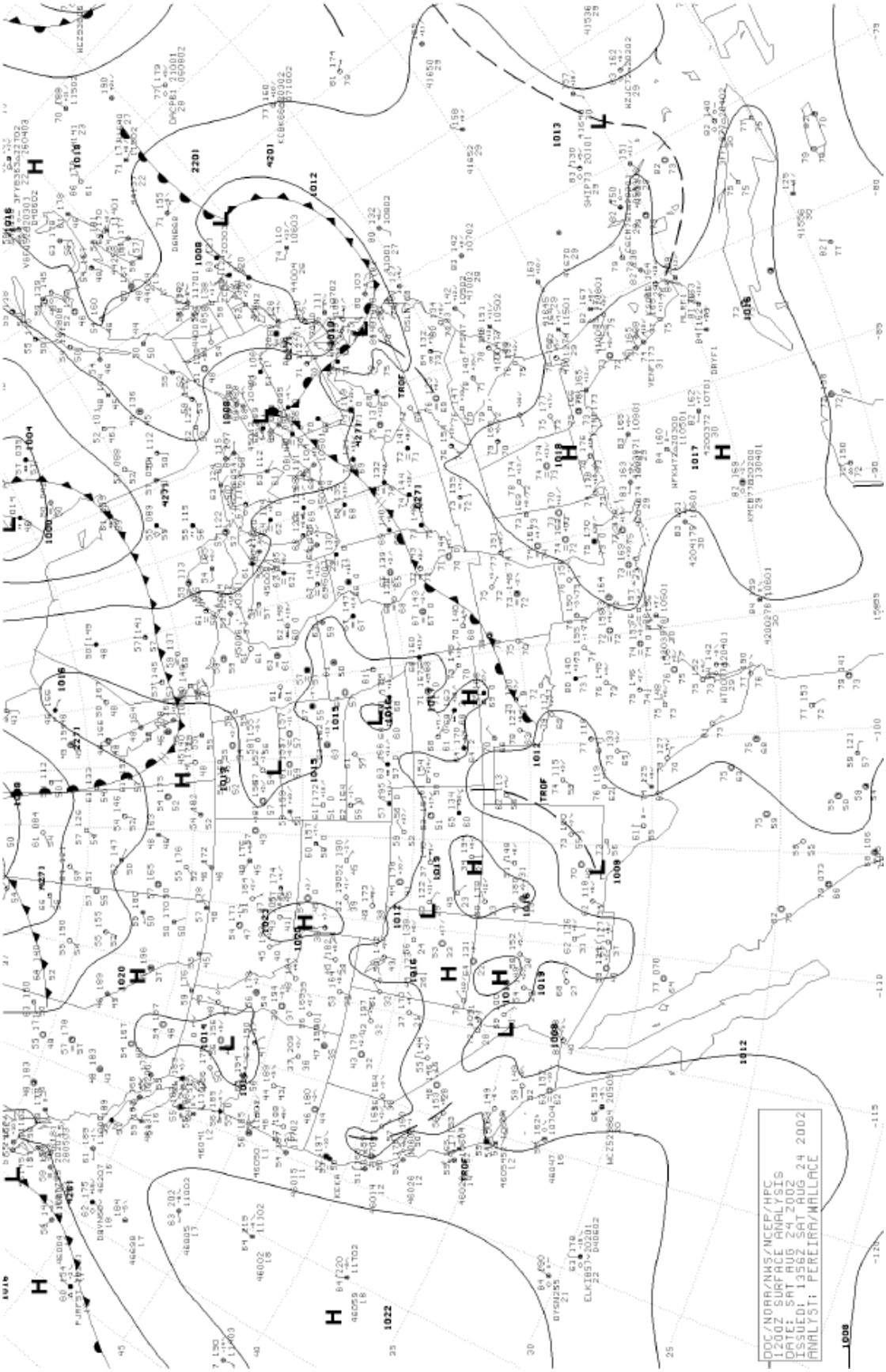
DOC/NOAA/NWS/NCEP/HPC
1200Z SURFACE ANALYSIS
DATE: SAT AUG 24 2002
ISSUED: 1356Z SAT AUG 24 2002
ANALYST: PEREIRA/WALLACE

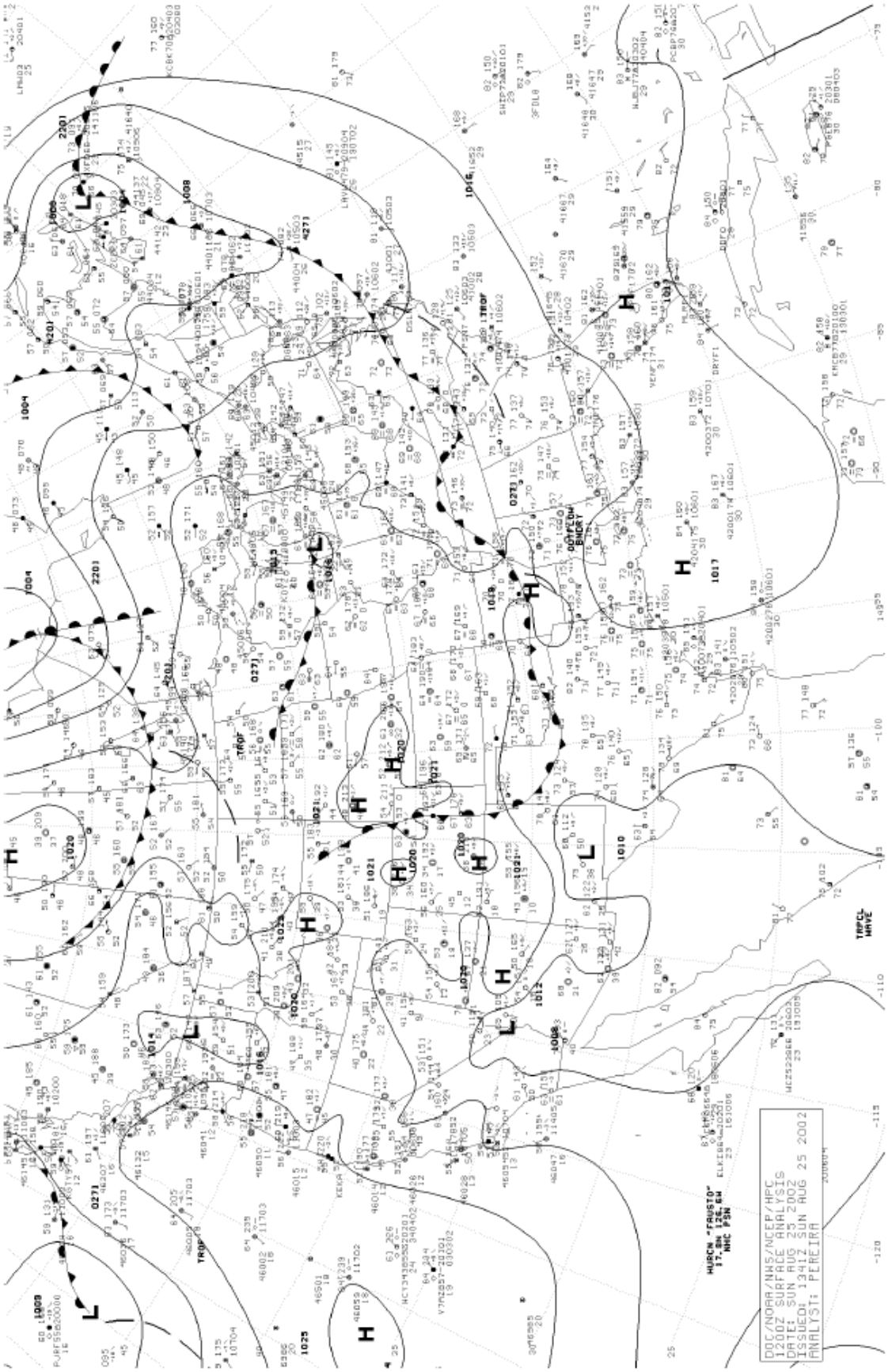
DOC/NOAA/NWS/NCEP/HPC
12OOZ SURFACE ANALYSIS
DATE: SUN AUG 25 2002
ISSUED: 13HLZ SUN AUG 25 2002
ANALYST: PEREIRA

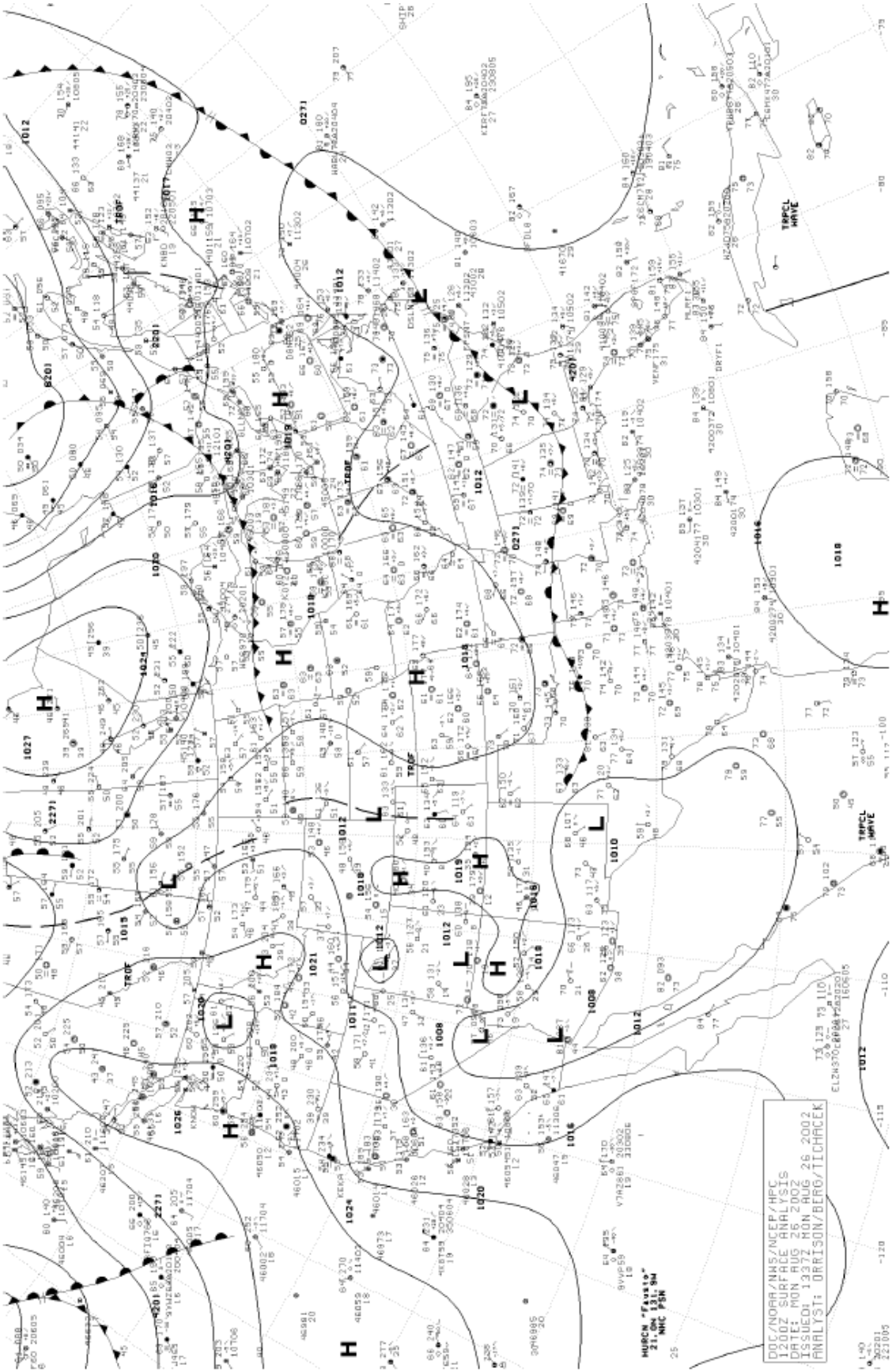
DOC/NOAA/NWS/NCEP/HPC
1200Z SURFACE ANALYSIS
DATE: MON AUG 26 2002
ISSUED: 1337Z MON AUG 26 2002
ANALYST: ORRISON/BERG/TICHACEK

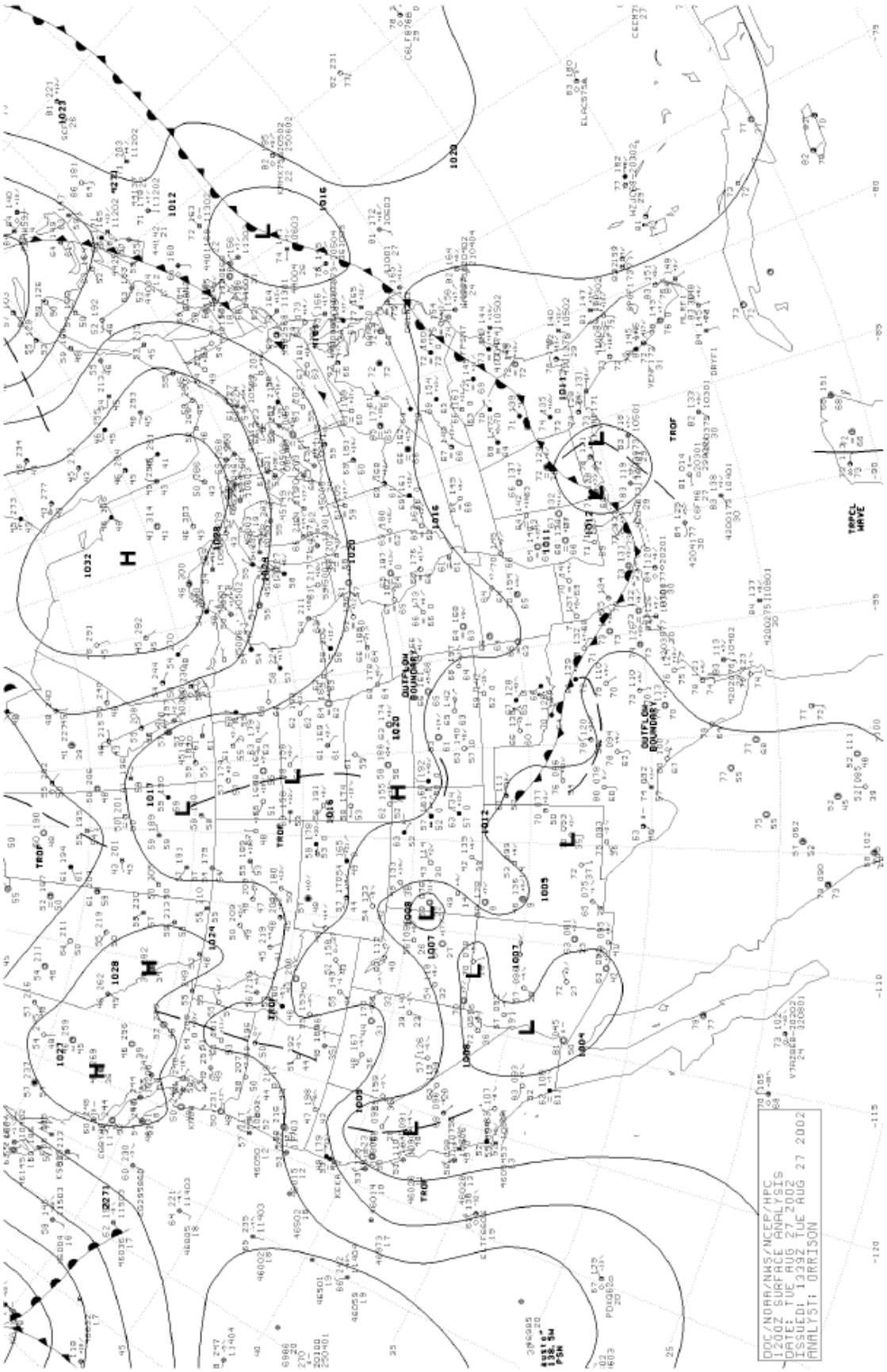
DOC/NOAA/NWS/NCEP/HPC
1200Z SURFACE ANALYSIS
DATE: TUE AUG 27 2002
ISSUED: 1339Z TUE AUG 27 2002
ANALYST: ORRISON

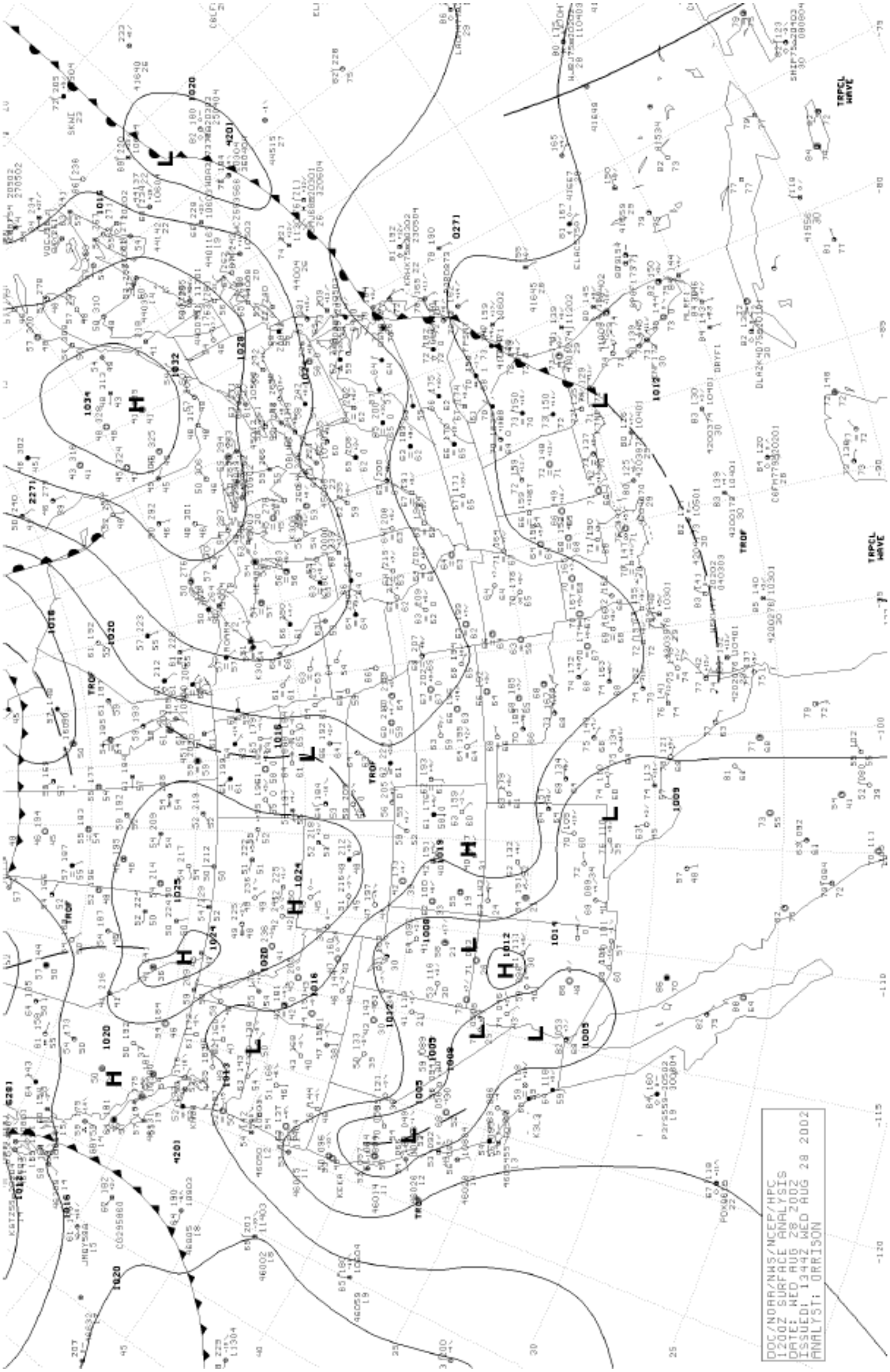
DOC/NOAA/NWS/NCEP/HPC
1200Z SURFACE ANALYSIS
DATE: WED AUG 28 2002
ISSUED: 1344Z WED AUG 28 2002
ANALYST: ORRISON

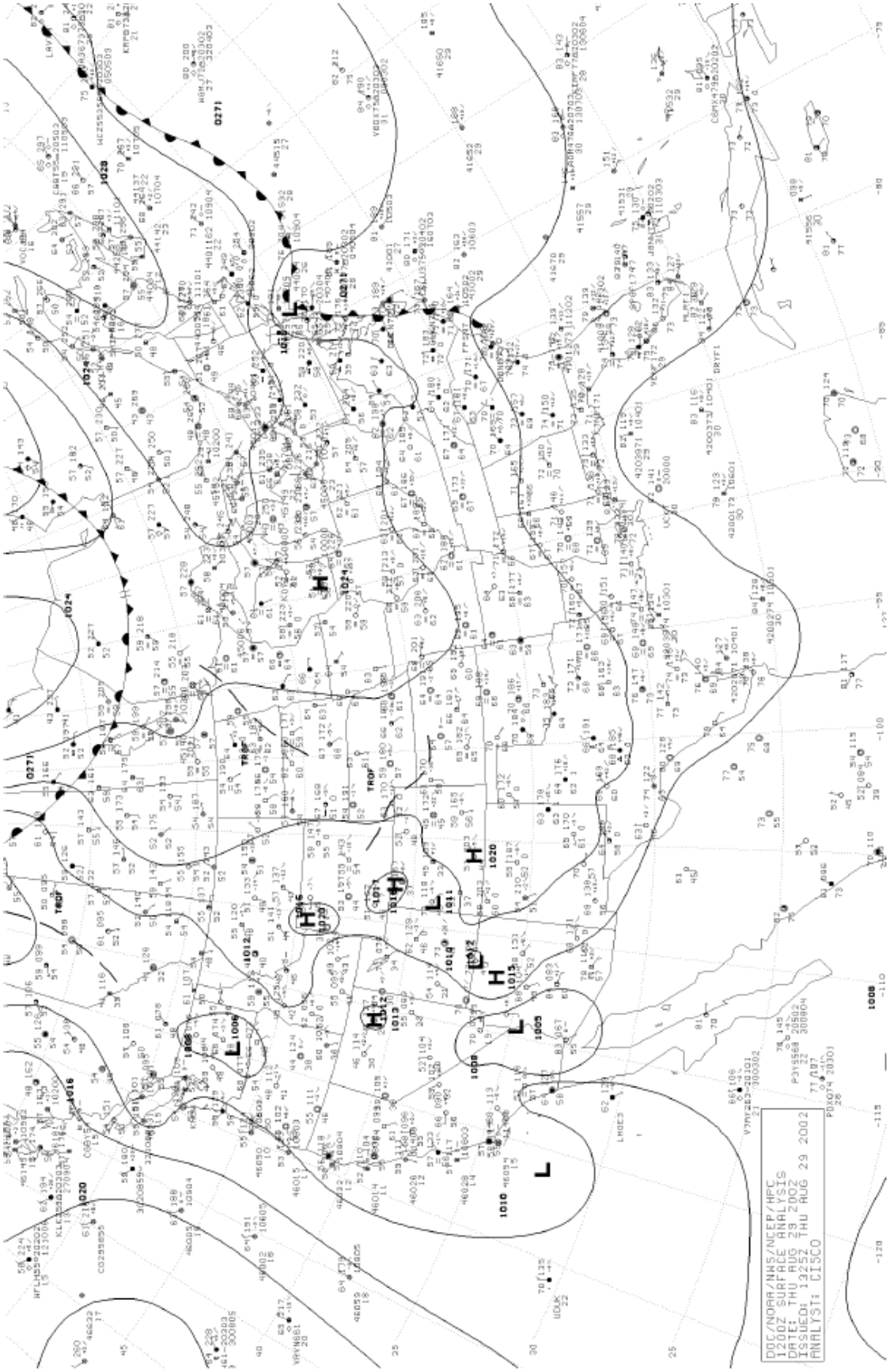
DOC/NOAA/NWS/NCEP/HPC
1200Z SURFACE ANALYSIS
DATE: THU AUG 29 2002
ISSUED: 1325Z THU AUG 29 2002
ANALYST: CISCO

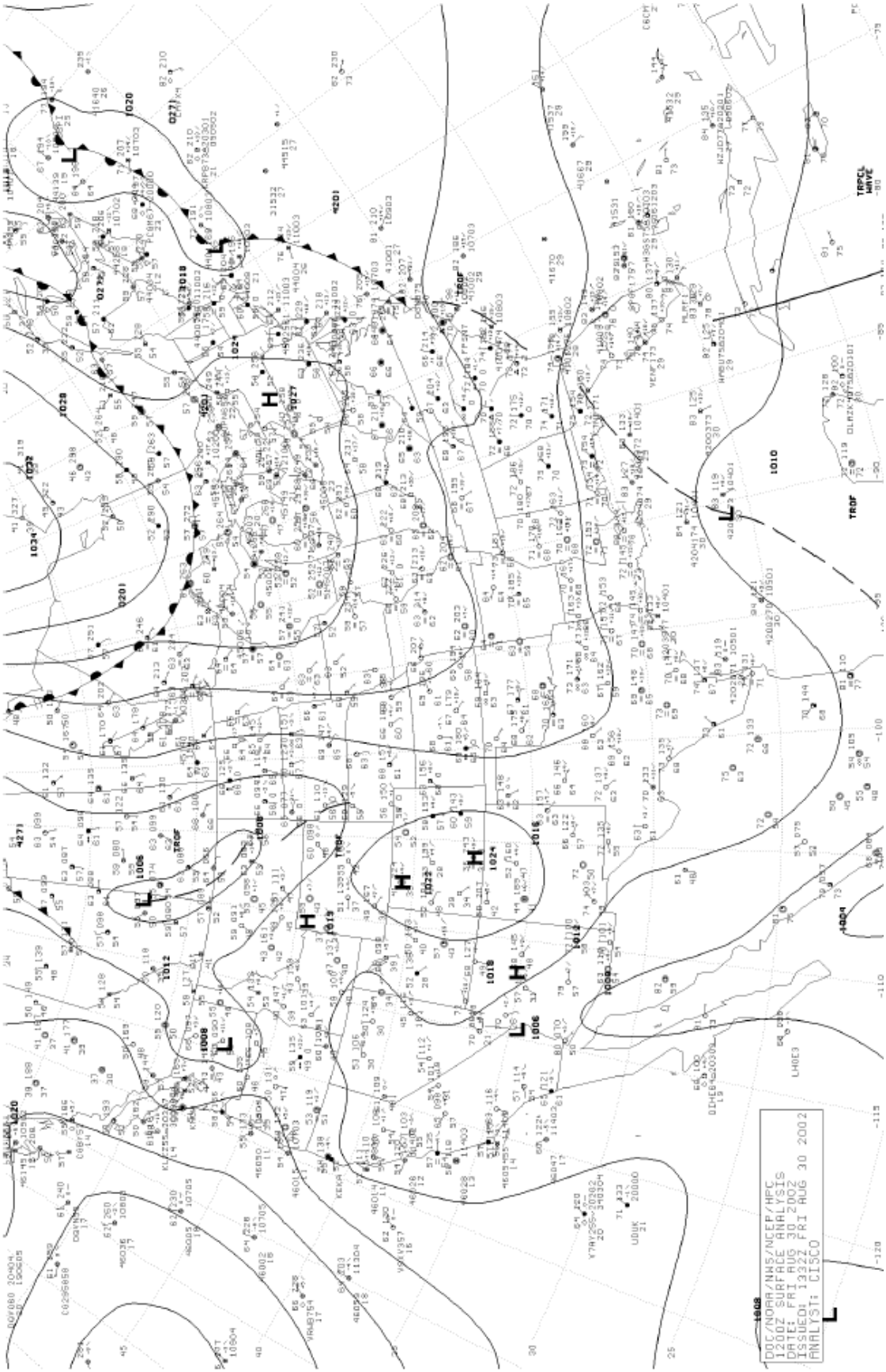
DOC/NOAA/NWS/NCEP/HPC
1200Z SURFACE ANALYSIS
DATE: FRI AUG 30 2002
ISSUED: 1332Z FRI AUG 30 2002
ANALYST: CISCO

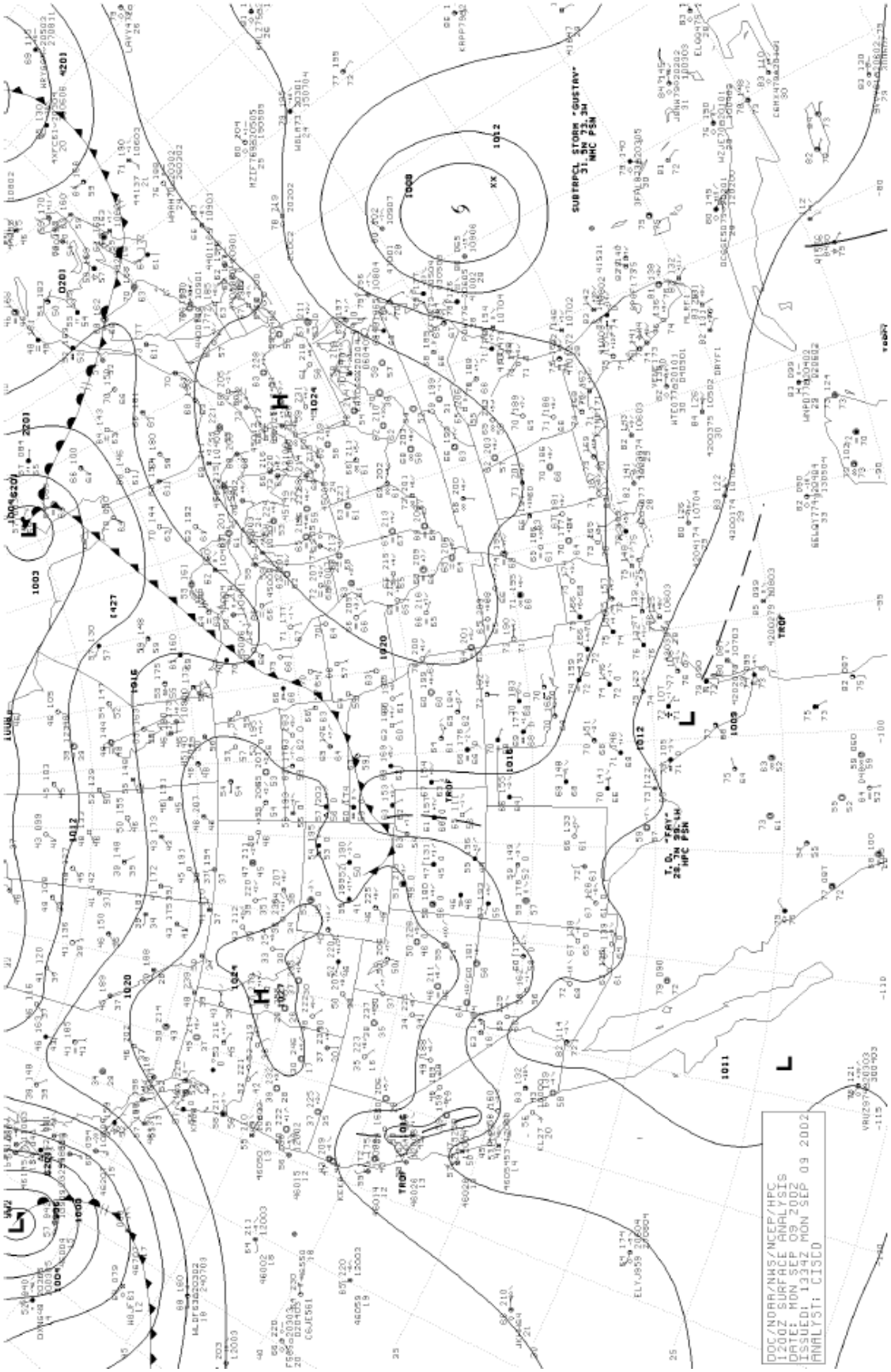
DOC/NOAA/NWS/NCEP/HPC
1200Z SURFACE ANALYSIS
DATE: MON SEP 09 2002
ISSUED: 1334Z MON SEP 09 2002
ANALYST: CISCO

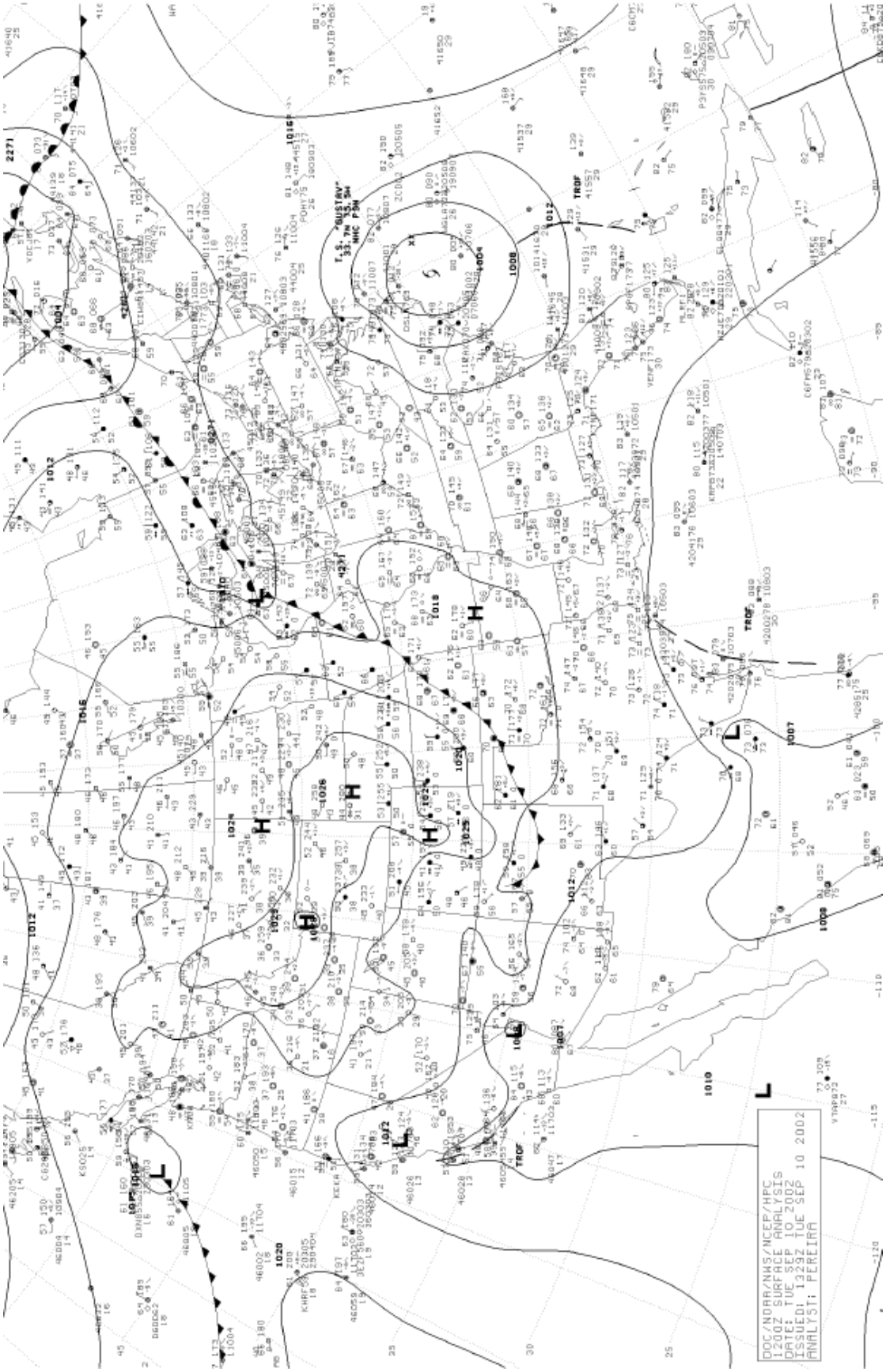
DOC/NOAA/NWS/NCEP/HPC
1200Z SURFACE ANALYSIS
DATE: TUE SEP 10 2002
ISSUED: 1329Z TUE SEP 10 2002
ANALYST: PEREIRA

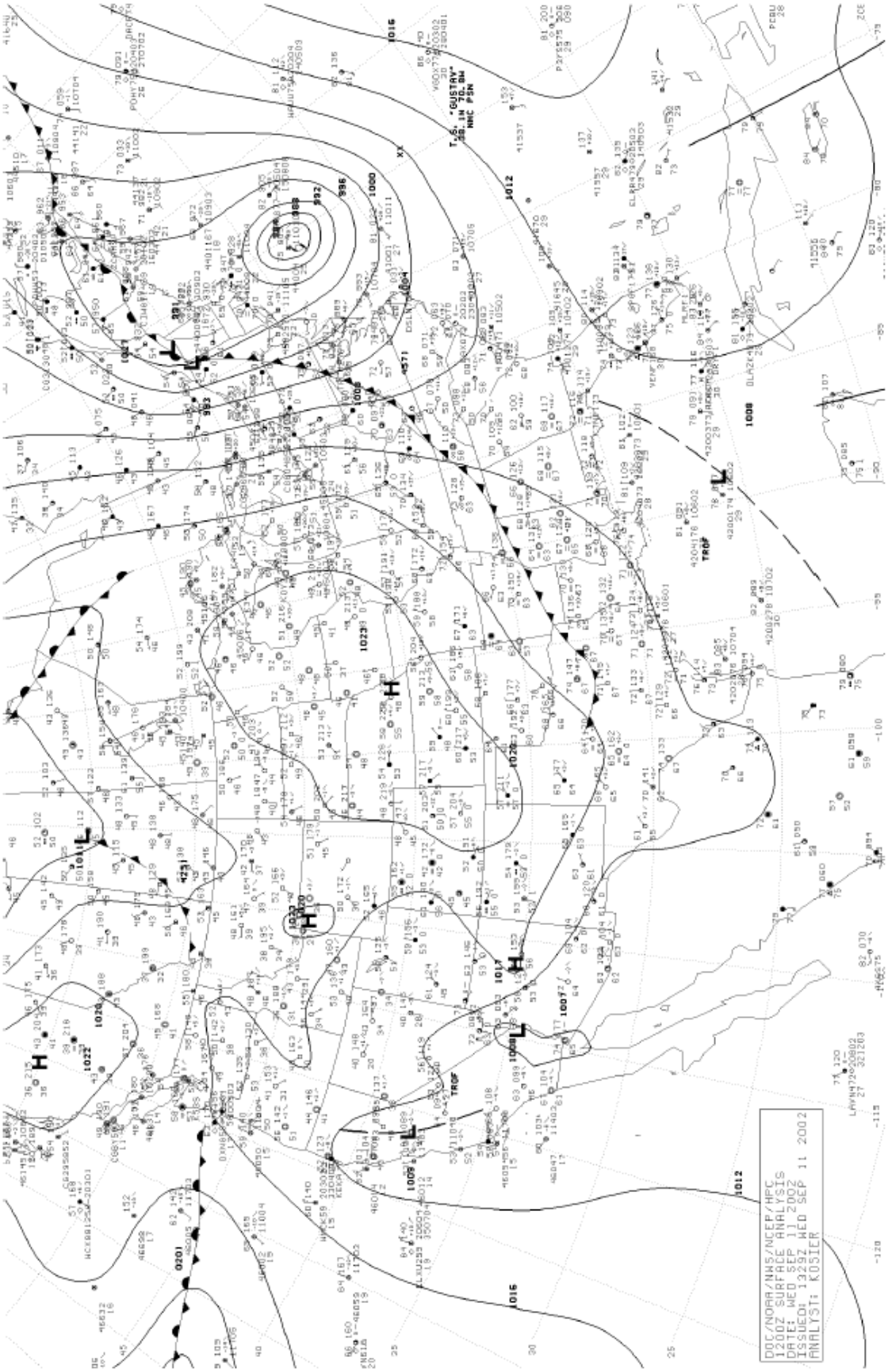
DOC/NOAA/NWS/NCEP/HPC
1200Z SURFACE ANALYSIS
DATE: WED SEP 11 2002
ISSUED: 1329Z WED SEP 11 2002
ANALYST: KOSIER

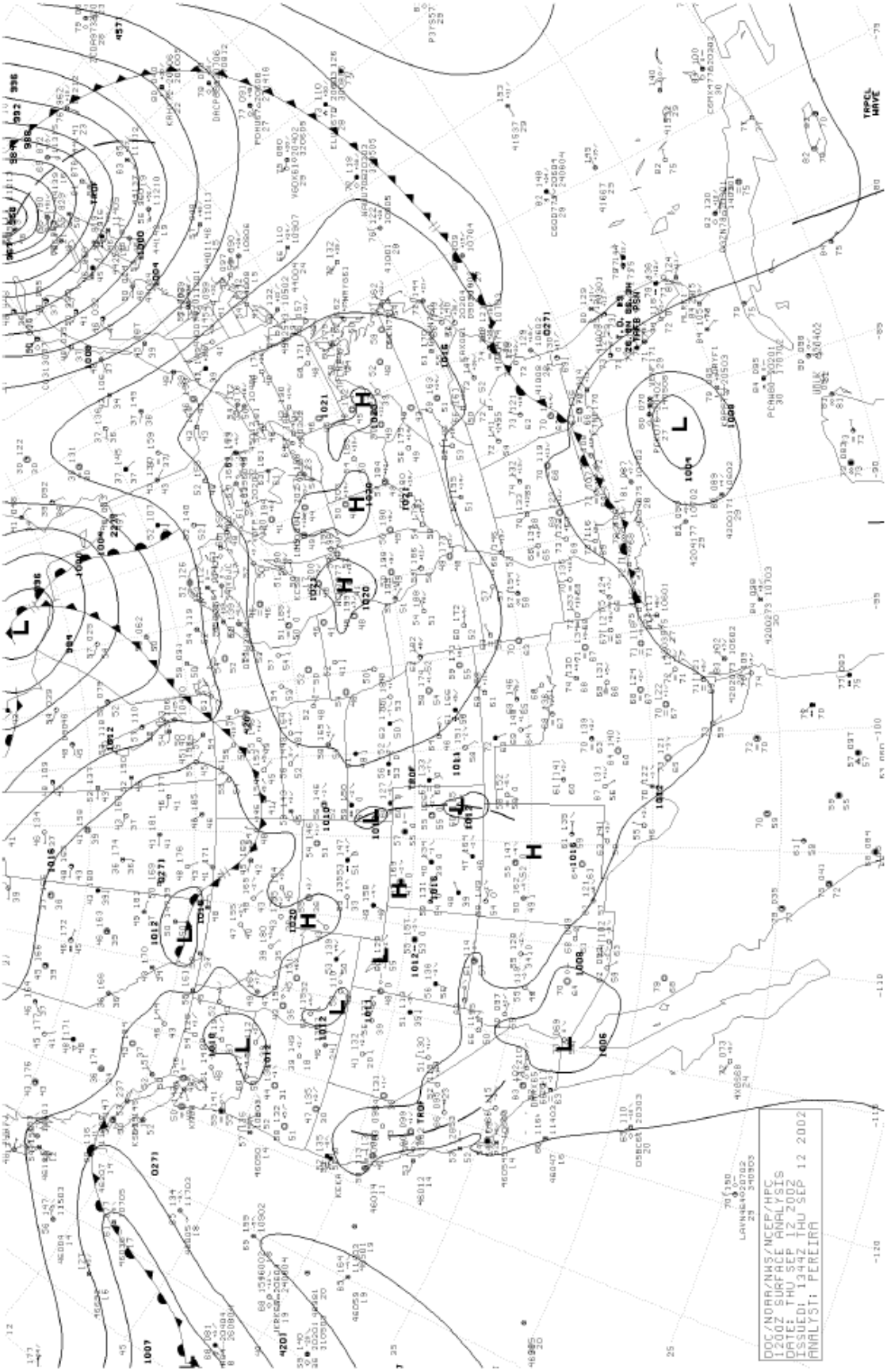
DOC/NOAA/NWS/NCEP/HPC
1200Z SURFACE ANALYSIS
DATE: THU SEP 12 2002
ISSUED: 1344Z THU SEP 12 2002
ANALYST: PEREIRA

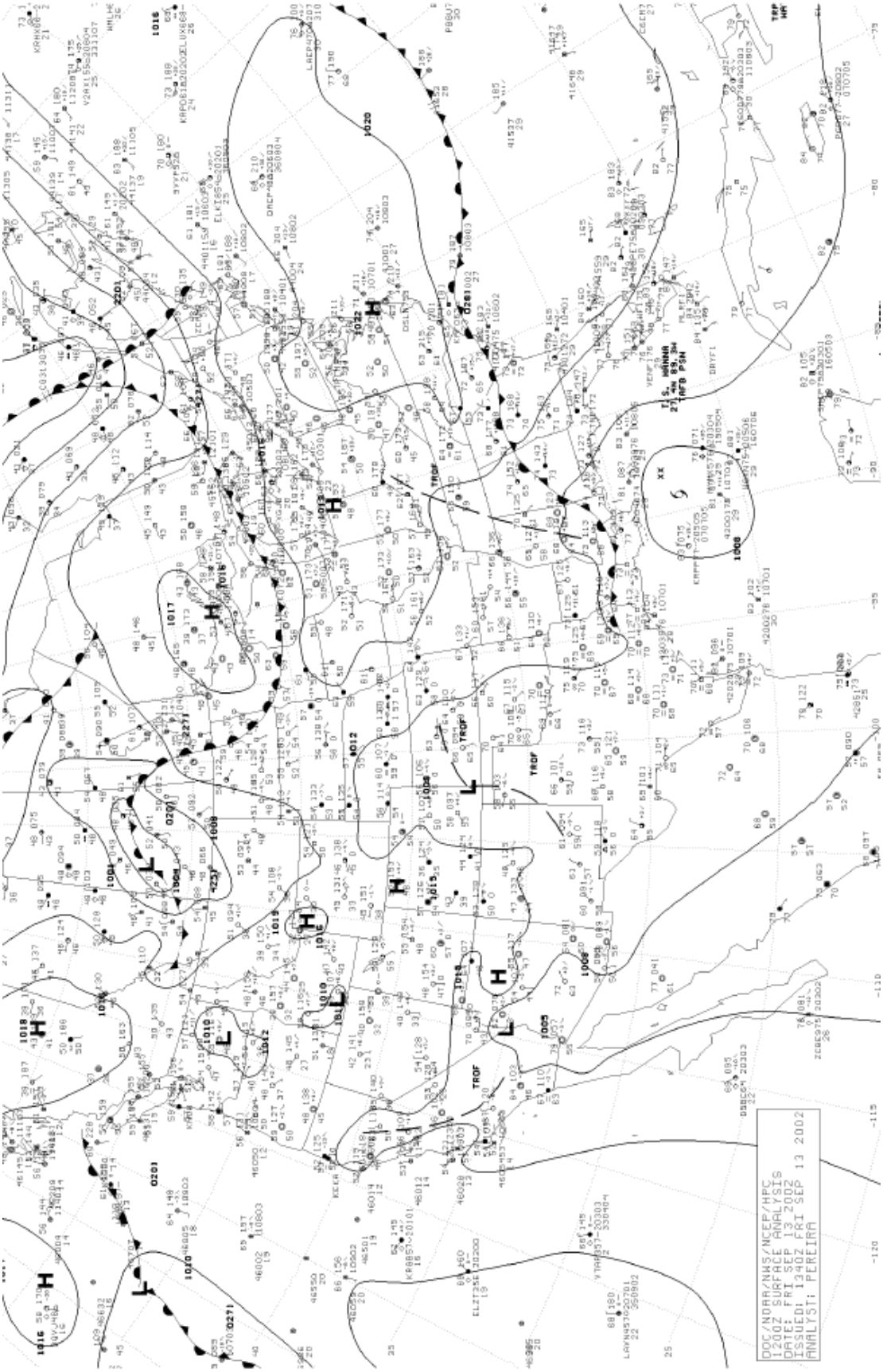
DOC/NOAA/NWS/NCEP/HPC
1200Z SURFACE ANALYSIS
DATE: FRI SEP 13 2002
ISSUED: 1340Z FRI SEP 13 2002
ANALYST: PEREIRA

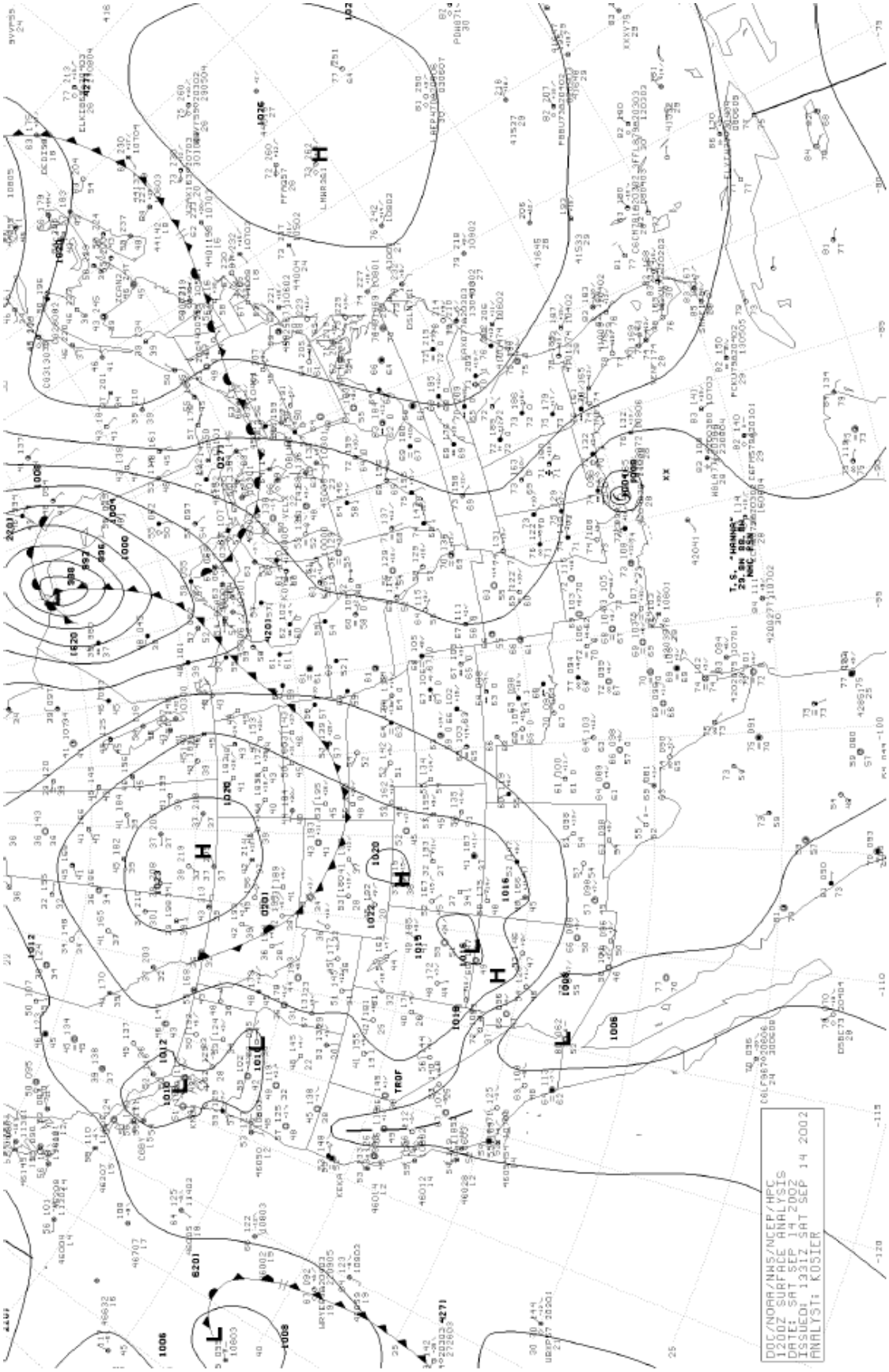
DOC/NOAA/NWS/NCEP/HPC
1200Z SURFACE ANALYSIS
DATE: SAT SEP 14 2002
ISSUED: 1331Z SAT SEP 14 2002
ANALYST: KOSIER

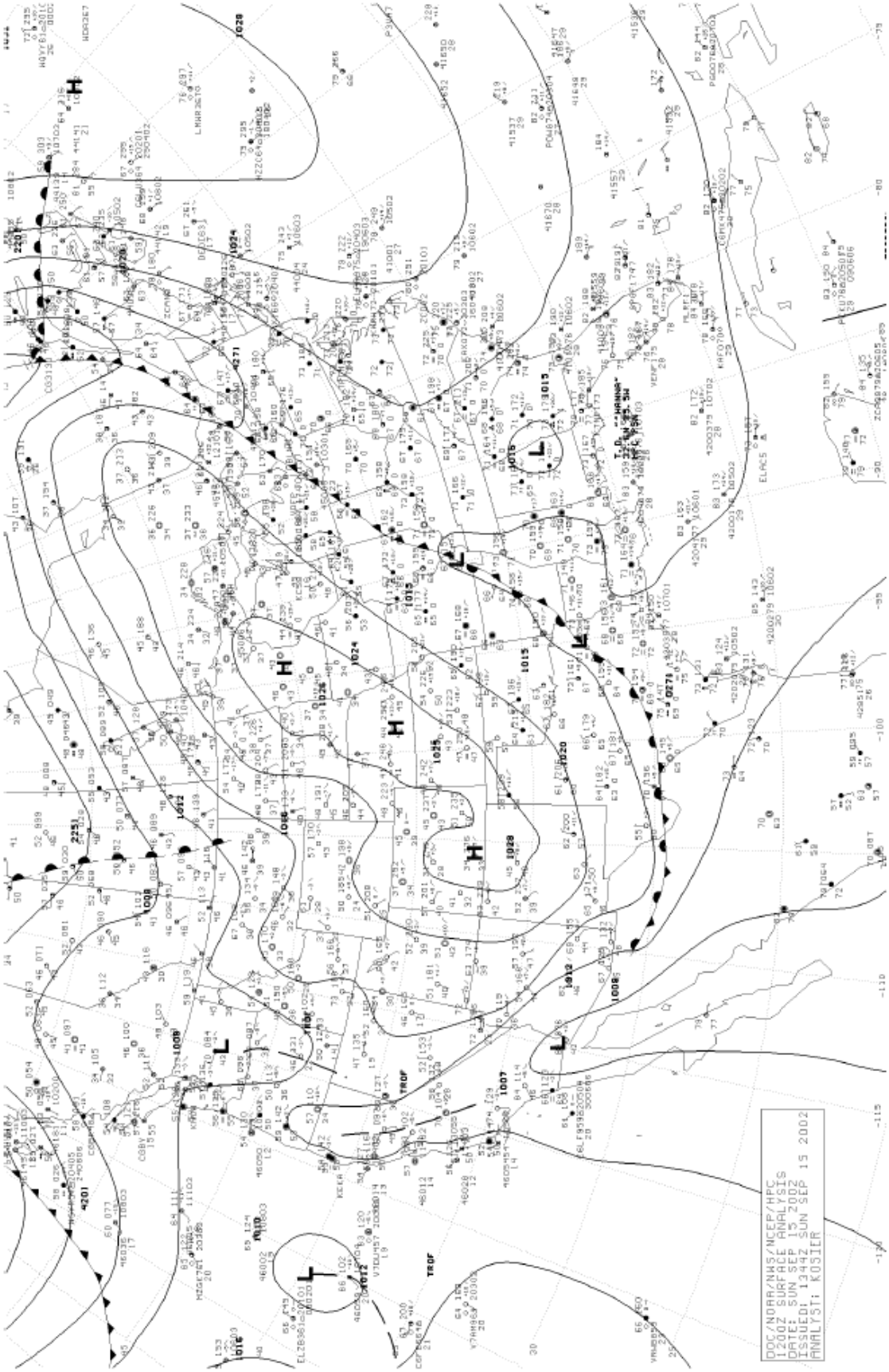
DOC/NOAA/NWS/NCEP/HPC
1200Z SURFACE ANALYSIS
DATE: SUN SEP 15 2002
ISSUED: 1342Z SUN SEP 15 2002
ANALYST: KOSIER

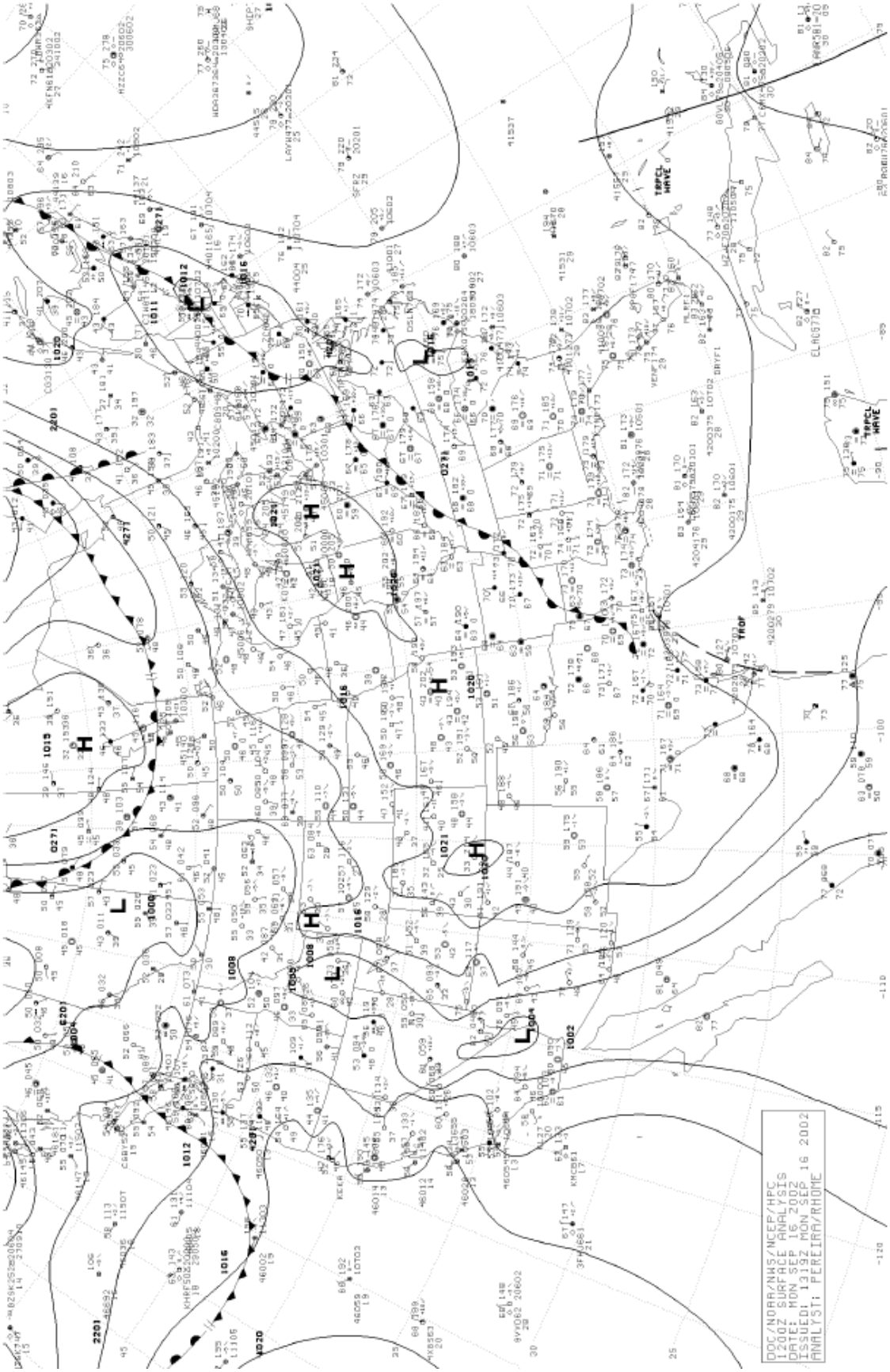
DOC/NOAA/NWS/NCEP/HPC
1200Z SURFACE ANALYSIS
DATE: MON SEP 16 2002
ISSUED: 1319Z MON SEP 16 2002
ANALYST: PEREIRA/RHOME

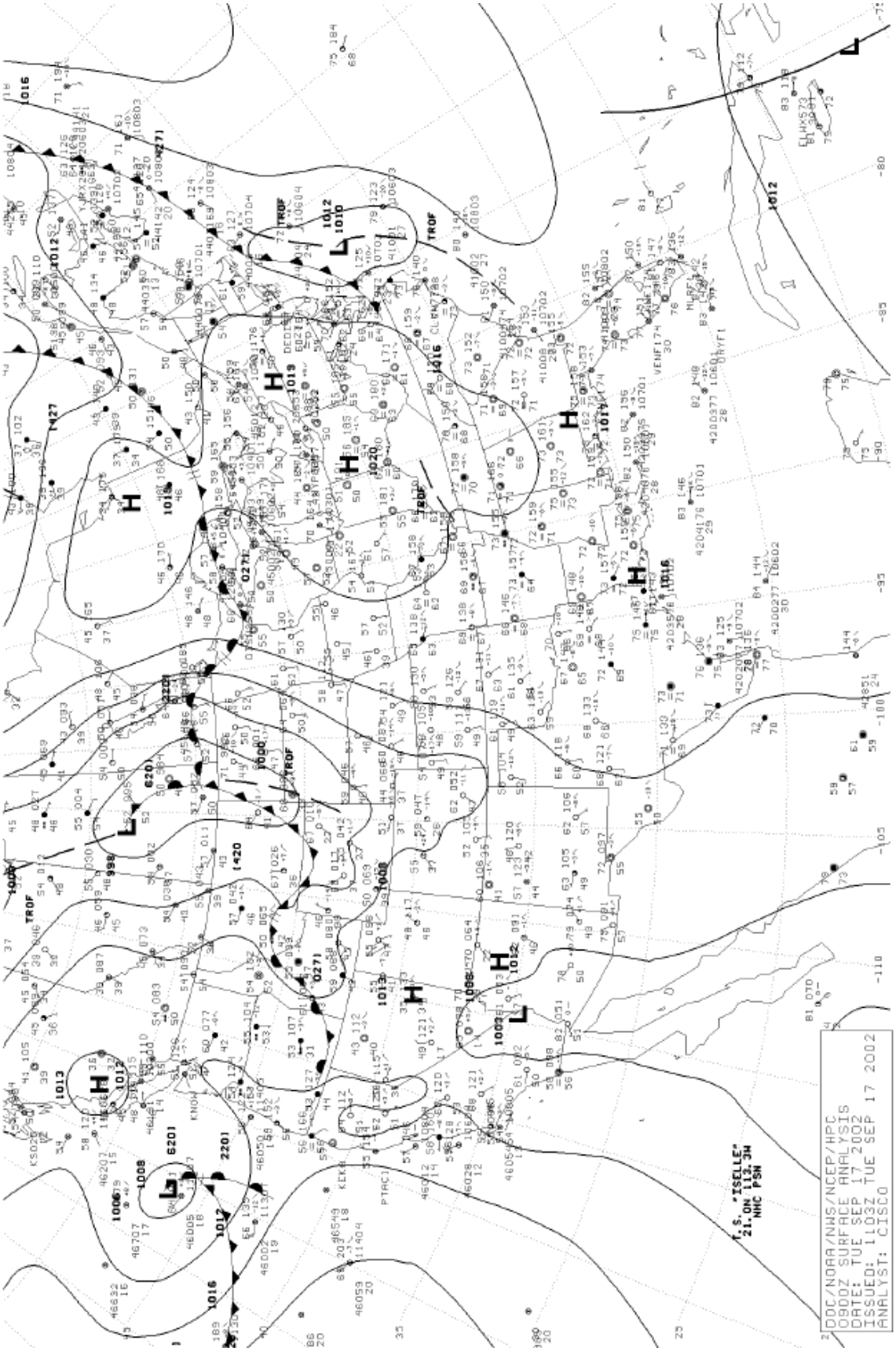
T.S. "ISELLE"
21. ON 1130 3H
NHC PSN
DOC/NOAA/NWS/NCEP/HPC
0900Z SURFACE ANALYSIS
DATE: TUE SEP 17 2002
ISSUED: 1103Z TUE SEP 17 2002
ANALYST: CISCO

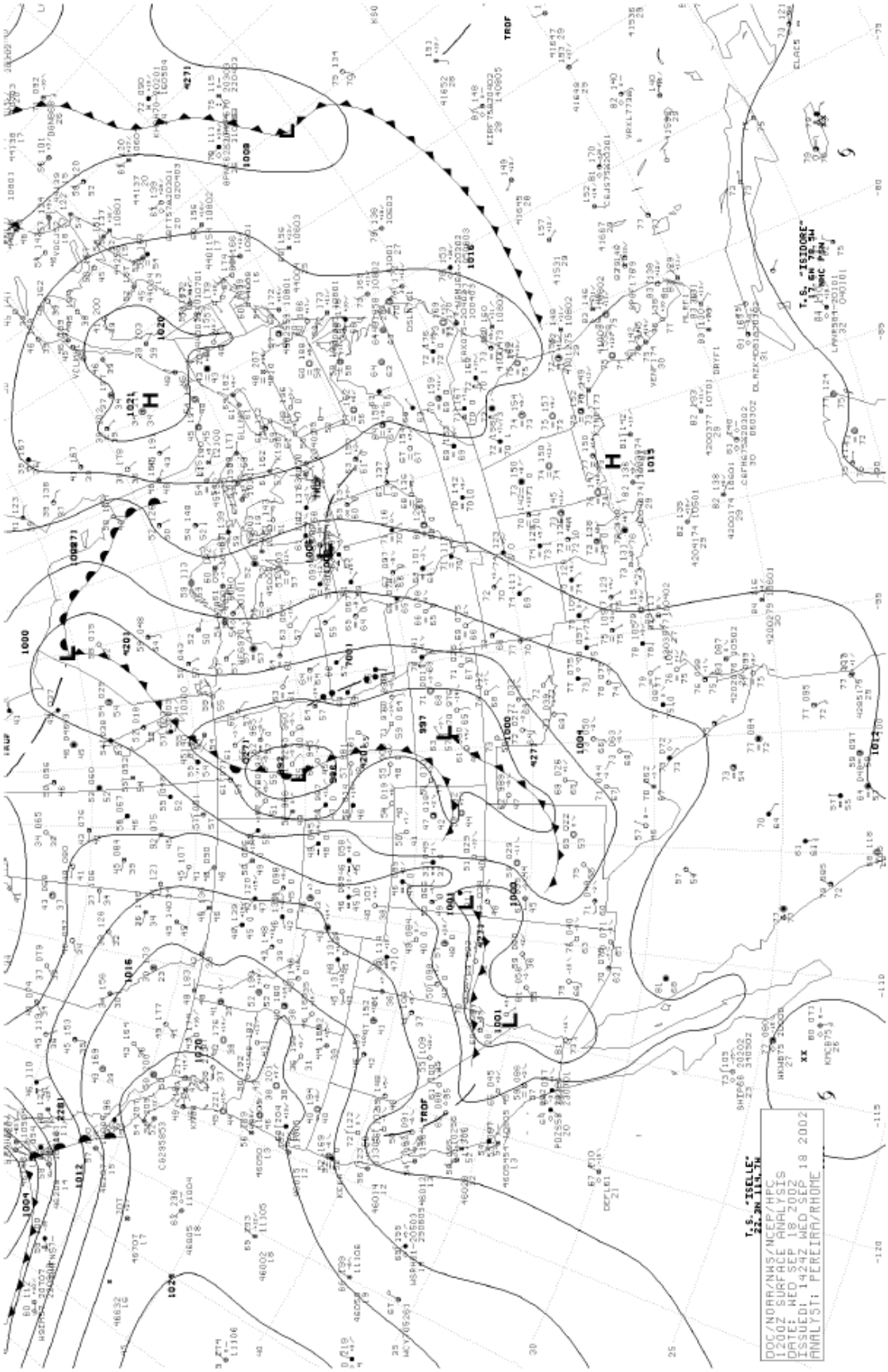
DOC/NOAA/NWS/NCEP/HPC
1200Z SURFACE ANALYSIS
DATE: WED SEP 18 2002
ISSUED: 1424Z WED SEP 18 2002
ANALYST: PEREIRA/RHOME

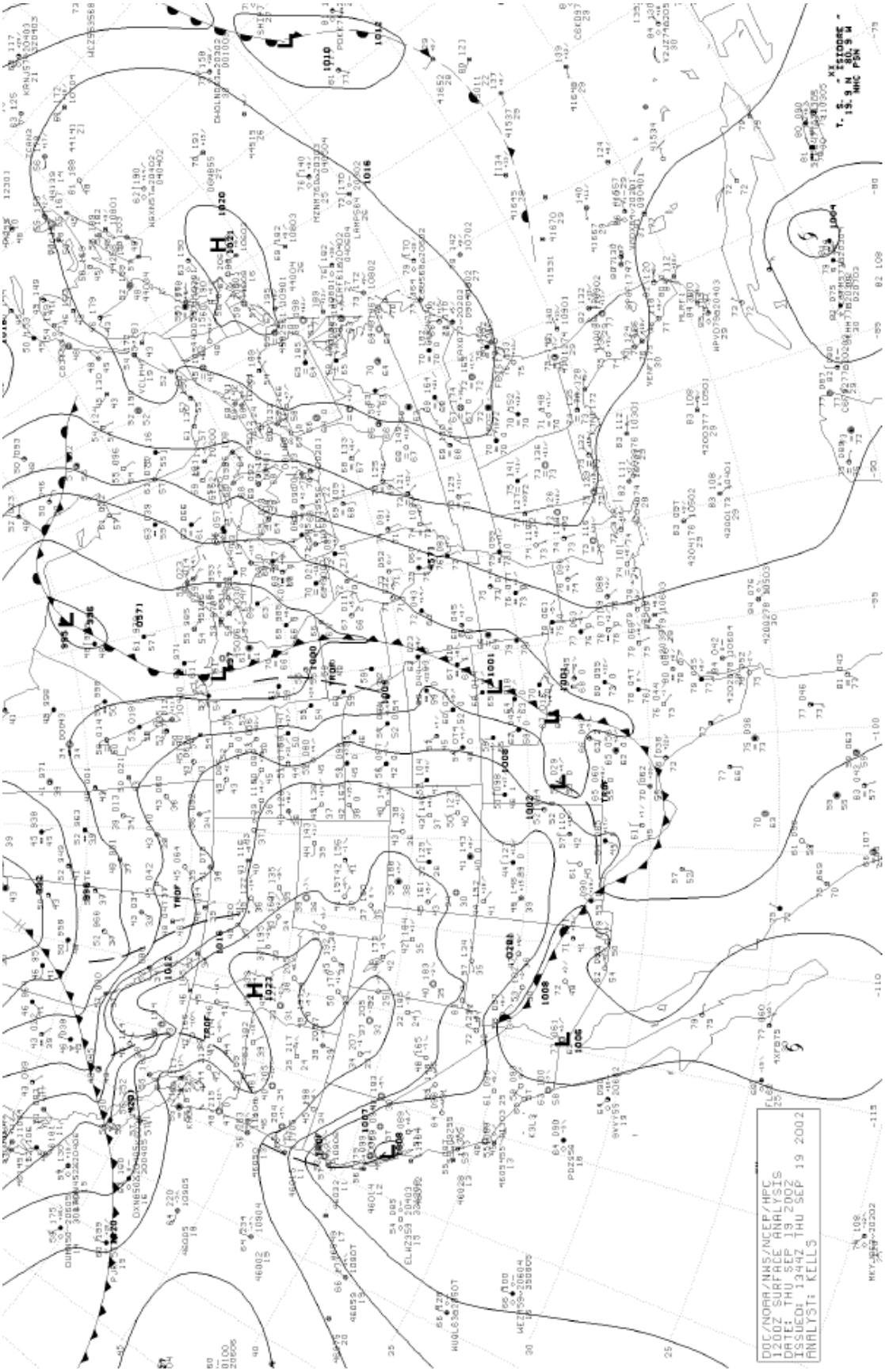
DOC/NOAA/NWS/NCEP/HPC
12OOZ SURFACE ANALYSIS
DESIGNED THU SEP 19 2002
ASSUEDLY 13HZ THU SEP 19 2002
ANALYST: KELLS

APPENDIX B

DRY-DEPOSITION MEASUREMENTS OF IMPORTANT IONIC SPECIES

Table B1. Anion Dry-Deposition During Pellston, Michigan Measurement Intensive

BDL = Below Detection Limit RI = Rain Influenced

Date On	Sample Period	Cl (mg/m2/pd)	NO2 (mg/m2/pd)	Br (mg/m2/pd)	NO3 (mg/m2/pd)	SO4 (mg/m2/pd)
6-Jun-01	Day	0.45	BDL	BDL	BDL	3.78
6-Jun-01	Night	1.43	BDL	BDL	BDL	BDL
7-Jun-01	Day	BDL	BDL	BDL	BDL	BDL
7-Jun-01	Night	BDL	BDL	BDL	BDL	BDL
8-Jun-01	Day	BDL	BDL	BDL	BDL	BDL
8-Jun-01	Night	1.35	BDL	BDL	BDL	BDL
9-Jun-01	Day	0.61	BDL	BDL	2.77	1.98
9-Jun-01	Night	BDL	BDL	BDL	BDL	BDL
10-Jun-01	Day	BDL	BDL	BDL	BDL	BDL
10-Jun-01	Night	RI	RI	RI	RI	RI
11-Jun-01	Day	2.70	BDL	BDL	BDL	BDL
11-Jun-01	Night	RI	RI	RI	RI	RI
12-Jun-01	Day	1.02	BDL	BDL	1.16	0.94
12-Jun-01	Night	BDL	BDL	BDL	BDL	BDL
13-Jun-01	Day	BDL	BDL	BDL	1.71	2.55
13-Jun-01	Night	BDL	BDL	BDL	1.95	2.51
14-Jun-01	Day	0.74	BDL	BDL	3.16	3.08
14-Jun-01	Night	BDL	BDL	BDL	1.28	2.52
15-Jun-01	Day	RI	RI	RI	RI	RI
15-Jun-01	Night	BDL	BDL	BDL	BDL	BDL

Table B2. Cation Dry-Deposition During Pellston, Michigan Measurement Intensive

BDL = Below Detection Limit RI = Rain Influenced

Date On	Sample Period	Na (mg/m2/pd)	NH4 (mg/m2/pd)	K (mg/m2/pd)	Mg (mg/m2/pd)	Ca (mg/m2/pd)
06/06/01	Day	BDL	BDL	0.52	BDL	0.53
06/06/01	Night	BDL	BDL	1.37	BDL	BDL
06/07/01	Day	BDL	BDL	BDL	BDL	BDL
06/07/01	Night	BDL	BDL	1.44	BDL	BDL
06/08/01	Day	BDL	BDL	0.51	BDL	0.61
06/08/01	Night	BDL	BDL	1.30	BDL	BDL
06/09/01	Day	0.69	BDL	0.84	BDL	0.81
06/09/01	Night	BDL	BDL	1.57	BDL	BDL
06/10/01	Day	BDL	BDL	1.84	BDL	BDL
06/10/01	Night	RI	RI	RI	RI	RI
06/11/01	Day	BDL	BDL	BDL	BDL	BDL
06/11/01	Night	RI	RI	RI	RI	RI
06/12/01	Day	BDL	BDL	BDL	BDL	BDL
06/12/01	Night	BDL	BDL	BDL	BDL	BDL
06/13/01	Day	BDL	BDL	BDL	BDL	BDL
06/13/01	Night	BDL	BDL	BDL	BDL	BDL
06/14/01	Day	BDL	0.74	0.21	BDL	0.46
06/14/01	Night	BDL	BDL	BDL	BDL	BDL
06/15/01	Day	RI	RI	RI	RI	RI
06/15/01	Night	BDL	BDL	BDL	BDL	BDL

Table B3. Anion Dry-Deposition During Clarksville, Michigan Measurement Intensives

BDL = Below Detection Limit RI = Rain Influenced

Sample On Date	Period	Cl (mg/m2/pd)	NO2 (mg/m2/pd)	Br (mg/m2/pd)	NO3 (mg/m2/pd)	SO4 (mg/m2/pd)
Apple Canopy Study						
8/20/2002	Night	BDL	BDL	BDL	BDL	BDL
8/21/2002	Day	BDL	BDL	BDL	1.3	1.4
8/21/2002	Night	RI	RI	RI	RI	RI
8/22/2002	Day	RI	RI	RI	RI	RI
8/22/2002	Night	RI	RI	RI	RI	RI
8/23/2002	Day	BDL	BDL	BDL	BDL	BDL
8/23/2002	Night	BDL	BDL	BDL	BDL	BDL
8/24/2002	Day	BDL	BDL	BDL	BDL	BDL
8/24/2002	Night	BDL	BDL	BDL	BDL	BDL
8/25/2002	Day	BDL	BDL	BDL	BDL	BDL
8/25/2002	Night	BDL	BDL	BDL	BDL	BDL
8/26/2002	Day	BDL	BDL	BDL	BDL	BDL
8/26/2002	Night	BDL	BDL	BDL	BDL	BDL
8/27/2002	Day	BDL	BDL	BDL	BDL	BDL
8/27/2002	Night	2.2	BDL	BDL	BDL	BDL
8/28/2002	Day	1.3	BDL	BDL	BDL	1.4
8/28/2002	Night	BDL	BDL	BDL	BDL	BDL
8/29/2002	Day	BDL	BDL	BDL	BDL	BDL
8/29/2002	Night	BDL	BDL	BDL	BDL	BDL
Soybean Canopy Study						
9/10/2002	Night	BDL	BDL	BDL	BDL	BDL
9/11/2002	Day	BDL	BDL	BDL	BDL	BDL
9/11/2002	Night	BDL	BDL	BDL	BDL	BDL
9/12/2002	Day	1.5	BDL	BDL	BDL	BDL
9/12/2002	Night	BDL	BDL	BDL	BDL	BDL
9/13/2002	Day	BDL	BDL	BDL	1.8	2.7
9/13/2002	Night	BDL	BDL	BDL	BDL	BDL
9/14/2002	Day	1.1	BDL	BDL	2.0	5.0
9/14/2002	Night	BDL	BDL	BDL	BDL	3.3
9/15/2002	Day	BDL	BDL	BDL	BDL	1.5
9/15/2002	Night	BDL	BDL	BDL	BDL	BDL
9/16/2002	Day	1.3	BDL	BDL	BDL	2.0
9/16/2002	Night	BDL	BDL	BDL	BDL	BDL
9/17/2002	Day	1.4	BDL	BDL	BDL	2.9
9/17/2002	Night	RI	RI	RI	RI	RI
9/18/2002	Day	BDL	BDL	BDL	BDL	BDL
9/18/2002	Night	BDL	BDL	BDL	BDL	BDL
9/19/2002	Day	BDL	BDL	BDL	BDL	1.3

Table B4. Cation Dry-Deposition for Clarksville, Michigan Measurement Intensives
BDL = Below Detection Limit RI = Rain Influenced

Sample On Date	Period	Na (mg/m2/pd)	NH4 (mg/m2/pd)	K (mg/m2/pd)	Mg (mg/m2/pd)	Ca (mg/m2/pd)
Apple Canopy Study						
08/20/02	Night	BDL	3.2	BDL	BDL	BDL
08/21/02	Day	BDL	1.7	BDL	BDL	2.3
08/21/02	Night	RI	RI	RI	RI	RI
08/22/02	Day	RI	RI	RI	RI	RI
08/22/02	Night	RI	RI	RI	RI	RI
08/23/02	Day	BDL	BDL	BDL	BDL	BDL
08/23/02	Night	BDL	BDL	BDL	BDL	BDL
08/24/02	Day	BDL	2.3	1.3	BDL	BDL
08/24/02	Night	BDL	2.5	BDL	BDL	BDL
08/25/02	Day	BDL	2.0	BDL	BDL	BDL
08/25/02	Night	BDL	BDL	BDL	BDL	BDL
08/26/02	Day	BDL	1.6	BDL	BDL	BDL
08/26/02	Night	BDL	1.8	BDL	BDL	BDL
08/27/02	Day	BDL	1.4	BDL	BDL	1.3
08/27/02	Night	BDL	BDL	BDL	BDL	BDL
08/28/02	Day	BDL	2.1	BDL	BDL	BDL
08/28/02	Night	BDL	BDL	BDL	BDL	BDL
08/29/02	Day	BDL	2.6	BDL	BDL	1.9
08/29/02	Night	BDL	BDL	BDL	BDL	BDL
Soybean Canopy Study						
09/10/02	Night	BDL	BDL	BDL	BDL	BDL
09/11/02	Day	BDL	1.6	BDL	BDL	BDL
09/11/02	Night	BDL	BDL	BDL	BDL	BDL
09/12/02	Day	BDL	4.2	BDL	BDL	1.3
09/12/02	Night	BDL	4.5	BDL	BDL	BDL
09/13/02	Day	BDL	4.0	BDL	BDL	1.6
09/13/02	Night	BDL	2.5	BDL	BDL	1.9
09/14/02	Day	1.1	4.3	BDL	BDL	1.8
09/14/02	Night	BDL	2.8	BDL	BDL	BDL
09/15/02	Day	BDL	3.4	BDL	BDL	BDL
09/15/02	Night	9.0	2.1	BDL	BDL	BDL
09/16/02	Day	4.1	2.4	BDL	BDL	BDL
09/16/02	Night	BDL	3.3	BDL	BDL	1.9
09/17/02	Day	1.7	4.6	BDL	BDL	2.2
09/17/02	Night	RI	RI	RI	RI	RI
09/18/02	Day	2.7	4.8	BDL	BDL	BDL
09/18/02	Night	1.7	6.8	BDL	BDL	2.6
09/19/02	Day	1.9	6.5	BDL	BDL	BDL